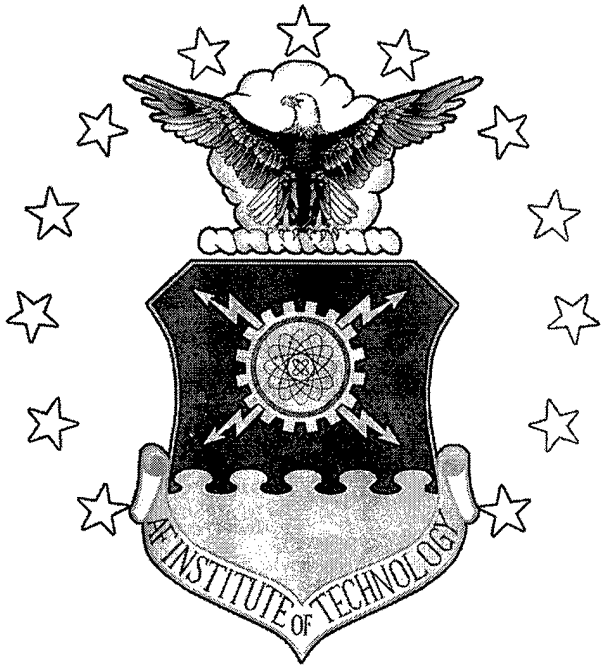

COMPARISON OF SPECTRAL ANALYSIS SOFTWARE PROGRAMS (RobWin and RSEMCA)

THESIS

Thomas E. Cartledge, Major, USA

AFIT/GNE/ENP/01M-1

DEPARTMENT OF THE AIR FORCE
AIR UNIVERSITY
AIR FORCE INSTITUTE OF TECHNOLOGY
Wright-Patterson Air Force Base, Ohio

The views expressed in this thesis are those of the author and do not reflect the official policy or position of the United States Air Force, Department of Defense, or the U. S. Government.

AFIT/GNE/ENP/01M-1

COMPARISON OF SPECTRAL ANALYSIS SOFTWARE PROGRAMS (RobWin and RSEMCA)

THESIS

Presented to the Faculty

Graduate School of Engineering and Management

Air Force Institute of Technology

Air University

Air Education and Training Command

In Partial Fulfillment of the Requirements for the

Degree of Master of Science in Nuclear Engineering

Thomas E. Cartledge, B.S.

Major, USA

March 2001

AFIT/GNE/ENP/01M-1

COMPARISON OF SPECTRAL ANALYSIS SOFTWARE PROGRAMS (RobWin and RSEMCA)

Thomas E. Cartledge, B.S.
Major, USA

Approved:

LTC James C. Petrosky (Chairman)	09MAR01 date
Larry W. Burggraf (Member)	8 Mar 01 date
Kirk A. Mathews (Member)	9 March 2001 date

Acknowledgments

I would like to express my sincere appreciation to my faculty advisor, LTC James Petrosky, for his guidance and support throughout the course of this thesis effort. Additionally, I would like to thank Dr Larry Burggraf and Dr Kirk Mathews for being committee members and providing their expertise to this research effort. I would, also, like to thank my sponsor, Lt Col John Anton, from the Defense Threat Reduction Agency for both the support and guidance provided to me in this endeavor. The insight and experience provided by all was certainly appreciated.

Thomas E. Cartledge

Table of Contents

List of Figures

Figure **Page**

List of Tables

Table **Page**

Abstract

The Defense Threat Reduction Agency (DTRA) has purchased two spectral analysis programs, RobWin and RSEMCA, to support arms control efforts. This thesis explored which program performed better for nuclear weapon identification and verification. The initial hypothesis was that both programs would perform similarly with only small differences in visual displays and operating functions.

The thesis investigated three areas in order to evaluate the software's capabilities. The first area studied the benefits offered by different detectors, specifically the NaI and CZT detector. The second area analyzed the quantitative and qualitative capabilities of each program, and the third area reviewed the software's ability to detect weapon grade plutonium (WGPu).

The results of the study show that RobWin performed better then RSEMCA. Only RobWin is capable of supporting DTRA's needs in treaty verification. RSEMCA is incapable of identifying WGPu due to a mathematical error associated with the peak count calculations. The detectors used in this thesis, the CZT and NaI, also failed to support DTRA's needs. Neither detector was capable of acquiring the necessary spectrum for identifying WGPu. Because of this thesis, recommendations were made for future work with CZT detectors, nuclear weapon detection, and software development.

COMPARISON OF SPECTRAL ANALYSIS SOFTWARE PROGRAMS (RobWin and RSEMCA)

I. Introduction

General Issues

The need for accurately detecting extremely low levels of nuclear isotopes is rapidly gaining importance in applications of nuclear counter-proliferation and verification. Current world events have established a need to detect and verify the accountability of nuclear materials. Reports of "loose nukes" from the former Soviet Union have identified accountability problems. States of concern, like Iraq, are attempting to clandestinely develop nuclear weapons. The United States and Russia are in the midst of large reductions in strategic weapons, but both need assurance that the other is complying. These events identify the need for accurate detection systems capable of identifying nuclear weapon's spectra. Improved methods to confidently detect trace signatures of isotopes based on gamma-ray spectra alone would improve remote-monitoring systems and greatly increase confidence levels in strategic arms control.

The United States and Russia are currently discussing a future strategic arms control treaty (START III). This treaty is likely to limit the number of nuclear warheads in addition to strategic delivery systems accountable under START I and START II. These limitations being discussed will require radiation detection equipment capable of verifying treaty compliance. DTRA has been assigned the mission to monitor and verify

START treaty compliance. As a result, DTRA is pursuing better technologies to improve confidence in measured results.

Problem

For better protection against this threat, nuclear surety, and treaty verification the need for more detailed information from nuclear detection is growing. DTRA developed two spectral analysis programs for use in weapon verification. It is necessary to evaluate their performance in detection and analysis.

Scope

The focus of this study is the performance of two spectral analysis software programs, RobWin by Constellation Technology Corporation and RSEMCA by Radiation Safety Engineering, Inc. The programs were used to analyze data collected using a Cadmium Zinc Telluride (CZT) detector from eV Products and a Harshaw Sodium Iodide (NaI) detector. DTRA is interested in exploring what benefits the higher resolution CZT detector offers compared to the NaI detector's capabilities. Emphasis was placed on detection of Uranium 235 (U-235), Plutonium 239 (Pu-239), and Plutonium 240 (Pu-240). DTRA specified that the analysis must include: the performance in evaluating data collected from low-resolution (NaI) detectors, the performance in evaluating data collected from a higher resolution (CZT) detectors, and analysis of data collected in high background environments.

Assumptions

Several assumptions were made for this thesis. To begin with, START I is the current standard for strategic arms inspections. START II has been signed and will be used as a standard, but at present, it has not been entered into force. All criteria for

weapon detection is based on the standards establish in START I and START II, to include the DoD/DOE thresholds and attributes associated with those treaties. This provides a limit to source size and criteria for determining weapon grade plutonium (WGPu). It is assumed that these will not change with the implementation of START II or future talks on START III.

Owing to the size of all the sources in relation to the detector, all sources used in this thesis are assumed to be point sources. Therefore, all efficiency calculations are based on the radius of the detector surface and the distance from the source.

It was also assumed that all Pu-239 weapons are implosion type weapons composed of single density Pu-239, $\rho = 19.85$ g/cm^3. This assumption standardizes the weapon's pit as spherical. Single density was assumed primarily for simplicity. The difference between using single density Pu-239 and double density, $\rho = 39.70$ g/cm^3, does not effect the thesis results.

The final assumption concerns the weapon's pit. The pit was approximated as a hollow sphere encased in approximately 18 inches of paraffin within a steel container. The gamma rays come from the surface of the sphere and not from within. This eliminates the need to account for gamma ray attenuation through the metal of the pit. Paraffin and steel are typical materials used when storing nuclear weapons. This assumption was necessary to determine the attenuation of Pu-239 gamma rays through the storage container. The attenuation will change if different materials are used.

Limitations

START I and II

Nuclear weapon verification inspections came about because of arms reduction efforts between the United States and Russia. A result of those efforts were the START I and Start II treaties. The START treaties allow each country to conduct inspect of the other country in order to verify treaty compliance. In an effort to keep a country's weapon designs a secret, limits were placed on the levels of verification. Neither country is required to open a warhead or container to physically show the presence of a nuclear weapon. In addition, the use of detectors to image the nuclear weapon inside a warhead or container is not allowed. These limitations established test conditions for this thesis. The detectors and software would need to identify a nuclear weapon of unknown shape and size contained within an unknown surrounding material.

DOE/DoD Limitations

To assist the United States with enforcing START I and START II, the Department of Energy (DOE) and the Department of Defense (DoD) established "Threshold and Attributes" to simplify means for nuclear weapon's accountability and treaty verification. The DOE/DoD Radiation Detection Working Group has identified 0.5 KG of weapon grade plutonium (WGPu) as the unclassified minimum threshold to detect. Anything more is potentially a bomb and lesser amounts are not likely under treaties verification. The 0.5 KG threshold provides a means to test detection equipment [17]. This minimum mass will be the hardest to identify and verify, and therefore will be used as the standard throughout the thesis.

Detector capabilities vary considerably. For weapon verification purposes, the ideal detector to use is the high resolution, liquid nitrogen (LN) cooled High Purity Germanium (HPGe) detector, but this is not always practical due to the cooling requirements. The default technology is to use the lower resolution room temperature NaI detector. The current regime favored by DoD/DOE working groups, and used by DTRA, involves using HPGe for detailed measurements at key places, and NaI detectors at other locations to save time/effort. The problem with this is that the low resolution NaI detector provides a very limited ability to verify nuclear weapons. DTRA is looking for better alternatives to replace the NaI detector. Therefore, this thesis will use the NaI detector as a base to compare other detectors against.

Detectors

There exist a wide variety of radiation detectors used to collect spectra. Two varieties that exist are active and passive detection systems. A passive system collects incident radiation as it is emitted from the source. An active detection system emits radiation into the source and collects the resulting spectrum. DTRA foresees safety and other intrusiveness issues in using active detection systems and does not want to pursue efforts in this area. DTRA has limited this thesis to passive detection systems only.

The experiment was also limited to two types of detectors, CZT and NaI. A secondary interest to DTRA was to find a detector that offers better portability than the high resolution liquid nitrogen cooled HPGe detector, and offers better resolution and more compact size than the room temperature NaI detector. CZT detectors offer a possible solution to DTRA's needs.

Paper Sequence

A more detailed analysis of the problem and testing procedures is discussed in the following chapters. Chapter II of this thesis describes the background information on the radioactive sources, detection equipment, and software. Chapter III provides software evaluation and testing procedures. Chapter IV describes experimental results and analysis. Chapter V contains concluding remarks, suggestions for changes to the spectral software, and recommendations for future study. Appendix A through Appendix K provide supporting calculations, tabulated data, and references used throughout the thesis.

II. Background

This chapter is broken into 3 sections. The first section provides a review of gamma ray interactions and detector characteristics for the Sodium Iodide (NaI) and Cadmium Zinc Telluride (CZT) detectors. The second section identifies the signature isotopes (SI) present in nuclear weapons and addresses the challenges in detecting the SI. The last section provides an overview of the RobWin and RSEMCA software programs to include the peak detection standards used by the software.

Section 1

Gamma ray interaction

Of the various ways gamma rays can interact, only three interaction mechanisms play a significant role in gamma-ray spectroscopy: photoelectric absorption, Compton scatter, and pair production. Figure 1 shows that the photoelectric absorption dominates for low-energy gamma rays (up to several hundred keV), pair production dominates for high-energy gamma rays (above 5-10 MeV), and Compton scattering is the most probable process over the range of energies between these extremes.

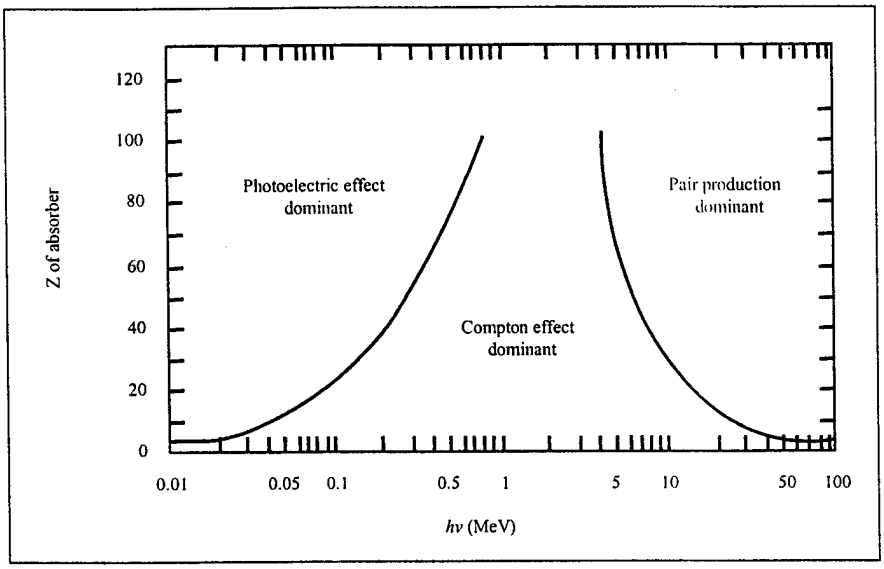

Figure 1 (Gamma-Ray Interaction)

At low energies, the primary interaction of concern is photoelectric absorption. Photoelectric absorption is an interaction in which the incident gamma-ray photon on the detector, or incident material, is absorbed. In its place, a photoelectron (e-) is produced from one of the electrons in the absorbing material with a kinetic energy equal to the incident photon energy minus the binding energy of the electron. Thus, the effect of photoelectric absorption is the liberation of a photoelectron, which carries off most of the gamma-ray energy.

During Compton scattering, a gamma-ray photon collides with an electron (e-). The result of this interaction is the creation of a recoil electron and a scattered gamma-ray photon, with the division of energy between the two. This can be problematic with gamma ray detection because the scattered gamma-ray photon can travel large distances and may escape the incident material, thus losing some of the energy from the original gamma ray.

Pair production occurs when a gamma-ray photon creates an electron-positron pair at the point of complete disappearance of the photon. A minimum gamma-ray energy of 1.02 MeV is required for this process to be energetically possible because an energy of $2M_0C^2$ is required to create the electron-positron pair. Any gamma-ray energy exceeding this will be transferred to the electron-positron pair.

It is very possible that all three interactions occur simultaneously within a detector. If the detector area is very large, the energy from these three gamma ray interactions would be captured within the detector as shown in Figure 2 with no loss to the original photon's energy. Unfortunately, a detector of sufficient size to capture all gamma ray energies would be impractical. Therefore, Compton scattering and pair production may create an escaping photon.

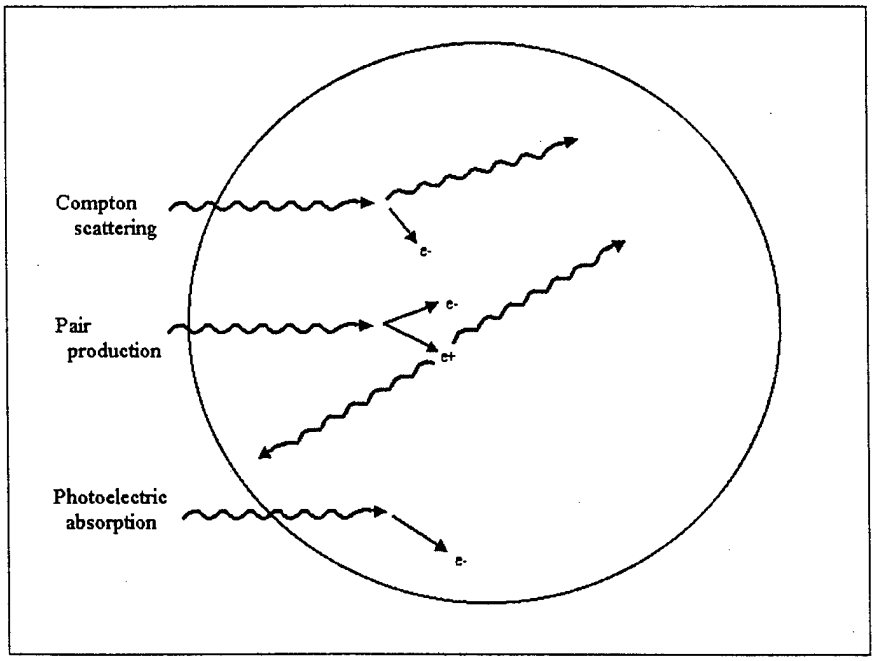

Figure 2 (Large Incident Area)

Figure 3 diagrams what happens in a detector of typical thickness. Photoelectric absorption is the preferred mode of gamma ray interaction with a detector because there is a greater probability of the entire energy being deposited in the detector. Therefore, it is desirable to detect low energy gamma rays so that the interactions are primarily photoelectric absorption. However, the situation is complicated by the fact that lower energy gamma rays (where photoelectric absorption dominates) are more easily shielded by the storage container.

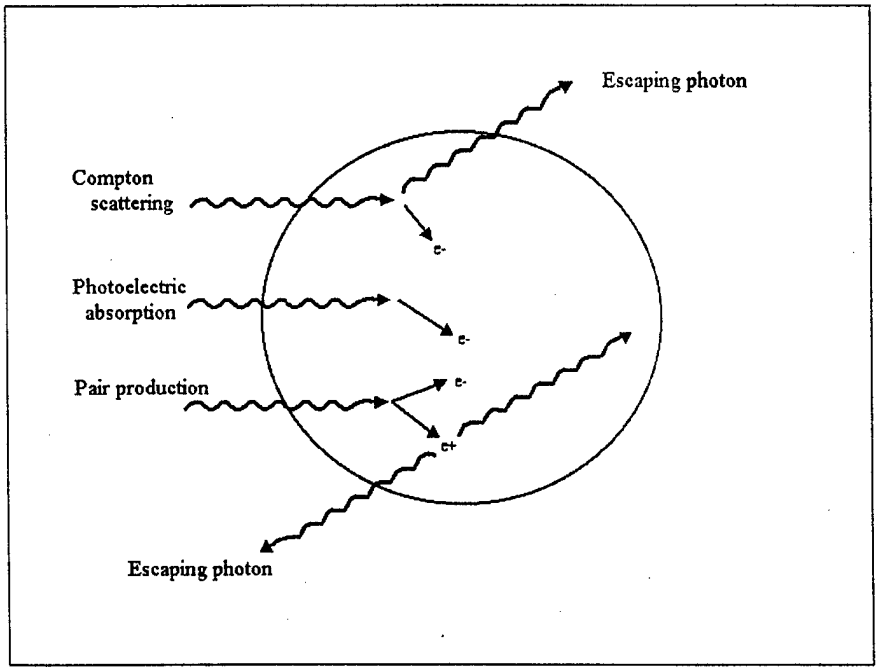

Figure 3 (Moderate Size Incident Area)

The gamma ray interactions through shielding are similar to those described above. The shielding around a nuclear weapon will absorb some of the gamma ray energy and create additional scatter events before the gamma rays reach the detector. This results in lost interactions with the detector due to absorption and the creation of

lower energy gamma ray interaction because of down scatter. Down scattering is a result of the Compton scattering events where some of the energy is absorbed in the shielding and a lower energy gamma ray is released that may have enough energy to cause additional interactions or escape the material. These additional lower energy gamma rays may add addition peaks and noise to the detected spectrum.

Detectors.

Without consideration of any other factors, high purity germanium (HPGe) would normally be the detector material of choice for nuclear safeguard inspections and nuclear non-proliferation because of its high resolution. DTRA's current default technology for higher resolution is the HPGe detector, but is seeking ways to get a room temperature replacement to avoid the logistics issues associated with transporting liquid nitrogen. DTRA's desired detector is a room temperature detector like CZT or HgI_2 (Mercuric Iodide), which offer higher resolution than the NaI detectors without the challenges of HPGe.

A NaI and CZT detector were available for this thesis, but the HPGe detector was not. Therefore, this thesis compared the spectral results from a NaI detector and a CZT detector to identify the benefits either offers to nuclear weapon detection or the spectral analysis programs. Because there was not an HPGe detector available, a comparison between the collected spectra from HPGE detectors and CZT detectors could not be done.

NaI Detectors

The NaI detector is an inorganic scintillator detector, which uses photomiltiplier tubes to collect spectra from incident gamma rays. As gamma rays deposit their energy in the scintillator material, electrons are excited. As the electrons de-excite they emit

light. The emitted light reflects and scatters until it is absorbed or escapes the scintillator. The light that reaches the photomultiplier tube is converted to electrons and collected to record the gamma ray's energy.

NaI crystals provide an excellent light yield and have become the standard scintillation material for routine gamma ray spectroscopy. The NaI detector operates at room temperature and has good detection efficiency due to its high density, large available sizes, and high atomic number (Z=53). The disadvantage of the NaI detector is the poor energy resolution, which results in the inability to distinguish between gamma rays within several keVs of each other [13, 219-259]. This can result in a single visible peak in the spectrum that is a combination of several different gamma ray energies.

NaI detectors currently used by DTRA are sufficient to determine the presence of plutonium or uranium, but provide insufficient information to determine the presence of WGPu. The NaI detectors lack the resolution to distinguish the key energy peaks to determine the mass percent of Pu-239 and Pu-240.

CZT Detectors.

The CZT detector, or CdZnTe, is a semiconductor based gamma-ray spectrometer made from a blended ratio of ZnTe and CdTe in a crystalline form. The semiconductor detector collects holes and electrons created by the interaction of a gamma ray in the semiconductor material. CZT detectors have shown significant improvement in both energy resolution and size over other room temperature gamma-ray spectrometers.

The CZT detector offers an advantage in resolution over the NaI detector. The advantage lies in the smaller ionization energy associated with CZT. Approximately 5 eVs are required to create an ion pair in CZT whereas NaI requires approximately 30

eVs. Thus, the number of charge carriers for CZT versus NaI is 6 times greater at any energy deposited in the detector. CZT detectors are also more efficient than NaI detectors. CZT detectors have a higher Z than NaI detectors, which have more electrons associated with the atoms and therefore more charge carriers [13, 477-486].

The size of the CZT detector offers an advantage over the NaI detector for portability. CZT detectors are significantly smaller than NaI detectors with crystal dimensions ranging from 5mm x 5mm x 1mm to 10mm x 10mm x 10mm compared to the NaI detector with minimum dimensions of 250 mm x 250 mm cylindrical. This is approximately a 12,270,000 mm^3 reduction in volume that would allow for significantly smaller detection systems for weapon verification inspections.

Unfortunately, the reduced size of the CZT detectors has a smaller collection area which limits the counts collected and increases statistical error. The CZT detectors are limited to small surface areas (10 mm x 10 mm) because current technologies cannot grow larger CZT crystals without a high impurity concentration. NaI crystals can be grown as large at 3 inches in dimension. The larger surface area of the NaI detector provides a larger area for gamma ray interactions, which improves the detector efficiency. Larger counts collected by the NaI detector reduce the statistical errors associated with the counts. The CZT detector used has a surface area of 25 mm^2 versus the NaI detectors surface area of 18241 mm^2.

The thickness of the crystal also affects the ability to collect spectra of gamma rays as they pass through crystal. Higher energy gamma rays are capable of penetrating deeper within a material than lower energy gamma rays. In the case of CZT detectors, many of the higher energy gamma rays, above 200 keV) will be capable of

passing through the crystal before depositing their energy. This will reduce the counting efficiency at higher energies. This is less likely to happen with the thicker 3 inch NaI detector.

Radiation damage to the detector is another disadvantage of the CZT detector compared to the NaI scintillator. Any extensive use of CZT detectors will result in some damage to the lattice because of the radiation damage. The radiation damage will trap charge carriers and limit complete charge collection. This will reduce the resolution of the CZT detector over time. This is not as much of a problem for NaI detectors because NaI detectors depend on the production of a photon through de-excitation. Once the photon is produced, radiation damage in the detector will not affect the photon's ability to travel.

Section 2

Nuclear Weapon Signature Isotopes (SI).

Since DTRA is concerned with determining the existence of a nuclear weapon, the SI are U-235, U-238, Pu-239, and Pu-240. U-235 and Pu-239 are of interest because they are the main fissile fuels in nuclear weapons. U-238 is included because many weapons have a depleted uranium tamper made of U-238 to improve weapon performance. In addition to its use as a taper, U-238 is fissionable and will add to the weapon's yield. Pu-240 is of interest because this helps establish the grade of plutonium.

The mass percent of Pu-239 and Pu240 is instrumental in determining whether the concealed plutonium is WGPu, which may indicate a weapon. Table 1 shows a mass percentage of 93.6 % or better Pu-239 indicates WGPu while Reactor Grade Plutonium

(RGPu) has a mass percent of 62% or less Pu-239. Anything between WGPu and RGPu is considered Fuel grade [18, A-3].

Table 1 (Isotope Mass Percents for different Plutonium Grades)

Isotope	238	239	240	241	242
WGPu	<0.0005	0.936	0.06	0.004	<0.0005
Fuel Grade	0.001	0.861	0.12	0.016	0.002
RGPu/Power Grade	0.100	0.620	0.22	0.120	0.030

SI Detection Challenge

The ability to identify the SI can be extremely challenging. Shielding of nuclear weapons is done to protect workers from harmful radiation and prevent neutrons from escaping and causing fission reactions. Nuclear devices are shielded primarily to absorb the neutrons emitted by the fissile material. Escaping neutrons are capable of initiating other fissions reactions. In a facility with many stored weapons, the cumulative effect of the escaping neutrons could possibly initiate a chain reaction. The shielding is not designed to absorb the emitted gamma rays. It does attenuate the gamma rays through absorption of low energy gamma rays and secondary interactions, or scatter, for the higher energy gamma rays. This scatter creates additional lower energy gamma rays, which add background noise to the spectrum. Appendix A contains the key gamma rays emitted for the SI.

Another effect from the shielding concerns the neutron absorption. Paraffin is typically used as a neutron shield because of its low Z. Paraffin like water has a high hydrogen density. Hydrogen serves to reduce the neutron energy to thermal energies, after which the neutron is captured. The neutron capture by hydrogen can produce a 2.22

combined scatter from all the Pu-239 gamma rays eliminates observable peaks below 200 keV.

Detection of plutonium offers an additional challenge. The detection of plutonium has to be able to distinguish between WGPu and RGPu. This occurs by identifying a Pu-239 peak and Pu-240 to calculate a mass percent from the peak counts for each respective peak. There are no identifiable peaks in the region below 200 keV. That only leaves a 212 keV and a 642 keV gamma ray for Pu-240. Pu-239 does not have a gamma ray around 212 keV, but does have a 645 keV gamma ray. It is essential to have gamma rays from Pu-239 and Pu-240 with approximately the same energy so the gammas are subject to similar conditions. The DoD/DOE working group has identified gammas in the 640 keV region where there is both a Pu-239 and Pu-240 peak to determine plutonium mass percents [17]. This thesis will focus on the detection of plutonium since it posses a much harder challenge to detect than HEU.

False Signals

The SI considered in this thesis result from a desire to verify the number of weapons a country may have in storage. In typical verification field investigations, spectra are gathered through a shielded medium. One must determine whether a weapon exists, "green light" or not, "red light" without being able to look inside the container. If a country provides a "look alike" pit within a shield, they may be able to fool the detector and divert the actual weapon for unauthorized use. A "True False" is when the detection system indicates the presence of a weapon when in actuality no weapon exists. The inspector has no means to verify the detector's results.

Another method to fool an inspector is if the opposition was willing to reshape the pit, they could cut it up into enough pieces to fall just above the 0.5 Kg threshold. This would provide the appropriate signal to the detector and the inspector would have no way to know that the concealed material was just a piece of an actual weapon. However, a lot of the cost comes from shaping the pit to high tolerances. So if they want to cheat, they would much rather divert a whole pit vice one that has been reshaped. By accepting a threshold value for verification, DOD/DOE has given up on a chance to catch pits being diverted a small piece at a time. That becomes a problem for a domestic safeguards/security program to prevent small quantities of weapons useful material being stolen, and domestic safeguards efforts operate under different constraints, without worrying about threshold "red light/green light" values.

DTRA is concerned about detecting weapons, not the domestic safeguards, and therefore this investigation uses the DOD/DOE threshold as minimum test standards. The initial focus has been on techniques that would be used to confirm, in reciprocal inspections, declarations of stocks of plutonium pits that each country had accumulated from dismantled warheads.

Section 3

Spectral Analysis Software Programs

This thesis involves the analysis of two software detection programs, RobWin and RSEMCA. A review of each program is provided below.

RobWin.

The approach used in RobWin is to fit of the entire continuum, followed by searches for nuclides. This approach emphasizes modeling the continuum for the spectrum as a single, continuous curve composed of cubic splines with optimized knot locations and coefficients. In each nuclide search, RobWin reoptimizes the energy and resolution calibrations and adjusts efficiency for attenuation in air. Because the RobWin analysis is not peak-search based, RobWin claims to report no false peaks.

The RobWin approach applies a great deal of computational effort to modeling the continuum as a single, continuous, smooth curve spanning the entire spectrum in a nonlinear minimization matrix-reduction procedure. The continuum fit is composed of cubic splines whose number, knot locations, and amplitudes are optimized to result in the smallest modified chi-square with the fewest splines.

The RobWin approach employs simultaneous, non-linear fitting of six key elements fit to the entire spectrum until no further gain in statistics can be achieved. These elements are: 1) the continuum for the entire spectrum as a composite of cubic splines, 2) the photopeak response function of all the lines of each search nuclide, 3) the relative intrinsic efficiency of the detector, 4) the photopeak resolution width, 5) energy calibration, and 6) modification to efficiency for designated isotopes due to attenuation by intervening matter. Only after this is done, is a conventional peak search made to locate peaks not yet associated with any of the nuclides chosen by the user. The key to this methodology is the accurate table of nuclides available within the program [1]-[3].

RobWin can possess computational challenges due to the computationally intensive nature of its algorithm. The developer indicates that computation time could

vary between seconds to several minutes on a modern computer because of a weak signal or small number of counts [4].

RSEMCA.

RSEMCA runs on a personal computer under Windows 95, 98, or NT operating system. The program can be used to control a Digital Signal Processor (DSP) connected to a CZT detector. RSEMCA has been developed specifically for use with an array of four CZT detectors. Because of this, it is capable of displaying and manipulating the spectra from several crystals, as well as displaying the spectrum. The offsets and gains for each crystal are not required to be the same. RSEMCA can be set to compensate for these differences by calculating and applying offsets and scale factors to the crystal spectra before constructing the total spectrum and when displaying the individual spectra.

The peak search algorithm looks for peaks in the spectrum and places a Region of Interest (ROI) around those found. The algorithm uses a generalized second difference method that was first introduced in the SAMPO spectroscopy code. The method identifies the extent of the peaks by finding a maximum in a weighted average of the numerical second derivative of the spectrum. Once the algorithm identifies a tentative peak as a local minimum in the smoothed second difference curve; it places a tentative ROI around it at the current FWHM. RSEMCA also has the ability to conduct a nuclide identification algorithm where it matches peaks in the spectrum to known peaks in a library file and computes the activity of identified nuclides contributing to those peaks.

RSEMCA offers the capability to calculate the enrichment of uranium using the Uranium Meter method. The meter method is based on the net counts in an ROI around

the 185.7 keV peak that increases with enrichment. To calculate the uranium enrichment, the software requires a calibration file of a uranium source.

Because of the complex algorithm, the software can take a significant amount of time to execute. No definition was provided for a significant amount of time [6].

Nuclide Standards

RobWin and RSEMCA both report to use data and standards provided by Brookhaven National Laboratories from the National Nuclear Data Center (NNDC) which includes the SI. NNDC produces these databases in cooperation with various national and international networks such as the International Nuclear Structure and Decay Network and the Nuclear Data Centres. In addition to Brookhaven National Laboratories, RobWin also uses the "Shirley" tables, which are now maintained by Berkeley [19]. This thesis will use the Brookhaven National Laboratories reference tables as a standard since both software programs claim to use this reference.

III. Methodology

This chapter provides the methodology for the spectral testing using the CZT and NaI detectors as well as both RobWin and RSEMCA spectral analysis software programs.

Test Objectives

Several tests were performed to investigate the detection capability of the CZT detector compared to the lower resolution NaI detector for used in treaty verifications. The spectra collected by the detectors were analyzed using both RobWin and RSEMCA. This provided data for analysis of the software programs. Three areas of interest were identified that influences the detection system. Those areas were: the type of detectors used, the software capabilities, and the WGPu spectrum. The test results were used to answer the following questions:

1. Detector Types. What is gained by using the CZT detector instead of the NaI detector on nuclear weapons material when analyzed using RobWin and RSEMCA?

2. Software Analysis. Does either RobWin or RSEMCA perform better in the area of spectral analysis?

3. WGPu Spectrum. Does one software program offer an advantage in identifying WGPu?

A multisource was used with the CZT and NaI detectors to characterize the detectors and gain an understanding of the software's analysis capabilities. Afterward,

both detectors were used to characterize a Pu-239 source in an attempt to model DOD's minimal threshold of a stored nuclear weapon. This was to help determine what benefit the higher resolution CZT detector offers for nuclear weapon detection. Constellation Technologies provided a WGPu spectrum that could be used to analyze the software's ability to identify WGPu should modeling efforts fail. Through all experiments, both RobWin and RSEMCA were used to analyze the data.

Characterize detectors

This involved determining the energy calibration, detector resolution, and detector efficiency for the NaI and CZT detectors. Known gamma ray sources were used in this calibration. The detector characteristics were essential to identify unknown sources and provided basic comparisons of the two detectors.

Characterize the Pu-239 Source

A thorough characterization of the Pu-239 source required the gathering of a shielded, and unshielded spectrum. The shielded spectrum helped to identify any downscatter effects from the shielding. This involved looking at the source by itself and with shielding materials to identify the down scatter that may result. Both detectors will collect a shield and unshielded spectrum from the Pu-239 source.

Software Analysis

RobWin and RSEMCA were used to analyze the spectral data collected throughout the experiment. Both software programs will be evaluated quantitatively, by the software's ability to analyze the data and identify the nuclear isotopes present, and qualitatively, by the software's ease of use.

Test priorities

The primary objective of the tests was to provide the necessary spectra to analyze the capabilities of the detectors and software programs. It is essential that the detectors and Pu-239 source were properly characterized before analyzing the detector and software's ability to detect WGPu nuclear materials.

Description of Tests

Characterize detectors

A known gamma ray source will be used to characterize both the NAI and CZT detectors. Although this source initially had nine nuclides present (Cd-109, Co-57, Te-123, Cr-51, Sn-113, Sr-85, Cs-137, C0-60, and Y-88) when activated in October 1994, only three are left at a detectable level. Those isotopes are: Cd-109, Cs-137, and Co-60. A pulser and oscilloscope were used to verify that the components of the detection system were operating properly. Figure 4 and Figure 6 show the setup for both detectors.

A 10 hour spectrum was collected of the multi source by both detectors. The multi source contained Cd-109, Cs-137, and Co-60. For the CZT detector, the source was placed directly in front of the detector's face to capture 50% of the available gamma rays assuming a point source with spherical divergence. For the NaI detector, the source had to be located 25 cm from the detector face to minimize dead time on the detector. Using the key gamma rays associated with Cd-109, Cs-137 and Co-60, an energy calibration for the spectra was determined. Spectra from separate sources of Cd-109, Cs-137, and Co-60 were used to confirm the location of energy peaks and the energy calibration.

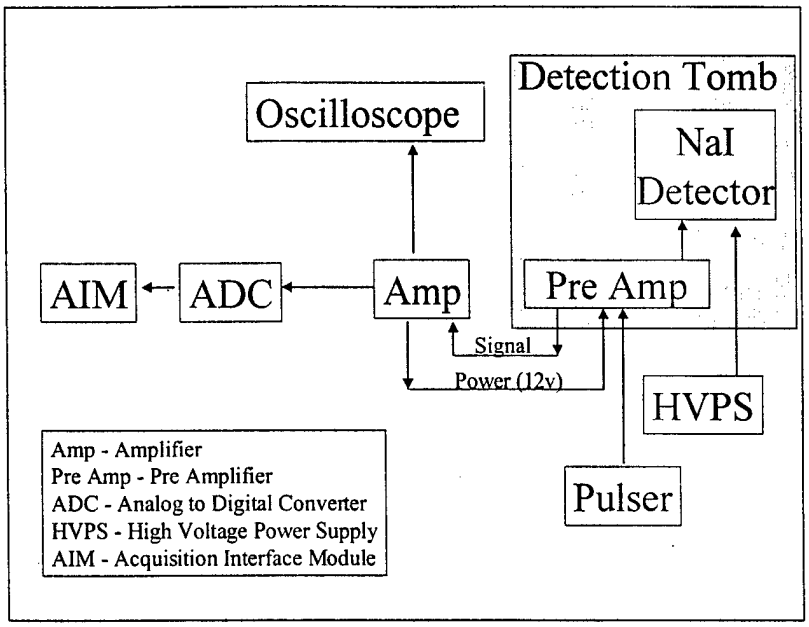

Figure 4 (NaI Detector Setup)

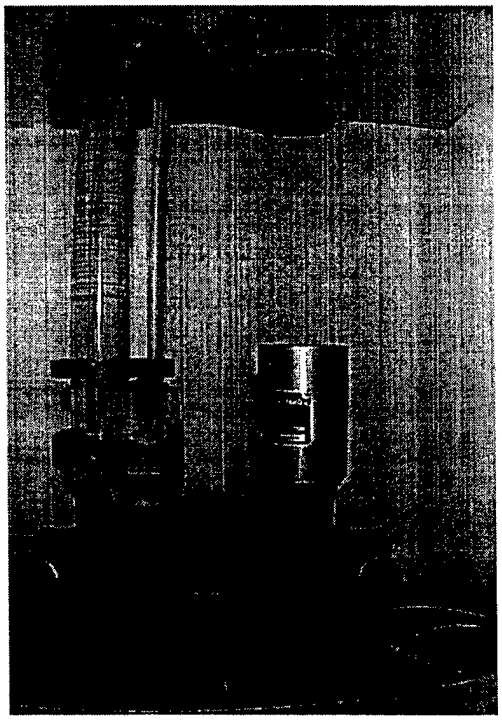

Figure 5 (NaI Detector Picture)

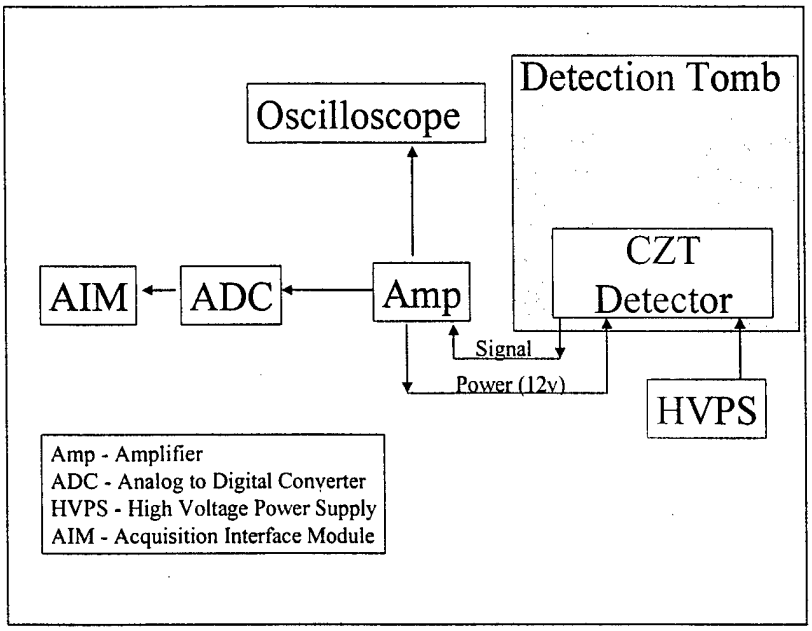

Figure 6 (CZT Detector Setup)

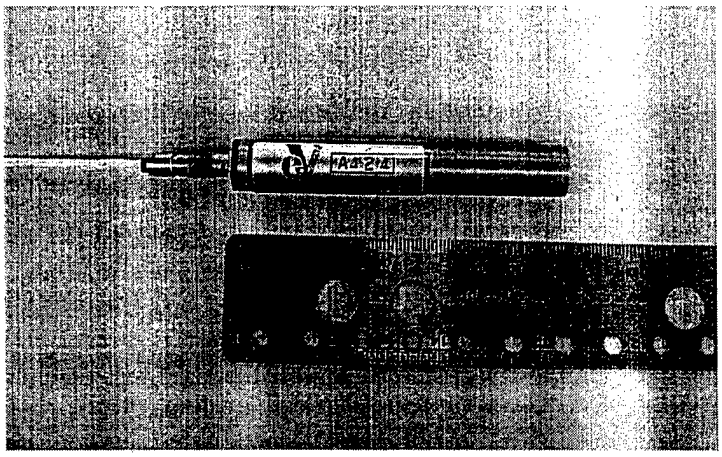

Figure 7 (CZT Detector Picture)

Characterize the Pu-239 Source

The Pu-239 source used in this experiment was an 11.994 mCi source with an initial activity date of 28 Feb 82. The source was characterized without shielding, with a

paraffin shield, and with a paraffin and a steel shield to account for the different downscatter events. The spectra were collected for 10 hours with both the CZT and NaI detectors to ensure sufficient counts were detected in key peak areas.

Nuclear Weapon Detection Capability

Using Appendix B and Appendix G, attempts were made to model the Pu-239 source as a stored weapon. Appendix B contains an approximation of the signal expected from 0.5 kg WGPu. Appendix G contains an approximation of the size of a 0.5 Kg weapon. Assuming a 360 spherical divergence of the escaping gamma rays, paraffin and steel can be used with the Pu-239 source to match those approximations. After the model was completed, the NaI and CZT detectors could collect a spectrum to analyze the detector's capabilities in nuclear weapon detection.

Analysis of RobWin and RSEMCA Software

The factors used to analyze the software are listed below. Upon assessing these factors, a determination of the benefits of each software program was made.

a. Quantitative:

1. Peak Search Capabilities
2. Energy Calibration
3. Resolution Calibration
4. Efficiency Calibration

b. Qualitative:

1. Installation
2. Instruction Manual/Help Files
3. Examples
4. Input files
5. Operating the Software
6. Software graphics
7. Library Files
8. Printing Results/Output
9. Developer Response

Special Requirements

Test Equipment

The equipment and settings used for each detector setup are listed in Appendix G. The following test equipment was necessary to test the detection components and system:

1. EG&G Ortec Model 419 Precision Pulse Generator
2. LeCroy Model 9310 Digital Oscilloscope
3. Fluke 77 Multimeter

Sources

The sources used in this thesis are listed in Appendix C. The need for a source to simulate 0.5 kg of stored WGPu poses the biggest challenge and limitation. If efforts to model a stored nuclear weapon failed, this thesis fails to answer the problem statement. Without a nuclear weapon spectrum, it would be challenging to determine the software and detector's capabilities for nuclear weapon identification and verification. As a backup should modeling efforts fail, Constellation Technology provided the spectrum from a 400 gram WGPu sample collected with an HPGe detector. Both RobWin and RSEMCA were used to analyze this spectrum.

IV. Test and Evaluation

The spectra were collected using Genie 2000 software made by Canberra. Both RobWin and RSEMCA have the ability to collect spectra, but could not be used in this way because of hardware requirements. RobWin and RSEMCA use electronics specific to their parent companies, which were not available.

A multi isotope source was used to characterize the detector. Spectra were collected for 10 hours with the CZT and NaI detectors. Spectra were also collected on individual sources of Cd-109, Cs-137, and Co-60 to confirm the location of the energy peaks in the multi source. Figure 8 and Figure 9 show the collected spectra for the multi source. Table 2 and Table 3 identify the peak centroids and Full Width at Half Maximum (FWHM) determined by RobWin and RSEMCA. The peak centroids and FWHM were used to derive an energy calibration and calculate an absolute efficiency for the detector.

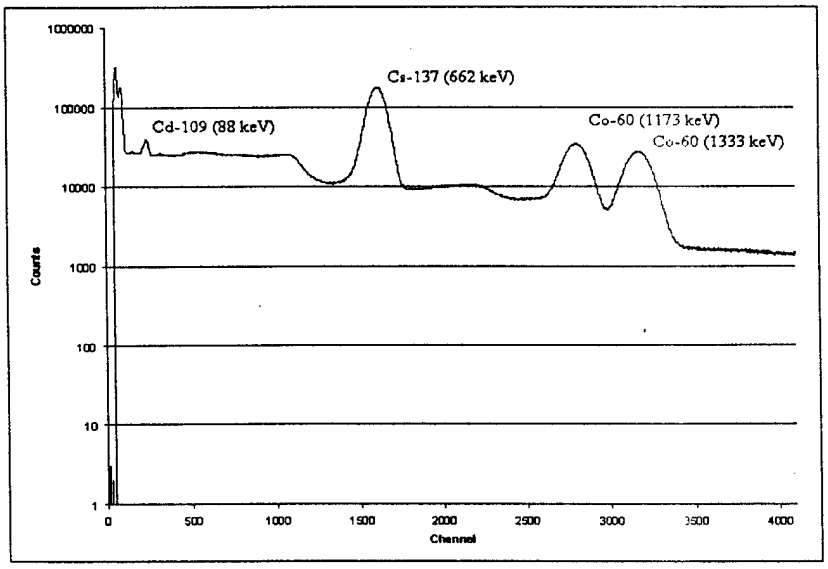

Figure 8 (Multi Source Spectra from NaI Detector)

Table 2 (Multi Source Peak Centroids and FWHM with the NaI Detector)

Isotope	Key Gamma (keV)	RobWin Peak Centroid (Channel #)	RobWin FWHM (Channel #)	RSEMCA Peak Centroid (Channel #)	RSEMCA FWHM (Channel #)
Cd-109	22.163	62.0	13.82	59.1	20.42
Cs-137	32.194	88.0	14.42	89.2	21.53
Cd-109	88.034	238.0	25.79	231.5	64.10
Cs–137	661.660	1610.0	117.72	1588.7	124.10
Co-60	1173.237	2807.0	152.97	2779.1	179.78
Co-60	1332.501	3172.0	169.03	3154.3	189.53

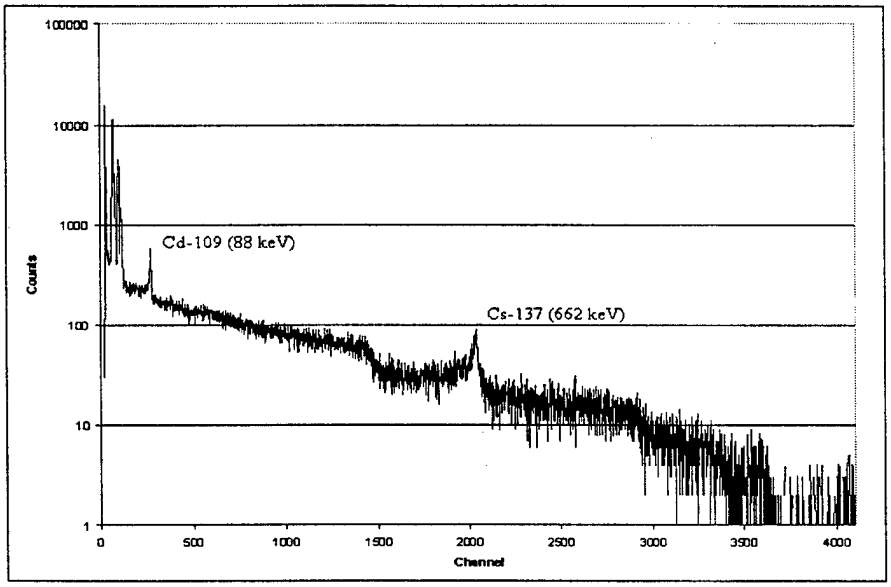

Figure 9 (Multi Source Spectra from the CZT Detector)

Table 3 (Multi Source Peak Centroids and FWHM with the CZT Detector)

Isotope	Key Gamma (keV)	RobWin Peak Centroid (Channel #)	RobWin FWHM (Channel #)	RSEMCA Peak Centroid (Channel #)	RSEMCA FWHM (Channel #)
Cd-109	22.163	69.0	5.63	65.9	6.59
Cd-109	24.900	78.0	3.48	96.7	6.88
Cs-137	36.400	114.0	5.62	111.1	8.19
Cd-109	88.034	272.0	7.20	268.0	13.14
Cs–137	661.660	2034.0	17.20	1976.6	27.54
Co-60	1173.237	3582.0	1.64	3543.1	1.50

The spectra collected from the CZT detector show several low energy peaks not visible in the NaI spectrum. Those peaks are the 22.163 and 24.90 keV gamma rays from Cd-109 and the 32.194 and 34.60 keV gamma rays from Cs-137. It is also shown that the CZT detector's ability to collect counts from gamma rays above 200 keV starts to degrade. The 1173 keV peak of Co-60 is barely visible and the 1333 keV peak is not recognizable.

Characterizing the Detectors

Energy and FWHM Calibration

Both software programs used the key gamma energies associated with each peak to perform a quadratic fit for the energy calibration. This converts the peak centroid (H_o) and FWHM from channel numbers into terms of energy. The equations provided by both software programs for the different detectors are listed below.

1) NaI w/RobWin: $y\ (keV) = (2.853031E\text{-}6)*x^2 + 0.4133294*x - 7.863638$

2) NaI w/RSEMCA: $y\ (keV) = (1.396E\text{-}5)*x^2 + 0.3789*x - 0.9978$

3) CZT w/RobWin: $y\ (keV) = (2.768152E\text{-}6)*x^2 + 0.3214926*x - 0.1301418$

4) CZT w/RSEMCA: $y\ (keV) = (6.824E\text{-}7)*x^2 + 0.3246*x - 0.9927$

Detector Resolution

From this point the detector's resolution (R) at different peak energies was calculated using:

$$R = \frac{FWHM(keV)}{H_0(keV)}, \qquad 2$$

where H_o is the energy at the peak centroid. The equations for energy calibration and FWHM were used for the respective systems in the calculations of the resolutions in Table 4.

Table 4 (Resolution calculations using RobWin and RSEMCA results)

	Key Peak Gamma Energy (keV)	RobWin FWHM (keV)	RobWin Resolution (FWHM/H_o)	RSEMCA FWHM (keV)	RSEMCA Resolution (FWHM/H_o)
NaI Detector	22.16	5.711	0.3213	7.77	0.3631
	32.19	5.960	0.2089	8.21	0.2503
	88.03	10.658	0.1175	24.69	0.2825
	661.66	48.659	0.0732	52.59	0.0821
	1173.24	63.227	0.0538	82.19	0.0709
	1332.50	69.867	0.0525	88.62	0.0665
CZT Detector	22.16	1.844	0.0862	2.14	0.0955
	24.90	1.141	0.0579	2.53	0.0996
	36.40	1.841	0.0509	2.66	0.0717
	88.03	2.358	0.0268	3.05	0.0346
	661.66	5.637	0.0085	9.02	0.0014
	1173.23	0.538	0.0005	0.49	0.0004

Detector Efficiency

Table 5 shows the absolute efficiencies for the different detectors with the different software programs. As expected, the absolute efficiency of the NaI detector is much larger than the CZT. Another observation is that the efficiencies associated with RSEMCA are generally better than the efficiencies associated with Rob Win. This is most likely a result of RobWin eliminating the background before fitting the peaks, so the peaks are generally smaller in counts than the RSEMCA peaks.

Table 5 (Absolute Efficiencies using RobWin and RSEMCA)

	Key Gamma Rays (keV)	Pulses recorded N (counts)	Number emitted S (counts)	Absolute Efficiency N/S
RobWin with NaI Detector	22.16	2709221	20734445	0.130662817
	32.19	1052679	6698894	0.157142209
	88.03	297529	1356003	0.219416181
	661.66	20271708	158352560	0.128016295
	1173.24	4456546	93082220	0.047877522
	1332.50	4141312	93093393	0.044485563
RSEMCA with NaI Detector	22.16	4045183	20734445	0.195094829
	32.19	1034219	6698894	0.15438653
	88.03	386482	1356003	0.285015594
	661.66	17494538	158352560	0.110478403
	1173.24	3037258	93082220	0.032629841
	1332.50	2767257	93093393	0.0297256
RobWin with CZT Detector	22.16	51790	20734445	0.002497776
	24.90	2999	6685732	0.000448567
	36.40	6373	2456261	0.002594594
	88.03	2510	1356003	0.001851028
	661.66	1182	158352560	7.46436E-06
	1173.24	96	93082220	1.03135E-06
RSEMCA with CZT Detector	22.16	55314	20734445	0.002667735
	24.90	-17258	6685732	-0.00258132
	36.40	2983	2456261	0.001214447
	88.03	2646	1356003	0.001951323
	661.66	2920	158352560	1.84399E-05
	1173.24	520	93082220	5.58646E-06

The comparison of absolute efficiency between the two detectors is not a fair comparison. Both detectors collected the spectra under different geometries. To account for those geometries a solid angle approximation is used. With the assumption of point sources, the solid angle for each detector was calculated using

$$\Omega = 2\pi\left(1 - \frac{d}{\sqrt{d^2 + a^2}}\right), \qquad 3$$

with d being the distance from the source to the detector and a being the radius of the detector face.

For the CZT detector, the sources were located directly on the face of the detector. With the source sitting directly on the face of the detector, d = 0 so $\Omega = 2\pi$ regardless of the size of the detector's face. For the NaI detector the sources were located 25 cm from the detector face with a detector radius is 1.5 inch or 3.81 cm. This equates to a solid angle of $\Omega = 0.0717$.

The following equation uses the solid angle to calculate the detector's intrinsic peak efficiency (ε_{ip})

$$\varepsilon_{ip} = N\frac{4\pi}{S\Omega}. \qquad 4$$

Where Ω is the solid angle, N is the number of radiation quanta incident on the detector, and S is the number of radiation quanta emitted by the source. This is a better efficiency to compare detectors because it takes into account the detector geometry. Table 6 uses a portion of the intrinsic efficiency equation to correct the collected pulse count for the different geometries of the CZT and NaI detectors. The NaI collected pulses are significantly higher than those from the CZT detector. If the intrinsic efficiencies were calculated, most of the NaI efficiencies would exceed 100%. The high efficiency is caused by a combination of the good collection efficiency of the NaI detector and the addition of background counts inherent with scintillator detectors.

Table 6 (Solid Angle Geometry Correction)

	Key Gamma Rays (keV)	Pulses Recorded N (counts)	Solid Angle Ω (steradians)	Pulses after Geometry correction N*4π/Ω (counts)
RobWin with NaI Detector	22.16	2709221	0.0717	474585993.9
	32.19	1052679	0.0717	184402346.4
	88.03	297529	0.0717	52119445.47
	661.66	20271708	0.0717	3551083019
	1173.24	4456546	0.0717	780672493.2
	1332.50	4141312	0.0717	725451586.1
RSEMCA with NaI Detector	22.16	4045183	0.0717	708612252.2
	32.19	1034219	0.0717	181168628.2
	88.03	386482	0.0717	67701728.31
	661.66	17494538	0.0717	3064594104
	1173.24	3037258	0.0717	532049658
	1332.50	2767257	0.0717	484752411.7
RobWin with CZT Detector	22.16	51790	6.28	103580
	24.90	2999	6.28	5998
	36.40	6373	6.28	12746
	88.03	2510	6.28	5020
	661.66	1182	6.28	2364
	1173.24	96	6.28	192
RSEMCA with CZT Detector	22.16	55314	6.28	110628
	24.90	-17258	6.28	-34516
	36.40	2983	6.28	5966
	88.03	2646	6.28	5292
	661.66	2920	6.28	5840
	1173.24	520	6.28	1040

Detectors Comparison

Table 2 and Table 3 show that RobWin and RSEMCA process the data differently since both have different centroid locations and FWHM values. Figure 10 shows a comparison of the multisource spectra collected using the CZT and NaI detectors. The NaI detector collected clearly defined peaks with large peak counts. The CZT detector had better resolution, but significantly lower counts at higher energies. Figure 11 expands the lower energy range where the CZT detector appears to perform better. The

CZT detector's better resolution resulted in the observation of additional peaks for Cd-109 and Cs-137. This proved to be an advantage to characterizing the detectors by adding additional peaks to fit the energy calibration. The NaI detector's poor resolution could not resolve these peaks. However, the NaI detector offers a much larger counting efficiency and better gamma ray detection at higher energy levels than the CZT detector.

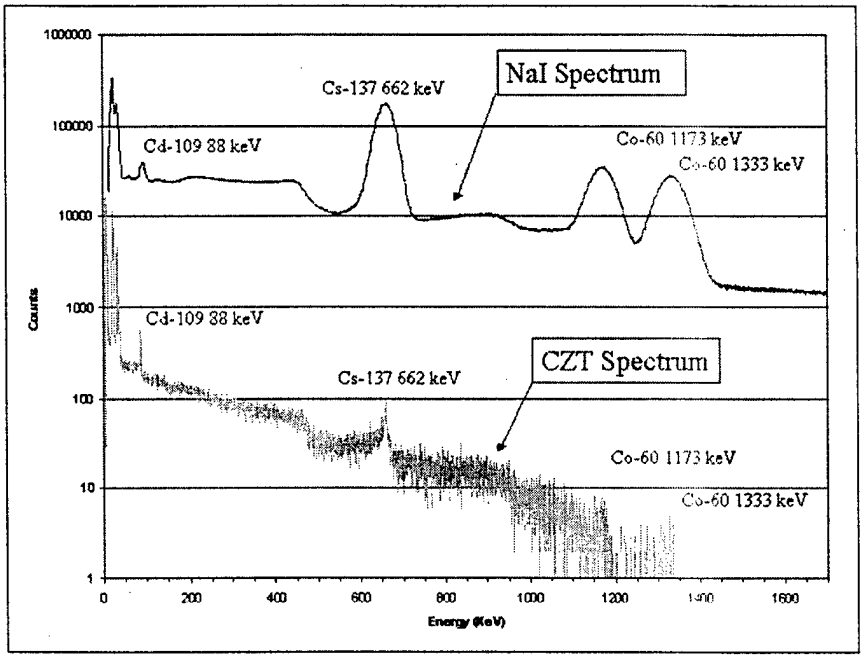

Figure 10 (Multi Source Spectra Comparison)

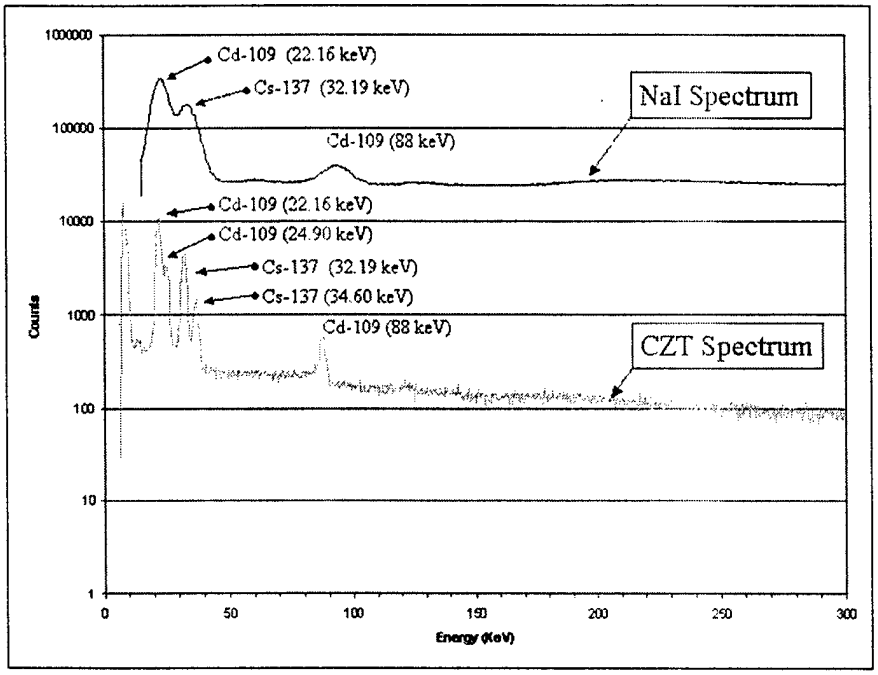

Figure 11 (Lower Energy Multi Source Spectra Comparison)

Due to the small collection surface (5 mm x 5 mm square) of the CZT detector compared to the collection surface (3 inch circular) of the NaI detector, the counts collected per channel are significantly lower. Figure 12 compares the NaI detector to the CZT detector spectra normalized to 1 mm^2 surface area. Again, the figure shows that the CZT detector's collection capability starts to degrade for energies above 200 keV. However, Figure 13 shows that the CZT detector is actually more efficient than the NaI detector per mm^2 below the 200 keV range. If money is not an issue, the lower count rate of the CZT detector can be corrected by using more CZT detectors in unison so that the total combined surface area of the CZT detectors is equivalent to the surface area of the NaI detector.

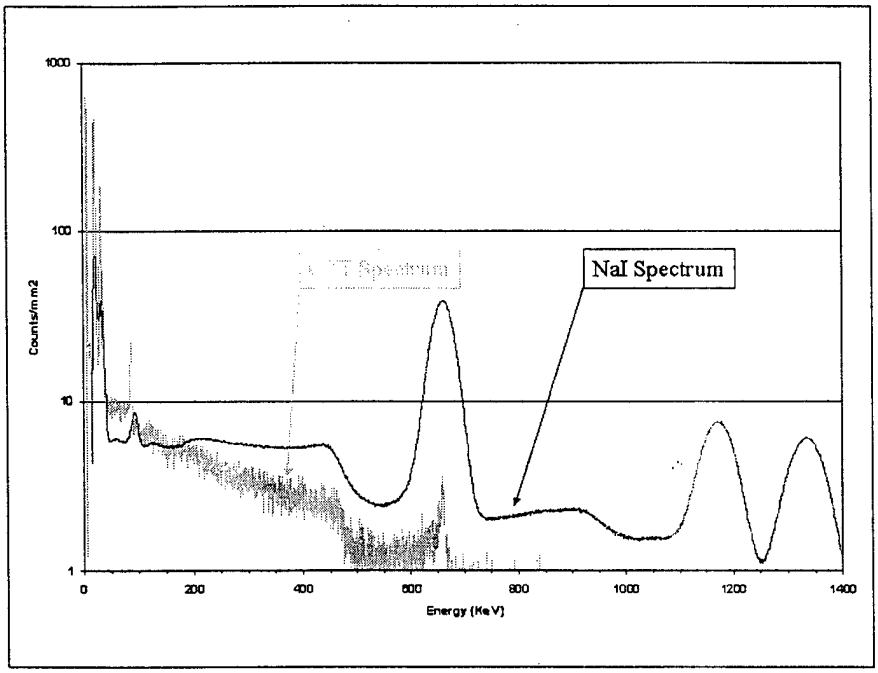

Figure 12 (Normalized CZT and NaI Spectra)

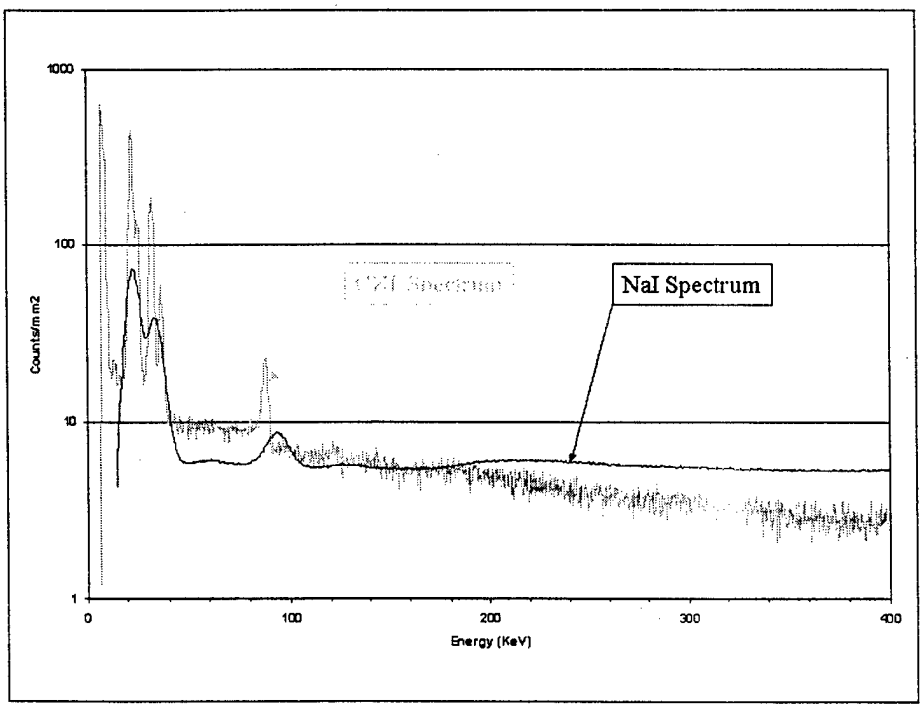

Figure 13 (Low Energy Normalized CZT and NaI Spectra)

Characterize the Pu-239 Source

Efforts to characterize AFIT's Pu-239 source and use it to model a stored weapon failed because of detector limitations. Figure 14 displays the spectra of the Pu-239 source collected by the CZT and NaI detector. The NaI detector lacked the resolution necessary to characterize the source and distinguish between WGPU and RGPu. The CZT detector was not capable of collecting counts at higher energy ranges to identify WGPu.

The makers of the CZT detector, eV Products, were contacted to see if anything could be done to improve the collection range of the CZT detector beyond 200 keV. eV Products recommended changing the pulse shaping time from 0.5 μs to 2.0 μs, dropping the conventional gain channels from 4096 to 512, and increasing the bias voltage from 504 V to 800 V. This was done and the results are in Figure 15. The spectrum collected using the recommended changes provides slightly better resolution at higher energies, but the tradeoff was a loss of resolution at the lower energy ranges. The newer spectrum cannot resolve the multiple peaks in the 98 keV and the 129 keV regions. Reducing the conventional gain from 4096 to 512 channels resulted in more counts per channel. With only 512 energy bins, the range of energies within the bin increases and more interactions are recorded per channel. This new spectrum offers no advantage because it still does not collect sufficient counts to form peaks in the 640 keV region.

Neither detector was capable of sufficiently characterizing AFIT's Pu-239 source and determining the grade of plutonium. Appendix F contains the analysis attempts to characterize the Pu-239 source. The detector limitations also affect the ability to model a

stored nuclear weapon because neither detector was capable of testing the model for accuracy.

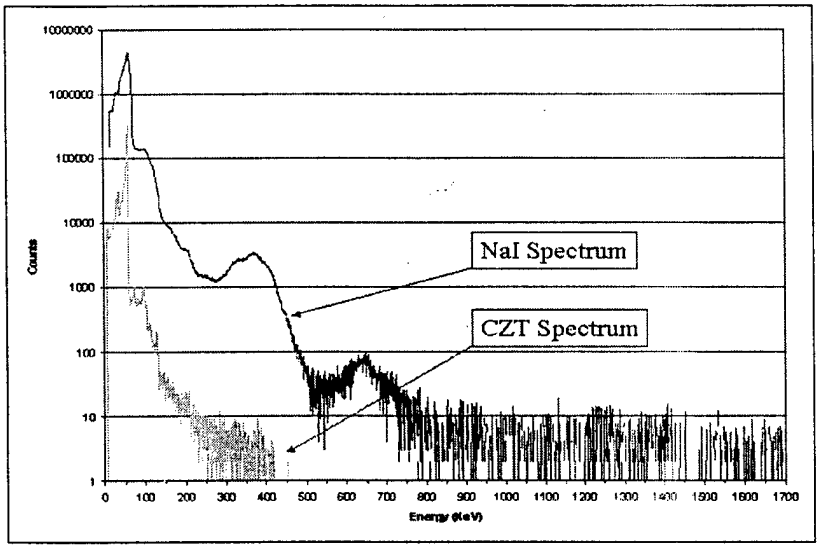

Figure 14 (Pu-239 Spectra Comparison)

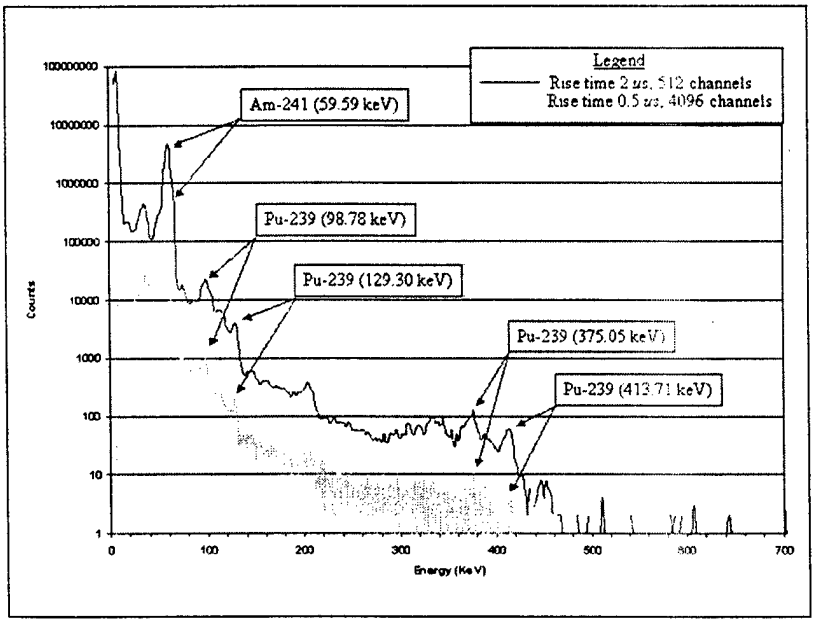

Figure 15 (CZT Detection Comparison)

Software Comparison

Quantitative Analysis.

Peaks Identified

RobWin and RSEMCA performed differently in peak detection. RobWin performed much better than RSEMCA. RobWin does not execute a peak search like most spectral analysis programs. To run RobWin, the operator identifies several regions of interest to initiate an energy calibration. The next step fits the continuum. After fitting the continuum, the operator identifies nuclides to search for. RobWin then uses the fits, the nuclides of interest and attempts to locate peaks for the nuclides of interest in the areas above the continuum. This was a significant advantage in trying to locate peaks and to adjust the energy calibration.

RSEMCA initiates its analysis with a peak search. The peak search may fail if tolerances are not within the search parameters. Figure 16 shows how RSEMCA identified a region with 4 peaks as an individual peak (shade area). This was corrected using ROIs set by the operator. A more significant problem was identified for areas with joint peaks such as in the region of the 22.16 and 24.90 keV peaks of Cd-109 in Figure 11 or the 639.99 and 642.35 keV peaks in Figure 38. In both cases, RSEMCA reported negative peak counts for the lower peak. RSEMCA calculates the net counts in a peak by subtracting a background count outside of the Gaussian fitted peak from the counts within the ROI. Because this occurs when two peaks are joined, it is possible that the background counts outside the Gaussian fit may include counts from the adjoining peak resulting in a total background count larger than the counts within the ROI. The designer of RSEMCA has been notified of this problem.

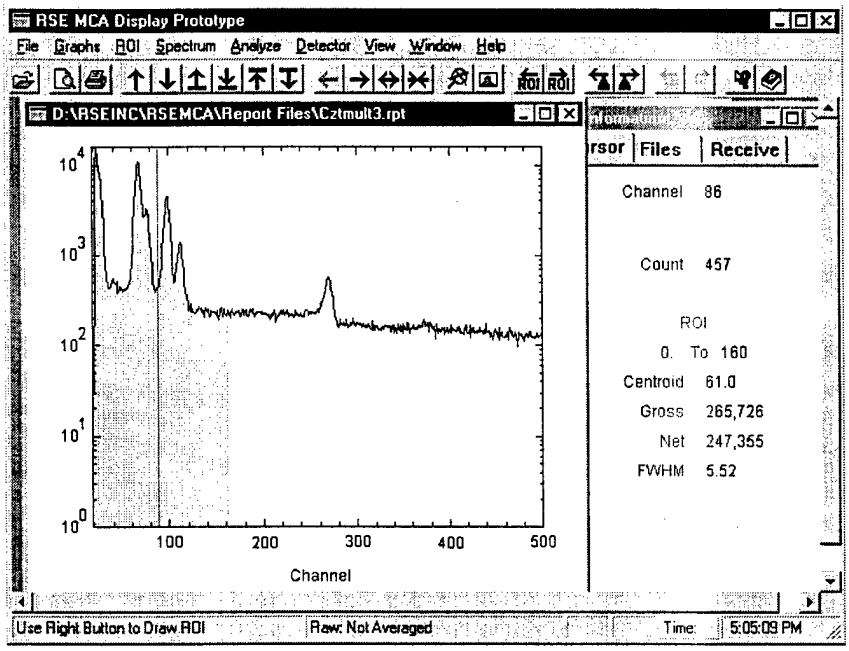

Figure 16 (RSEMCA Peak Search)

Energy calibration.

Both RobWin and RSEMCA performed similarly when calculating an energy calibration. RSEMCA made the effort a little more challenging because of a limited library, but this is addressed later in this study. Table 7 and Table 8 display the results of the energy calibration and how both programs compare to the standards from Brookhaven National Labs. RobWin results have an average percent difference of 0.011 with a standard deviation of 0.013. RSEMCA results produced an average percent difference of 0.014 with a standard deviation of 0.010. Both programs produced results within 1 to 2% of the National Standard.

Table 7 (RobWin Energy Calibration Accuracy)

	Isotope	Brookhaven National Laboratory Standards	RobWin Calibrated Results	Percent Difference
CZT Results	Cd-109	22.16	21.404	0.0343
	Cd-109	24.90	24.353	0.0212
	Cs-137	36.40	36.149	0.0069
	Cd-109	88.03	87.922	0.0013
	Cs-137	661.66	665.286	0.0055
	Co-60	1173.24	1171.220	0.0017
NaI Results	Cd-109	88.03	90.670	0.0299
	Cs-137	661.66	664.992	0.0050
	Co-60	1173.24	1174.830	0.0014
	Co-60	1332.50	1331.920	0.0004

Table 8 (RSEMCA Energy Calibration Accuracy)

	Isotope	Brookhaven National Laboratory Standards	RSEMCA Calibrated Results	Percent Difference
CZT Results	Cd-109	22.16	22.4	0.0107
	Cd-109	24.90	25.4	0.0201
	Cs-137	36.40	37.1	0.0192
	Cd-109	88.03	88.2	0.0019
	Cs-137	661.66	645.2	0.0249
	Co-60	1173.24	1159.6	0.0116
NaI Results	Cd-109	88.03	87.4	0.0072
	Cs-137	661.66	640.3	0.0323
	Co-60	1173.24	1159.8	0.0115
	Co-60	1332.50	1333.1	0.0005

Energy Resolution

Both RobWin and RSEMCA performed similarly when calculating the energy resolutions for the gamma ray energies. Table 4 contains the resolution calculations for RobWin and RSEMCA with both the CZT detector and the NaI detector. Both software programs produce similar results. In general, RobWin's calculated resolutions were slightly lower than RSEMCA's calculated resolutions. This may be attributed to the way each program fit the spectrum. By fitting the continuum first and eliminating the

background, RobWin may produce a thinner peak. RSEMCA fits the peak first with the background still present. Extra counts from the background may be part of the peak fit producing a wider peak.

Efficiency Calculation.

Overall, RSEMCA offers an advantage over RobWin when calculating efficiency by allowing the operator to enter certificate file information on the source of interest. It then uses the certificate to update the activity of the source every time efficiency is calculated. This provides the user with an absolute detector efficiency.

At the start of this analysis, RSEMCA had an error associated with the efficiency calculations that caused a general protective fault and terminated the program. Upon further inspection, it was found that RSEMCA had a Y2K problem associated with the activity calculations. The software developer was notified of this fault, corrections to the software were made, and a newer version was provided, that fixed the Y2K problem.

RSEMCA could improve the certificate file. The certificate file requests the initial source activity in units of counts/sec. Most sources are listed in units of Curies. The software should allow for activity in curies, or provide an option to enter either unit.

At no time did RobWin require the initial source activity. RobWin calculates a relative efficiency describing the relative likelihood that a gamma ray will deposit all of its energy in a particular detector. This efficiency is calculated during the analysis of data by using information from the tables of the relative strengths of nuclides in the spectrum. Because it is impossible to tell from the spectrum alone what the absolute activity of the sources was, the efficiency can only be determined as a relative function of the nuclides present.

Quantitative Decision Matrix

A decision matrix was used to tally the results of the quantitative analyses. Weighting of any factor was not used for the quantitative areas. Each area was essential in characterizing detectors and source identification. Program attributes were graded by better (+), neutral (0), or worse (-).

Table 9 shows that both software analysis programs quantitatively perform similarly. This comparison assumes that RSEMCA's negative count rate error will be corrected. Should this not be possible then RSEMCA fails the quantitative analysis.

Table 9 (Quantitative Decision Matrix)

Decision Matrix		
	RobWin	RSEMCA
Peak Search	+	-
Energy Calibration	0	0
Resolution Calculations	0	0
Efficiency Calculations	-	+
Total	**0**	**0**

Qualitative Analysis.

The software programs were also compared based on qualitative features that affect ease of use. The qualitative features are: installation, instruction manuals/help menus, examples, input files, operating the software, software graphics, library files, output results, and developer's responsiveness.

Installation.

Each software program was installed onto three Pentium II computer systems with Windows 95 and 98 operating systems. Two of the computers used were part of a

network, one of the networked computers used Windows 95 and the other networked system used Windows 98. The third computer was a stand-alone system using Windows 98. RobWin proved to be much simpler to install than RSEMCA.

RSEMCA is a Windows based system that uses standard Windows installation files. RSEMCA was loaded on the 3 different computers, but the software would not operate on the two networked systems. The developers recommended checking the registry and removing a registry file titled, "HKEY_CURRENT_USER/Software/RSE" if the file existed. This corrected the problem. This software did not come with installation instructions. The instruction manual needs to include installation instruction, warnings of potential errors, and how to correct the errors.

RobWin was provided through an internet download and came with installation instructions and a password. RobWin downloads into a separate folder with no Windows installation required. The program can be transported to other computers by simply copying the files. To remove RobWin from a computer is just a matter of deleting the files. This also allows RobWin to be transported around on a zip disk for use on different computer systems. RobWin can operate from the zip disk or quickly copied on to a computer hard drive.

Instruction Manual/Help Menu.

This area addressed the instruction manual and help menus provided for each software program. Both software programs offer a pull down help menu very similar in style and amount of assistance offered. RSEMCA offers an advantage with the printed instruction manual and the ability to print sections or the entire manual from the help menu. This is beneficial to a new user since it can be very burdensome switching back

and forth between a help screen and the software program while trying to learn how to use the software program. RobWin did not come with a printed instruction manual and to print anything from the help menu was a page-by-page process. For example, the example problem was listed on fifteen pages, each page had to be opened separately to print a hard copy of the example. An option to print the entire help menu, a section of the help menu, or an individual page offers more flexibility to the user.

Examples.

The Example section refers to instructional examples provided by the developer to assist the user in learning how to use the software. RobWin provides an excellent example that walks the operator through an example problem and covers the majority of RobWin's capabilities. RobWin's example uses a multisource spectrum and includes establishing ROIs, fitting the continuum, identifying known peaks, conducting a peak search, changing screen views, conducting an energy calibration, etc.... RSEMCA provides a very limited example using a Ba spectrum. The example demonstrates a peak search, defining ROIs, and producing an energy calibration for the spectrum. The example barely demonstrates the many capabilities of the software.

RSEMCA needs to develop a better example to help instruct operators how to use the full capabilities of the software. Additionally, both developers need to add an example using an unknown source to assist the operator with how to use the software to analyze an unknown spectrum.

Input Files.

Input file operations proved difficult. RobWin and RSEMCA have the capability to collect spectra, but require hardware specific to their respective developers, which was

not provided. Both programs use developer specific file formats to store collected spectra. RSEMCA files are tagged *.rse and RobWin uses *.sp. Since RobWin and RSEMCA could not collect the spectra, Canberra Genie 2000 software with a Canberra MCA and AIM were used to interface between the detectors and computer. Then, the collected spectra were adjusted to meet input file formats required by RSEMCA and RobWin.

Genie 2000 stores the collected spectrum in *.cnf files, which are binary files holding all the information about the spectrum. From *.cnf file, numerous reports can be generated that provide different displays of the data. Genie generates a report file (*.rpt), which is located in the "Rptfile" folder inside the "Genie2K" folder. The file is automatically given the same prefix name as the *.cnf file. For example, CZTCd109.cnf would create the report file CZTCd109.rpt. Each time a report is generated, it overwrites any previous report file from the *.cnf file.

RSEMCA is capable of reading several different report formats to include the Canberra report file (*.rpt), but the Canberra report must be in a specific format. Unfortunately, the format required by RSEMCA is not a generic report offered by Genie. This required writing new report commands for Genie 2000 to produce the proper format. Two reports were written for Genie and copies are provided in Appendix J.

The "Data2.tpl" file generates a report that contains only the channel numbers and respective counts per channel. RSEMCA could open and read this file, but errors occurred during detector efficiency calculations causing RSEMCA to terminate the program. The error occurred because the report did not pass the date and time the spectrum was collected. RSEMCA needs the date and time of the collected spectrum to

determine the current activity of the source. The only way to input this information is through the report file.

"Data.tpl" generates a *.rpt file which passes a header section containing the collection time and a data section with only the counts per channel. This corrected the problem with RSEMCA and allowed for a complete analysis.

RobWin proved to be much more accepting of input files. RobWin reads the Genie 2000 *.cnf files. The *.cnf file is the base data file and does not change after the spectrum is collected. The *.cnf file is better to use since it does not change, while the report format can take on a variety of formats. RobWin requires 16384 channels of data passed even when the conventional gain is set to lower channel collections of 512, 1024, 2048, 4096, or 8192.

RobWin performed much better than RSEMCA at accepting input files from Genie, whereas RSEMCA required a great deal of manipulation to get the proper format. Examples of the report formats should be included in the instruction manual for both programs to eliminate the guesswork for converting input files. Both programs have at least one spectrum file in their library of the different formats, which was the only way for the operator to determine the proper file format. Additionally, DTRA should specify in the contract requirements specific report formats required.

Operating the Software.

The term "Operating the Software" pertains to the operator's ability to use the software without fatal errors or reboots. RobWin performed much better than RSEMCA in this comparison. RSEMCA is not forgiving to the inexperienced operator. When an operator attempts a task not required or in the wrong sequence, an error results. This

error presents a window stating, "You have performed an Illegal Operation" and only offers the operator the option to close the program without being able to save any results. While learning how to use this program, it required numerous restarts of the software. This was very frustrating having to continually restart the software. It is recommended that the developer edit the software to return the operator to the previous step with a warning message, or at a minimum provide a save option before shutting down.

RSEMCA also had a Y2K problem that was identified when trying to input data. RSEMCA uses the date the source was activated and the date the spectrum was collected to calculate the current activity of the source. The program only read the last two digits of the year, for example 2000 was read as 00. This resulted in a fatal error and terminated the program. The developer was notified, rewrote the program, and provided an improved version for use. This eliminated the Y2K problem and allowed the analysis to continue.

RobWin is much friendlier to the operator. When an operator attempts an improper task, the software presents a window stating, "That operation is not available with version 1.0" and allows the operator to return to the main screen and try something different. One drawback with RobWin is when the window is adjusted, the analysis fit of the peaks and continuum disappear from the display. This is easily returned to the screen by selecting "Plot Fits" and the analysis plot fit quickly reappears. Although this does not affect the analysis, it can become monotonous when looking at multiple peaks in a small region that requires zooming in and out and having to reapply the fit for each change of the viewing window.

Software Graphics.

This topic refers to the visual graphics presented by the program. Both software programs allow the operator to adjust color schemes to the user's personal preference and offer setup options to adjust the displays.

RSEMCA displays the graphics on several windows within the software program as shown in Figure 17. There can be as many as 5 windows open at once. Those windows are: the spectrum plot, the information window that displays the cursor location and ROI information, the report window, a calibration plot, and a calibration window. This can become very busy and confusing for the operator because of the many open windows. In addition, the size of the windows affects the operator's ability to view the data displayed. Figure 18 shows several of the windows with incorrect sizing. The window tab allows the operator the ability to organize the windows, but the automatic sizing results in poor data displays.

RobWin offers two windows, one for the graphic shown in Figure 19 and the other for the report window shown in Figure 20. The operator has the ability to toggle between the graphics window and a report window. RobWin offers a better quality graphic display that does not require organizing multiple windows and adjusting poorly sized.

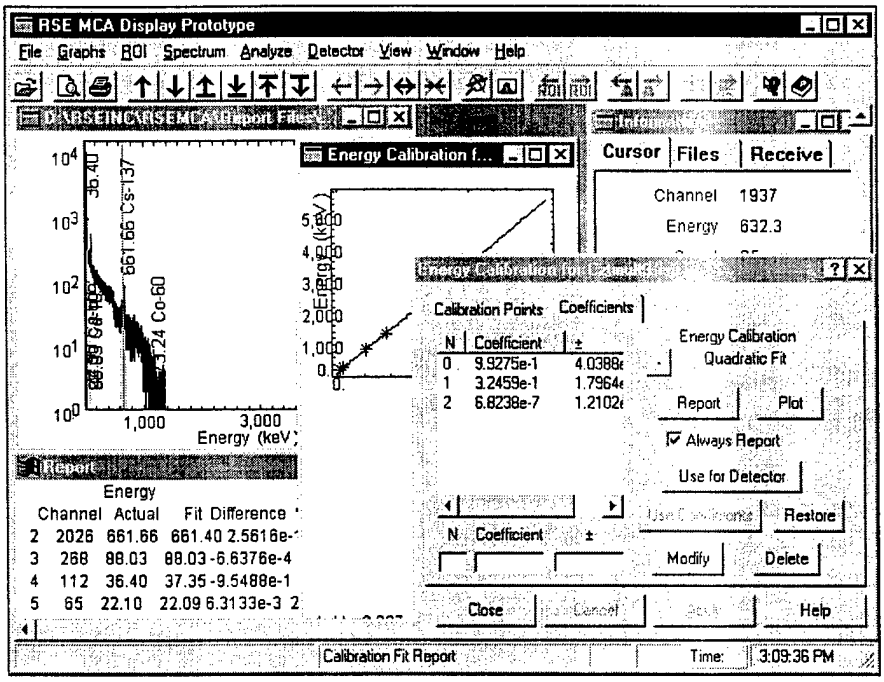

Figure 17(RSEMCA Active Windows)

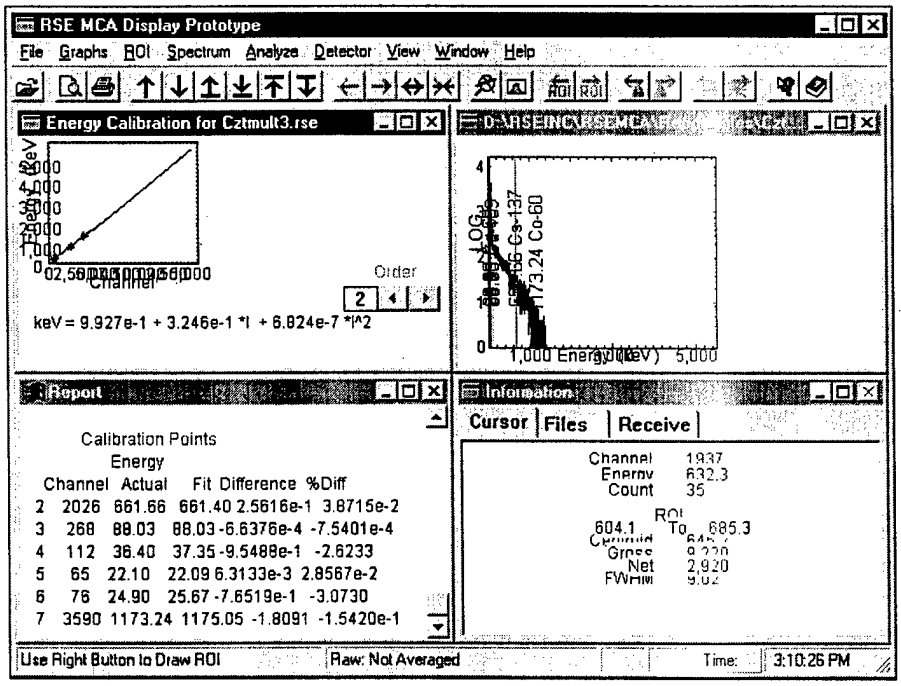

Figure 18(RSEMCA Window Size Problems)

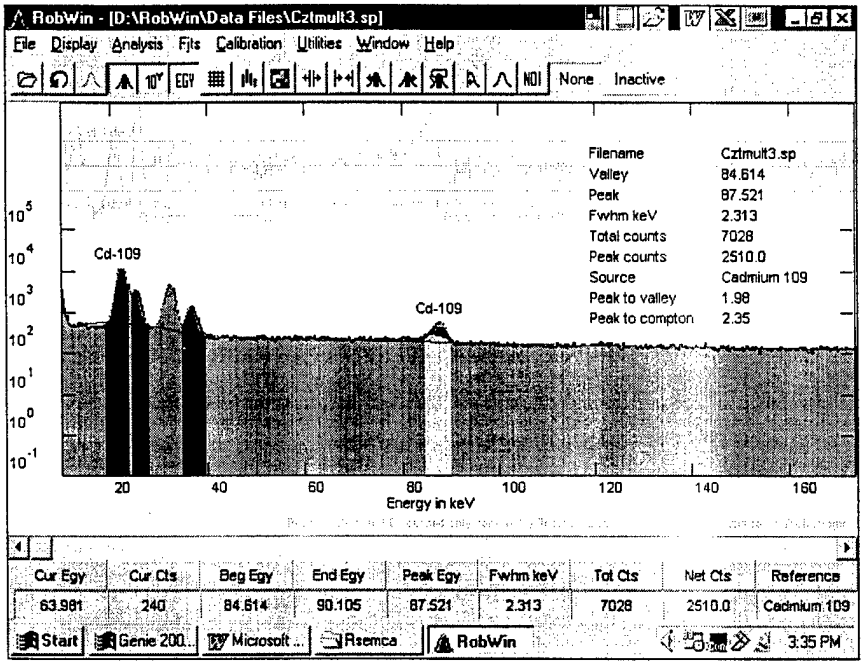

Figure 19(RobWin Window)

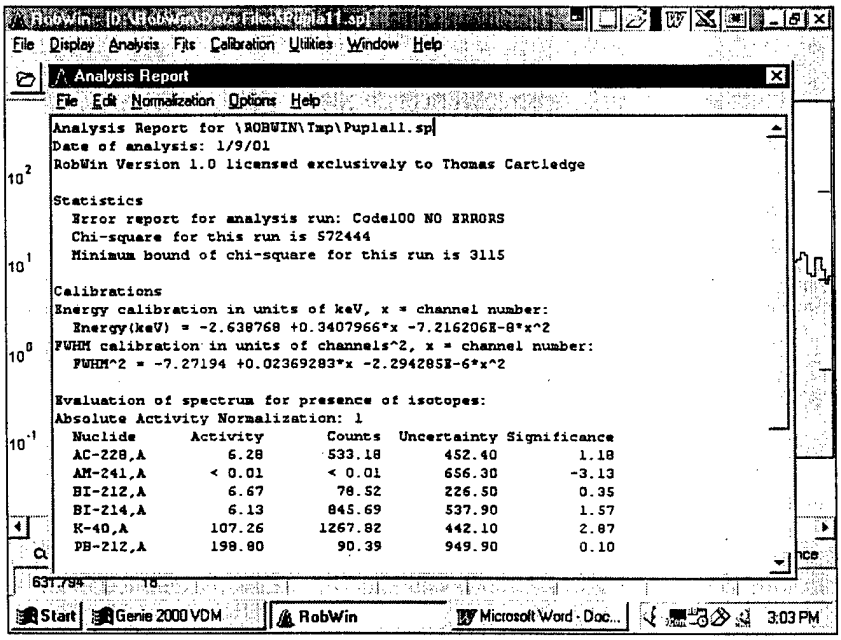

Figure 20 (RobWin Report Window)

Library Files.

Both programs claim to use Brookhaven National Labs as the reference source for their master library files for gamma ray energies. Despite using the same source, RobWin offers a more extensive library of data for the nuclides than RSEMCA. RobWin uses Brookhaven National Labs, but also incorporates data from the "Shirley" tables, which are maintained by Berkeley.

RSEMCA's limited library interferes with the software's ability to perform energy calibrations and calculate the detector efficiency. This occurs because RSEMCA's library files do not include the complete list of key gammas from the nuclides. For instance, only the 88.034 keV gamma ray for Cd-109 was available and no information was available for the 21.99, 22.16 and 24.90 keV gamma rays, also part of Cd-109 decay. This was also the case for Cs-137 where only the 661 keV gamma ray was available, even though it has 31.82, 32.19, and 36.4 keV gamma rays. These lesser peaks were visible, but associated energy peaks could not be assigned to the peaks and used as part of the energy calibration. Without these lower energy data points, the energy calibration was skewed slightly to the right (higher energy).

The operator has to manually enter the ROIs with associated energies to correct the energy calibration. It becomes more of a problem with the efficiency calculations. The software calculates the efficiency for the identified peaks. The problem exists because RSEMCA cannot associate peak identifications for the lower energy peaks of Cd-109 and Cs-137. RSEMCA must have an associated energy peak in the library to calculate the efficiency. This reduces the number of data points to fit the efficiency calculations. The software did not provide a method to correct this problem. The

multisource was limited to three data points, which makes it impossible to determine how well the energy calibration and efficiency fit the results. Ideally, seven points are needed for a quadratic fit.

RSEMCA also has several special library files, but the names for several are confusing. One library file is titled "Pu-239" and contains data for AM241, Pu-239, Pu-240, Pu241, and Pu-242. Another library file is titled "Pu" but does not contain Pu-239, Pu-240, Pu-241, and Pu-242. These titles should be renamed to eliminate confusion.

Printing Results.

Overall, both programs produce similar printed products. RSEMCA provides an option to print the results from each active window by going to the File Tab and toggling "Print Active Window." These windows include the spectrum plots, the calibration plots, and the report window. Figure 21 shows a spectrum plots with energy peaks identified. Notice the isotope's name and energy are listed for each peak identified. The software automatically places the name and energy on the plot. Sometimes the name and energy go above the peak and can exceed the borders of the plot. There are other times that the name and energy are placed below the peak and will not appear on the printed results because of color schemes. These graphics are sized poorly and the quality is unsuitable for presentation purposes. Figure 22 shows a calibration plot and Figure 23 shows a report file. Both are of acceptable quality.

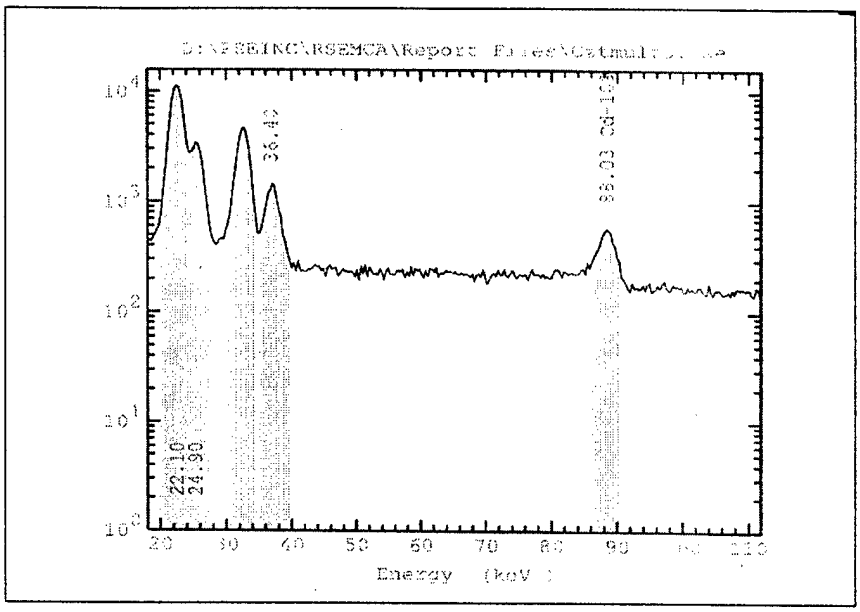

Figure 21 (RSEMCA Spectrum Plot)

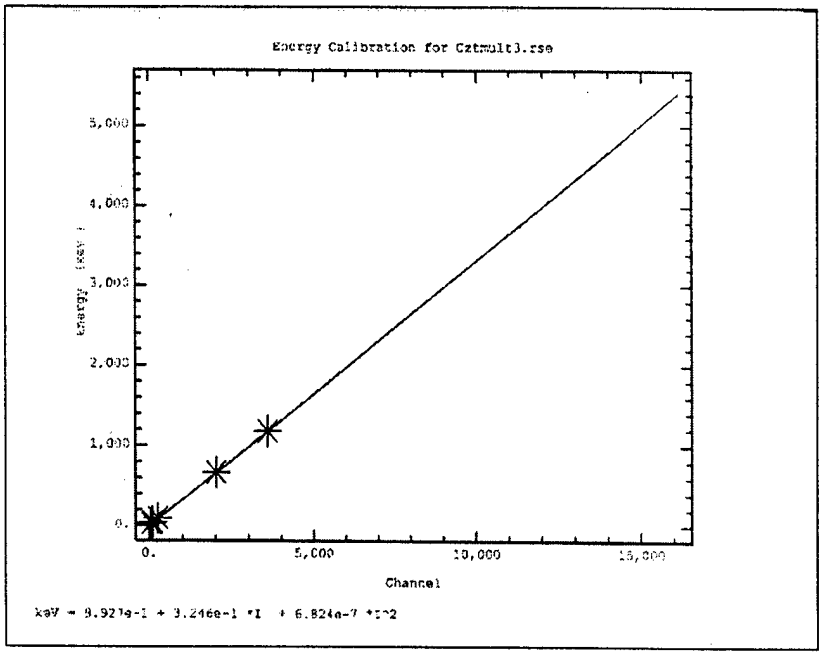

Figure 22 (RSEMCA Calibration Plot)

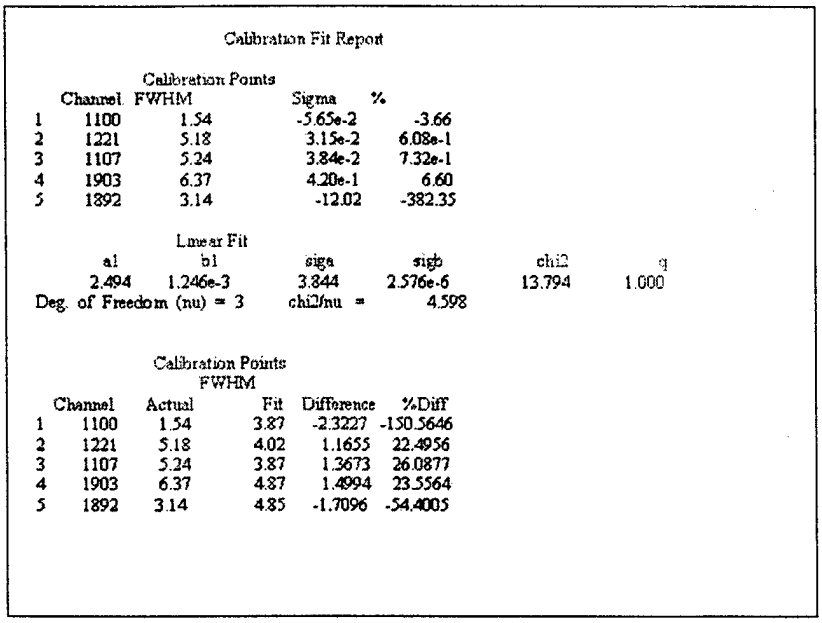

Calibration Fit Report

Calibration Points

	Channel	FWHM	Sigma	%
1	1100	1.54	-5.65e-2	-3.66
2	1221	5.18	3.15e-2	6.08e-1
3	1107	5.24	3.84e-2	7.32e-1
4	1903	6.37	4.20e-1	6.60
5	1892	3.14	-12.02	-382.35

Linear Fit

a1	b1	siga	sigb	chi2	q
2.494	1.246e-3	3.844	2.576e-6	13.794	1.000

Deg. of Freedom (nu) = 3 chi2/nu = 4.598

Calibration Points FWHM

	Channel	Actual	Fit	Difference	%Diff
1	1100	1.54	3.87	-2.3227	-150.5646
2	1221	5.18	4.02	1.1655	22.4956
3	1107	5.24	3.87	1.3673	26.0877
4	1903	6.37	4.87	1.4994	23.5564
5	1892	3.14	4.85	-1.7096	-54.4005

Figure 23 (RSEMCA Report Output)

RobWin is somewhat limited in printing because it does not allow the operator to print directly. To print plots, the operator uses the display pull down tab and "Copy Display to Message Board." Then the operator can paste the results into another suitable program to print. Figure 24 and Figure 25 show examples of this output product. The operator can print the reports upon request similar to Figure 26. All prints from RobWin are of acceptable quality.

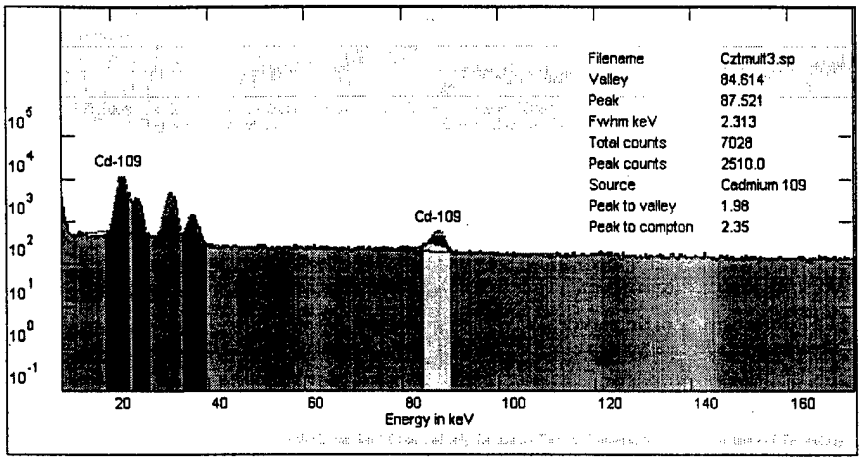

Figure 24(RobWin Spectrum Plot Output)

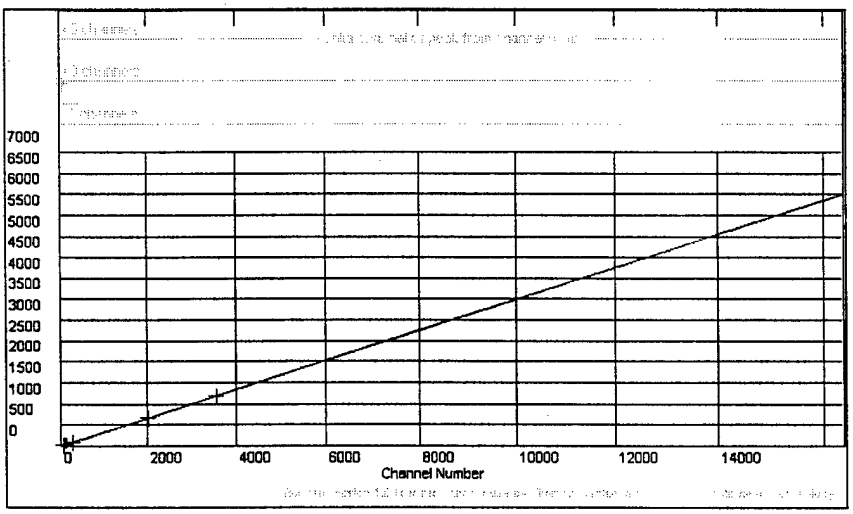

Figure 25(RobWin Calibration Plot Output)

Decision Matrix

A decision matrix was used to summarize the qualitative analysis of the two software programs. Since DTRA does not know how each of these programs will be employed, no weighting was used. Although the quantitative analysis did not reveal major differences between RobWin and RSEMC, the qualitative analysis shows a greater difference in the software programs. Table 10 shows that RobWin operated significantly better than RSEMCA in most of the evaluated areas.

Table 10 (Qualitative Decision Matrix)

Decision Matrix		
	RobWin	RSEMCA
Installation	+	-
Instruction Manual/Help Menu	-	+
Examples	+	-
Input Files	+	-
Operating the software	+	-
Software Graphics	+	-
Library	+	-
Printing Results	0	0
Owner Response	0	0
Total	**+5**	**-5**

Software's Capability to Detect WGPu

Most nuclear weapons and nuclear weapon materials are stored within shielded containers or delivery systems. Due to the shielding, gamma ray energies below 200 keV cannot be detected. START II prohibits the removing material from the container during inspections; so consequently, the peaks between 200 keV and 800 keV are relevant for analysis. Owing to this, DOE has identified the 642 keV gamma ray for Pu-240 and the

645 keV gamma ray for Pu-239 critical for WGPu identification and verification purposes [16].

The detectors used for verification must have sufficient efficiency and resolution in the 640 keV region. As shown previously, the NaI detector lacked the resolution to show key energy peaks for Pu-239 and Pu-240. The CZT may have the resolution to distinguish between the critical peaks, but the detector's efficiency severely degrades above 200 keV. At this time, neither detector used in this thesis is capable of supporting the weapon verification program.

George Lasche of Constellation Technology provided a spectrum from a 400 gram WGPu source collected using a HPGe detector. The spectrum was collected with a real time of 368.36 seconds and a live time of 300.68 seconds over 8192 channels. This file was used to test the software's ability to identify WGPu.

RobWin Results

RobWin performed very well in identifying the WGPu source. Two initial peaks of 375.054 keV and 413.713 keV were identified and the continuum was fitted. Once this was done, a nuclide search was conducted. Since the search was for WGPu, the isotopes to search for were: Pu-239, Pu-240, Pu-241, Pu-242 and Am 241. It is best to include all the likely isotopes in the nuclide search so RobWin can account for the different gamma rays in the analysis. The results of the initial nuclide search are shown in Figure 27. 28 knots were used to fit the continuum. The operator must use caution in the number of knots used to fit the continuum. Too many knots will cause the continuum fit to start fitting the peaks.

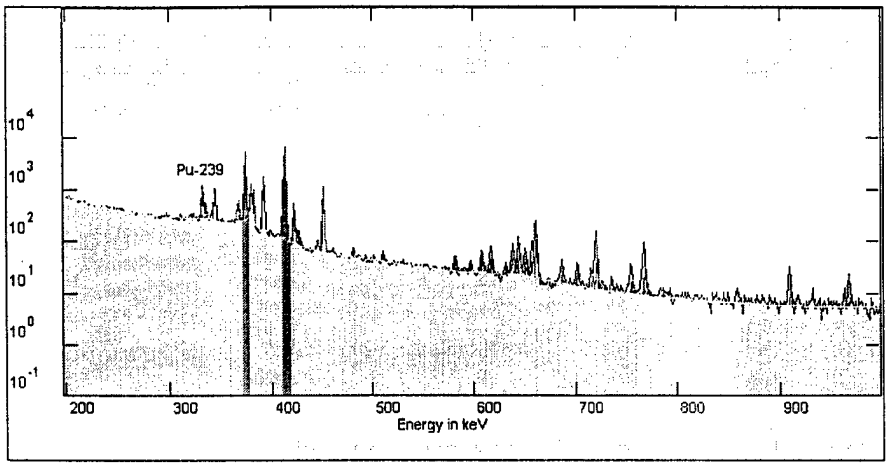

Figure 27 (RobWin Initial Search)

The initial nuclide search provided a very crude calibration for the spectrum. Upon expanding the window in the 635-665 keV range (Figure 28), it was obvious that the fitted continuum and peaks were slightly higher in energy than the actual spectrum.

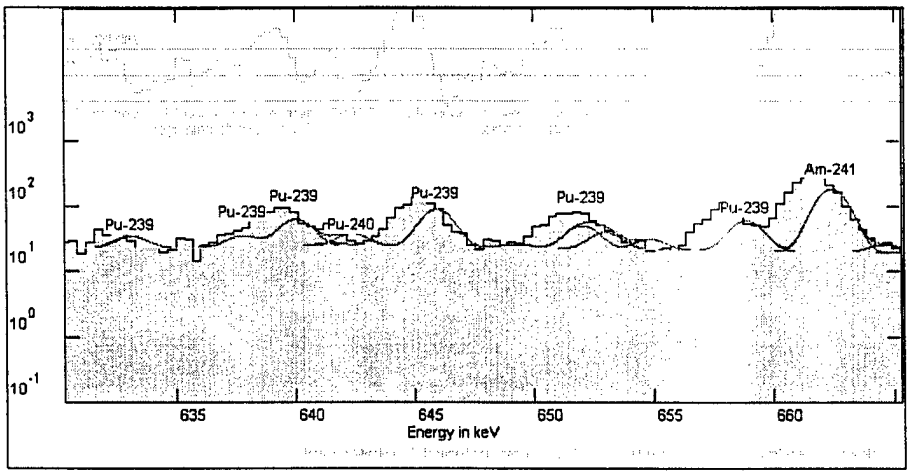

Figure 28 (RobWin Initial Continuum and Peak Fit)

To correct this difference, the energy peaks for Pu-239 at 645.940 keV and for Am241 at 662.400 keV were added to the energy calibration. This adjustment was

sufficient to align the spectruum with the fitted continuum and peaks as shown in Figure 29. This fit clearly identified the Pu-240 peak at 642.350 and Pu-239 peak at 645.940.

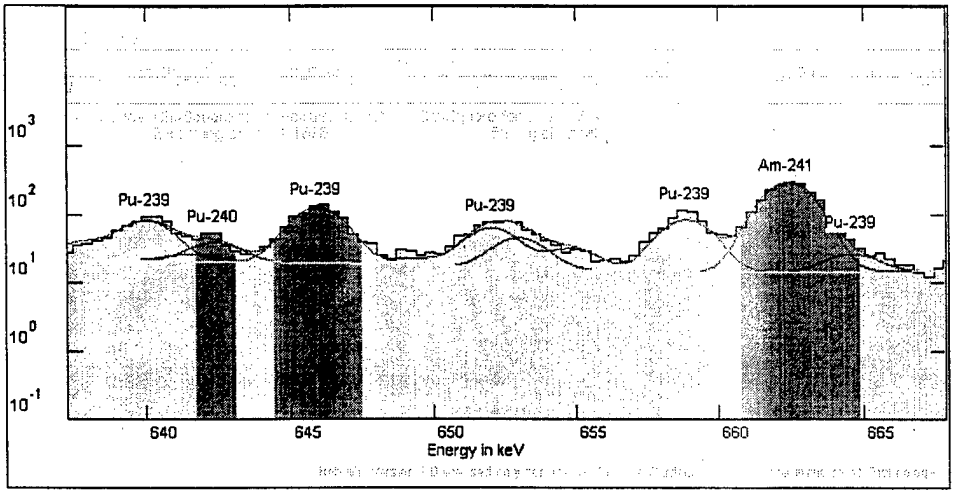

Figure 29 (Improved RobWin Continuum and Peak Fit)

The energy and FWHM calibration generated by RobWin were:

$$Y\ (keV) = 1.436837E\text{-}8*x^2 + 0.3402688*x - 1.795263$$

$$FWHM^2 = 30.53346 - 0.004895885*x$$

Figure 30 and Figure 31 show the spectrum and key peaks identified by RobWin . With the detector efficiency known at these energies, it is possible to determine a mass percent for Pu-239 and Pu-240. It is also possible to use the peak counts for Pu-239 and Pu-240 to calculate a mass percent and determine if the spectrum was from WGPu. Table 11 contains the calculation of the mass percent which show approximately 94% Pu-239 and 4% Pu-240, confirming that the spectrum was WGPu.

Table 11 (WGPu Mass Percent Calculation)

	Pu-239 (645 keV peak)	Pu-240 (642 keV peak)
Counts per peak	448	32
Total counts using % occurrence	448/0.0000002 = 2.24E+9	32/0.0000001 = 3.20E+8
Counts/sec using collection time	2.24E+9 counts/368 se = 6.09E+6 Bq	3.20E+8 counts/368 se = 8.70E+5 Bq
Mass using inverse of isotope decays/gram	6.09E+6 Bq/2.30E+9 Bq/gr = 2.65E-3 gr	8.70E+5 Bq/8.43E+9 Bq/gr = 1.03E-4 gr
Mass percent	2.65E-3/(2.65E-3 + 1.03E-4) = 0.962	1.03E-4/(2.65E-3 + 1.03E-4) = 0.038

A quantity approximation is possible using absolute efficiencies, but may not be reliable. A good shield will reduce the counts detected resulting in a lower quantity calculation. Adjustments for the absolute efficiency will not counter the effects of shielding. Without knowing the composition and geometry of the shielding, a reliable quantity cannot be derived from the spectrum.

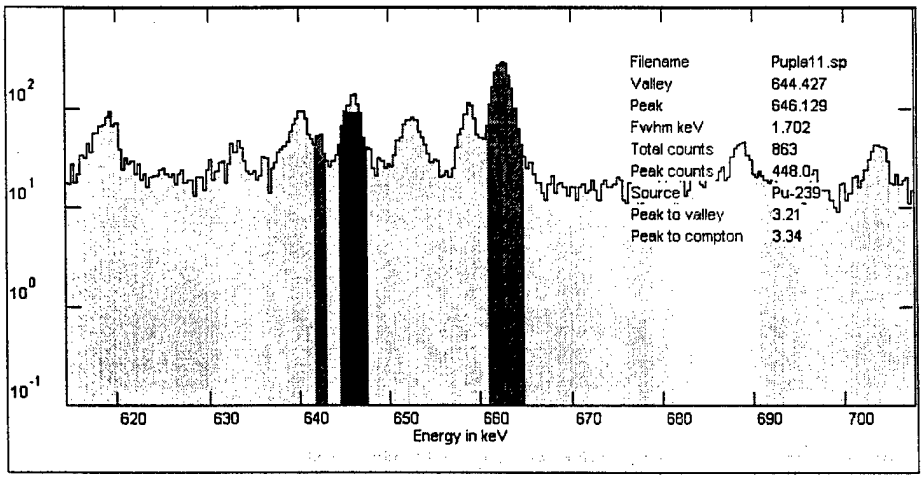

Figure 30 (645 keV Peak for Pu-239)

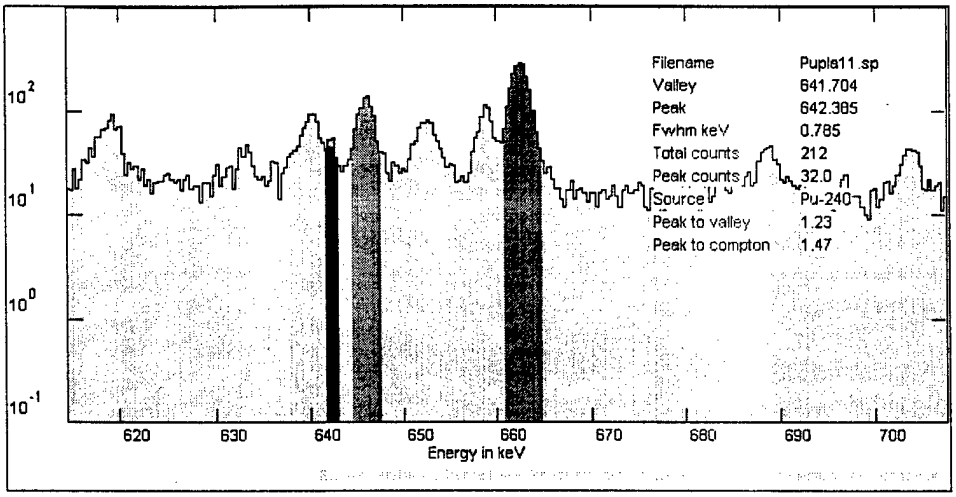

Figure 31 (642 keV Peak for Pu-240)

RSEMCA Results

RSEMCA did not perform as well as RobWin in the area of WGPu detection. Attempts were made to enter the energy calibration equation from the detector characterization with the multi source. RSEMCA does not have a method to enter the energy calibration equation. Instead, the calibration file from the characterization was used. Figure 32 shows that not only does it provide an energy calibration, but it also contains the peak names and energies from the multisource.

Loading the calibration file from the multisource was not a good option. The calibration of the WGPu source was restarted as an unknown source. First, a peak search was conducted, but as Figure 33 shows, no peaks were identified. Next, the operator identified several peaks in the spectrum (Figure 34) and a new energy calibration was calculated. The new energy calibration provided by RSEMCA was:

$$Y\ (keV) = -1.2337E\text{-}7*X^2 + 0.34080*X - 2.2357.$$

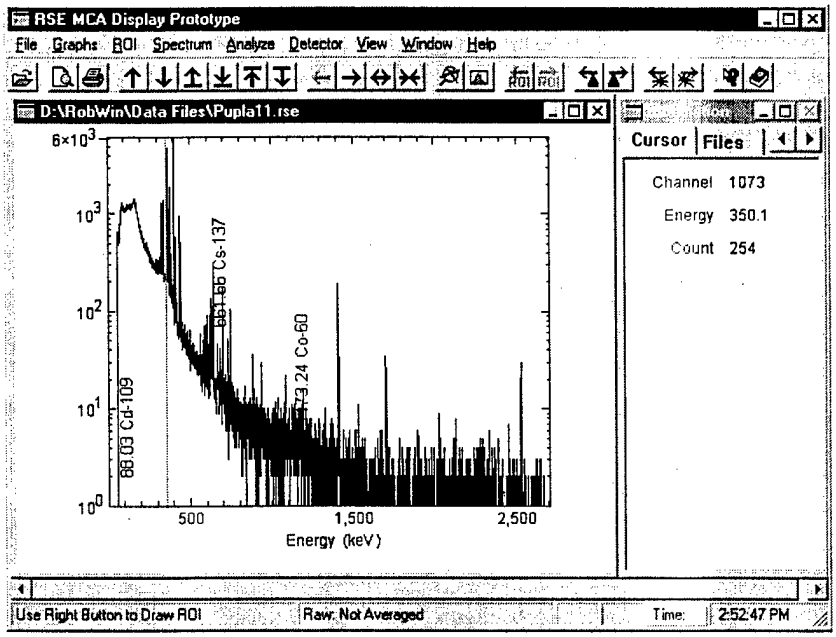

Figure 32 (RSEMCA Initial Calibration)

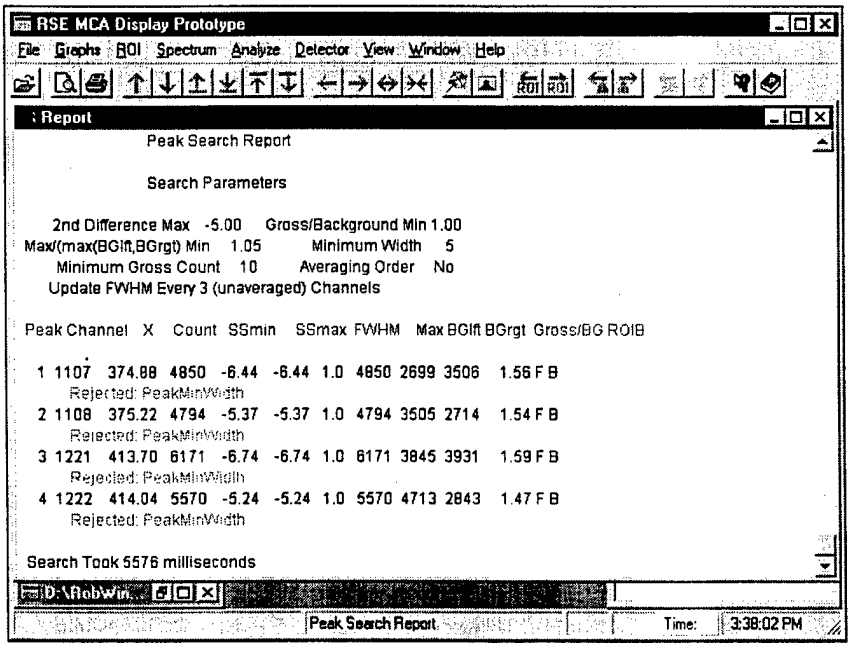

Figure 33 (RSEMCA Peak Search Report)

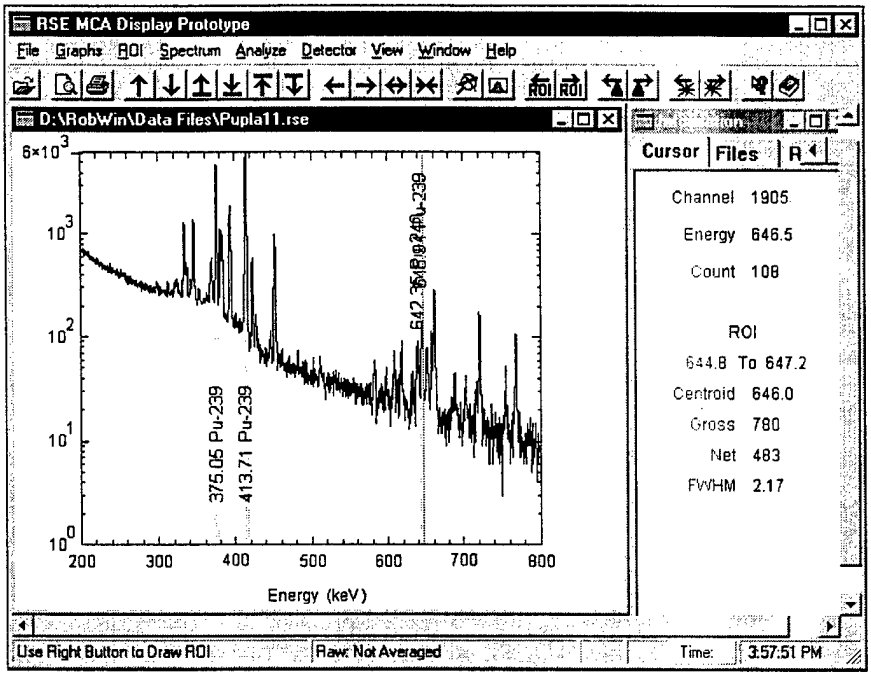

Figure 34 (RSEMCA Improved Calibration)

As with RobWin, RSEMCA's graphics display the peaks of interest in the 640 keV region. However, the peaks highlighted in Figure 35 were identified through operator input and identification. The software was not able to identify the peaks or provide any assistance in locating the peaks.

As before, the key gamma peaks for Pu-239 and Pu-240 (640 keV region) are needed to determine the mass percent of Pu-239 and Pu-240. Figure 36 identifies the 645.94 keV peak for Pu-239 and Figure 37 identifies the 642.35 keV peak for Pu-240. There is an error associated with the 642.35 keV peak because the software reports a net counts under the peak of –4. RSEMCA is not capable of determining WGPu because of this computation error.

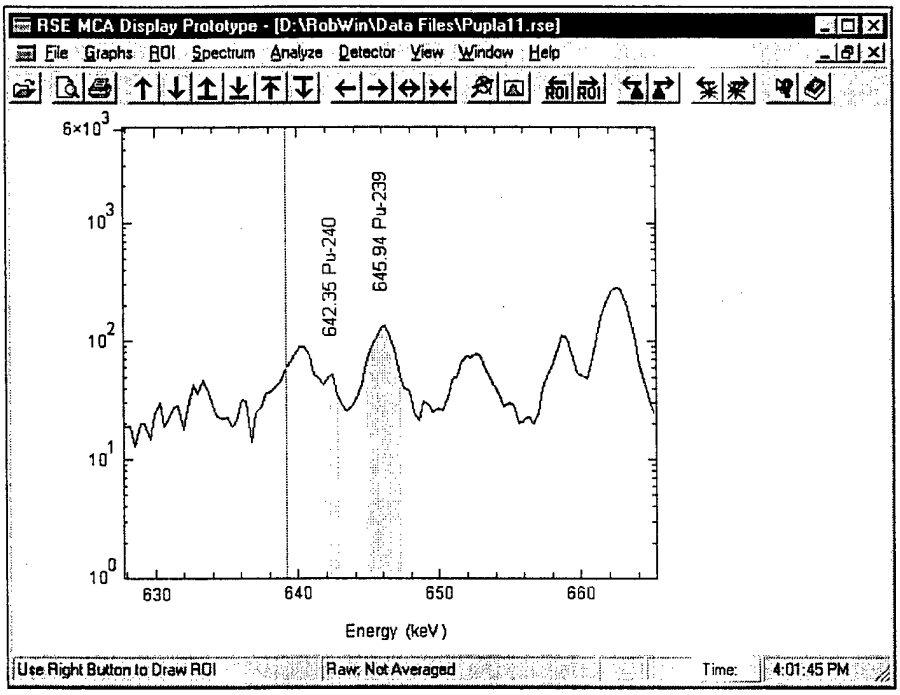

Figure 35 (RSEMCA 640 keV Region)

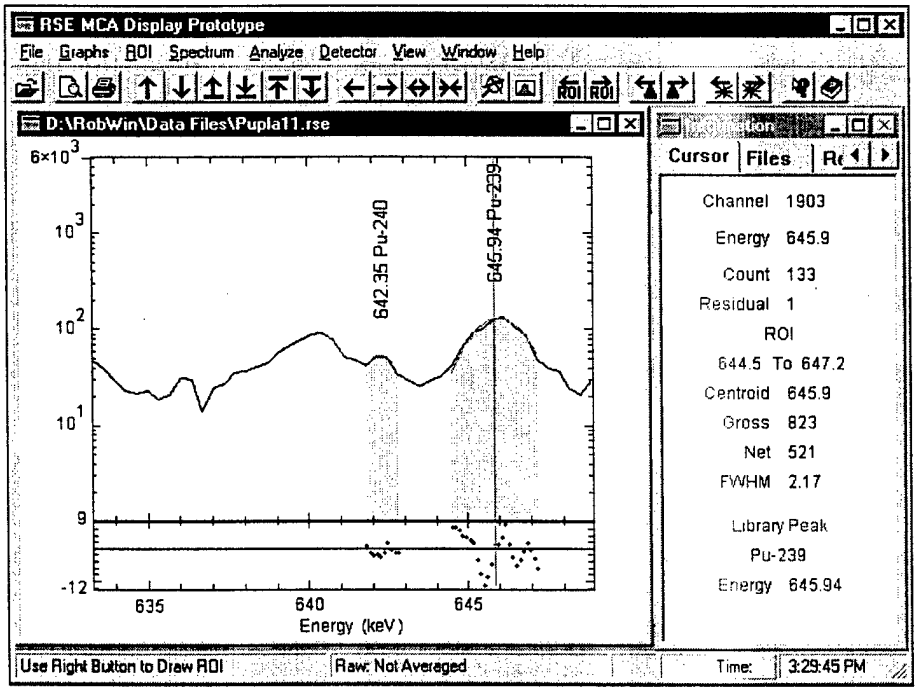

Figure 36 (645.94 keV Peak for Pu-239)

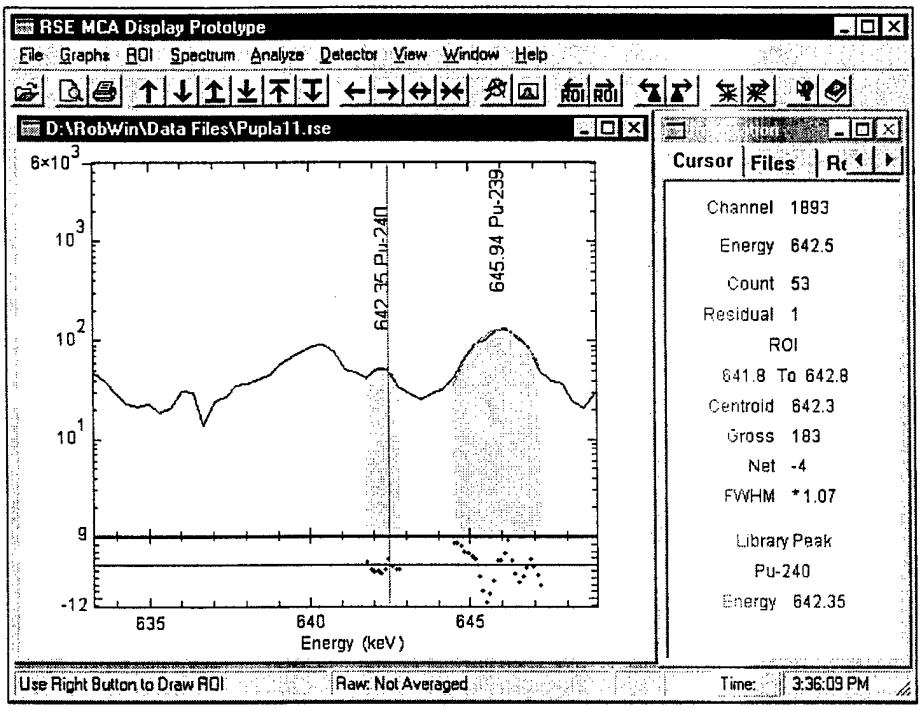

Figure 37 (642.35 keV Peak for Pu-240)

V. Discussion

General Discussion

Many challenges were experienced throughout this research. The absence of an HPGe detector placed several limitations upon the scope of the thesis and reduced the extent of the research. This report set out to answer the following three questions.

1. What is gained by using the CZT detector over the lower resolution NaI detector in nuclear weapons identification and verification using RobWin and RSEMCA?

2. Does either RobWin or RSEMCA perform better in the area of spectral analysis?

3. Are both software programs capable of analyzing and identifying nuclear weapons? If so, does one software program offer an advantage in identifying nuclear weapons?

In an effort to answer these questions, the research opened several additional areas of discussion. When comparing detectors, is it better to have a more accurate detector, or a more precise detector? While searching for WGPu, how certain are the results? Finally, why does the CZT spectrum lose efficiency and have a different shape than expected? Each of these areas will be addressed below.

Accuracy versus Precision.

The discussion on accuracy versus precision relates to resolution versus efficiency. It can be argued that the NaI detector is more accurate due to its ability to collect large count rates, which reduces the statistical error. However, it can also be said that the NaI detector is less precise because it cannot resolve many of the individual gamma ray peaks within 5-10 keVs of each other. Meanwhile, the CZT detector is more precise being able to resolve gamma rays within 2-3 keV of each other, but less accurate because it has such a small surface area to collect counts, and its thickness is small minimizing its stopping power for larger energy gamma rays.

This is a double-edged sword. Is it better to give up accuracy for better precision or vice a verse? The answer lies in the detection needs. To identify nuclear weapons, precision is necessary to identify the key gamma ray peaks in the 640 keV region. The NaI detector is not capable of doing this. However, to get that precision there is a loss of accuracy. This adds to the uncertainty of the results. For this thesis, it became obvious that the NaI detector was not capable of determining WGPu because it lacked the precision, while the CZT detector was incapable because it lacked the accuracy. Not much can be done to improve the NaI detector's precision, but better CZT detectors exist capable of greatly improving the CZT detectors accuracy.

Weapon Certainty/Uncertainty

Trading off resolution for efficiency or vice a verse creates uncertainty in the results. In the case of the CZT spectra collected at energies above 200 keV, the majority of peaks of interest had less than 500 counts. Most of the peaks ranged from 20 counts to 100 counts. Statistically, this produces associated errors of 4.5 counts to 10 counts. That

is a 27% to 10% range of difference. It will be challenging to make accurate determination of WGPu with errors as large as 27%. The mass percent of Pu-239 for WGPu is 93.8% while the mass percent for fuel grade plutonium is 86.1%. A statistical error of 27% associated with only 20 counts could produce a different conclusion as to the actual grade of plutonium.

An additional area of uncertainty lies in the determination of a plutonium weapon. The mere presence of WGPu does not guarantee a nuclear weapon exists. DoD/DOE have decided that 0.5 Kg of WGPu indicates the existence of a weapon.

Appendix F calculates the approximate size of a 0.5 Kg hollow mass of WGPu. The thickness of the plutonium shell was 0.01 cm. That is not much more than a coating of paint. Someone with the intention to deceive could paint a ball with an isotope source similar to WGPu. For in inspector, it would be difficult to determine the difference between the painted ball and a hollow mass of only 0.5 Kg based on the shielded spectra alone. Without being able to see within the container, no one can be 100% certain of the conclusion.

CZT Spectra

With the CZT detector, the signal is determined by the ability of the detector to fully collect the electrons and holes, which is limited by their respective mobility and trapping. Charge trapping has a major impact on the performance of CZT detectors and creates peak shapes that are not Gaussian with a distinctive low energy tail. This low energy tail is a result of poor mobility of the holes and is known as hole tailing. The shaping of the tail and the importance of hole tailing depend strongly upon the energy of the incident photon. Low energy photons will always stop near the front contact, and will

experience complete charge collection and hole tailing will be negligible, while high energy photons with an attenuation long relative to the detector thickness present the greatest amount of hole tailing. This is because at higher energies, more of the interactions take place further from the surface, so the effects of poor hole mobility are more pronounced creating the tail [20].

It is unclear whether the CZT detector will be useful for nuclear weapons verification. The CZT offers the potential to identify WGPu since it showed the capability to resolve energy peaks that within 2-3 keVs. Figure 11 shows that the CZT detector resolved the 22.16 keV and 24.90 keV peaks from Cd-109. The effects of a wider FWHM and hole tailing at higher energies will reduce the resolution of the CZT detector. The actual amount of change in resolution is unknown. Besides for the 645 keV peak, Figure 38 shows that Pu-239 also has a 639.99 keV peak joined with the Pu-240 peak at 642.35 keV. The CZT should be able to distinguish between these two peaks as long as enough counts exist to form the peaks. The challenge will be finding a CZT crystal with a larger surface area to improve the count rate, and thicker to increase the stopping power for the higher energy gamma rays.

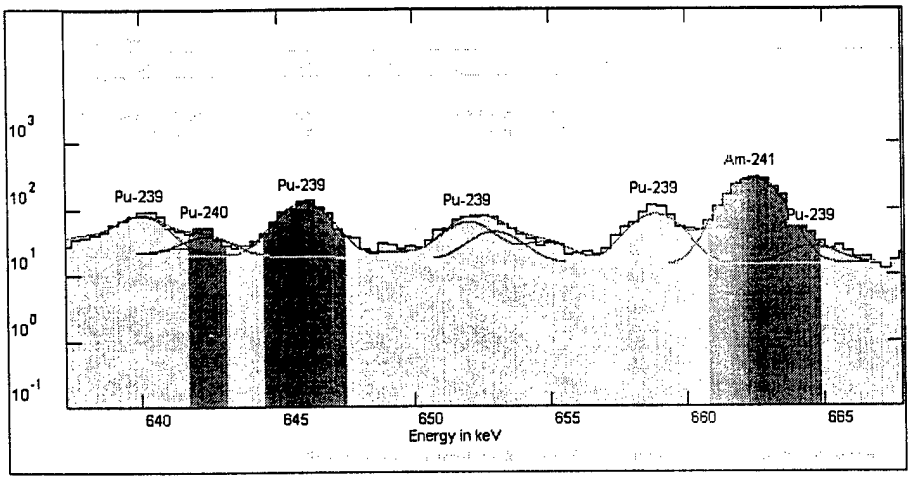

Figure 38 (WGPu-239 Spectrum)

Recommendations for Future Work

This research opens the door into several areas for future research. The limitations on the thesis because an HPGe detector was not available and the small count rate for the CZT detector due to its size left several questions unanswered.

Weapon Simulation

Without the HPGe detector, this research could not investigate the modeling of a stored nuclear weapon. The subject of nuclear weapon identification and verification will be of interest for many years to come. With the growing stockpile of spent reactor fuel and the dismantlement of nuclear weapons, methods are needed to identify and verify stockpile control. Detection systems need to be able of determining the difference between WGPu and RGPu. Modeling stored nuclear weapons is essential to test detector capabilities and define confidence levels associated with detection results.

Appendix B contains approximations of the escaping gamma ray activity. Appendix G provides an approximation of the minimal size of a stored Plutonium weapon of 0.5 Kg. The thickness for the Pu-239 shell was established so that it was less

than one mean free path for gamma rays energies equal to and greater than 80 keV. Assuming a constant density throughout the material, the attenuated gamma rays escaping the surface diverge spherically from the surface area of the sphere. Dividing the escaping gamma ray activity by the surface area provides an activity per surface area. This provides a reference scale to model a nuclear weapon.

In addition to simulating a real weapon, research should be conducted in the simulation of a false weapon. A ball painted with an isotopic source could provide a false signature of a weapon. Research in this area could identify insight into detection of false weapons.

Detectors Research.

The CZT detector offered tremendous potential due to its smaller size and higher resolution. The detector used was too small to complete the full scope of work. The small crystal size limited the counts incident upon the 25 mm^2 detector face and the thickness lacked the stopping power to absorb gamma rays of higher energies. As a result, the detector's collection capabilities severely degrade beyond 200 keV.

Larger CZT crystals exist and would greatly improve the performance. Using a 1 cm x 1cm crystal instead of a 5 mm x 5 mm crystal would increase the detection surface area by 4 and thus increase the peak counts by a multiple of 4. This in turn reduces the statistical error by a factor of 2. For example, if the 5 mm x 5 mm detector collected 100 counts for a given energy peak this would have an error of +/- 10 counts; whereas, a 1 cm x 1 cm detector should collect 400 counts at the given energy with an error of +/- 20counts. The percentage error in the counts changes from 10% to 5 % with the larger surface area.

If possible, a thicker crystal should be used which would increase the stopping power and improve collection capabilities above 200 keV. A thicker crystal would have a greater probability of capturing the higher energy gamma rays. Due to difficulties in growing CZT crystals, this may not be possible.

The 5 mm x 5 mm x 5 mm was capable of collecting counts for the 662 keV peak. A larger surface area should improve the number of counts and may produce better results. This may not be enough for detection of WGPu. Due to the low energy tailing associated with CZT detectors, distinct peaks within 2-3 keV may not be noticeable. eV Products offers a variety of CZT detectors. Their recommendation was to use a 1 cm x 1 cm x 3 mm coplanar design. This would offer the larger surface area and the coplanar design would reduce some of the tailing. Constellation Technologies recommends using a HgI_2 detector that does not require cooling, has a higher Z than CZT, is relatively small, and offers larger crystal sizes than CZT. HgI_2 detectors have an additional benefit in that they do not have the low energy tailing associated with CZT. Both options offer promise and deserve further research.

Software Research.

Experimenting with the two different spectral analysis programs has raised question in what the user would like the software to perform. Ideally, the software should identify things in the spectrum not obvious to the observer. Several different ideas were proposed that would improve a user's ability to analyze a spectrum.

Recommendation 1.

Due to the variety of spectral analysis software programs, and the constant need to improve and upgrade software, there exist many spectral data formats. Even within a

single office, the purchase of a new spectral software program may not be compatible with the previous version. For this reason, software developers need to provide a copy of the input data formats so users can adjust different data files to the correct format required by the software. At a minimum, a single standard should be declared for interoperability of recognized spectral analysis software programs. The spectral analysis programs should be able to read from or write to this "industry standard" report. The International Atomic Energy Agency (IAEA) is an international authority in this area has a specified format (*.spe) for spectrum collections. This format should be adopted as the "industry standard."

Recommendation 2.

Neither software program offers the ability to identify and calculate the quantity of WGPu or RGPu. Both programs are capable of identifying the key peaks needed to determine plutonium grade; therefore, both programs should be capable of determining the plutonium grade. Shielding should not affect the mass ratio calculations, because both the Pu-240 and Pu-239 gamma rays are approximately the same energy and should experience the same attenuation thereby maintaining the same ratio in peak counts.

Calculating the quantity is possible, but may not be a beneficial effort. If the shielding of a weapon is unknown, the actual amount of attenuation is also unknown and based upon assumptions of the shielding material and geometry. To calculate the quantity of plutonium, the software can use the detector efficiency, peak counts, and the frequency of occurrence at the particular energy. The following steps provide a rough template to calculate the quantity of an isotope present in a spectrum.

Step 1 – Calculate the number of radiation quanta emitted by the source at a particular energy using the solid angle, detector efficiency, and the number of pulses recorded.

Step 2 – Calculate the total activity of the source using the total counts from the source for a particular energy peak from Step 1 and the frequency of occurrence for that energy peak.

Step 3 – Calculate a mass quantity using the total source activity from Step 2 and the activity per gram rate.

Recommendation 3.

The process of identifying unknown sources can be confusing because of the existence on numerous gamma ray peaks. By eliminating those peaks that are known or suspected to exist, then some insight to what remains may be gained. This process would be more involved than the previous recommendation.

Step 1 – – Calculate the number of radiation quanta emitted by the source at a particular energy using the solid angle, detector efficiency, and the number of pulses recorded.

Step 2 – Calculate the total activity of the source using the total counts from the source for a particular energy peak from Step 1 and the frequency of occurrence for that energy peak.

Step 3 – Calculate the activity for each associated gamma ray using the total activity from Step 2 and the frequency of occurrence for all gammas associated with the isotope

Step 4 – Calculate an approximate number of pulses recorded for each gamma in the isotope using the activity for each gamma ray from Step 3, the solid angle and the detector efficiency for the different gamma energies.

Step 5 – Subtract isotope spectra from total spectra.

DTRA

A significant challenge encountered during this research involved the opening of input files. A considerable amount of time was spent altering files from the data collected using Genie 2000 to a format readable for RobWin and RSEMSA. Both software programs use different file formats. DTRA needs to specify to the developers specific input and output file formats for the software.

Conclusion

This thesis conducted research in three areas to evaluate the spectral analysis software's ability to identify and verify the existence of nuclear weapons. The first area investigated the advantages different detectors offered to the software. The results were disappointing. The CZT detector offered much better resolution than the NaI detector at energies below 200 keV, but beyond 200 keV, the CZT detector experienced poor charge collection and its superiority diminished. The NaI detector had great efficiency, but because it lacks sufficient resolution to identify critical gamma ray peaks, offers little use in nuclear weapons detection. Neither detector used in this thesis can support nuclear weapon detection.

The second area investigated the accuracy and capabilities of each program. Overall, RobWin performed better than RSEMCA. Quantitatively both produced similar results, while qualitatively RobWin offers significantly better features providing better

ease of use for the operator. RSEMCA is still a prototype and has several problems to work out before it will be compatible with RobWin.

The third area investigated was the software's ability to detect weapon grade plutonium. In the area of WGPu identification, RobWin easily identified the key peaks in the 640 keV region used to identify WGPu and determine the mass percent of Pu-239 and Pu-240. RSEMCA required the user more interface and knowledge of the WGPu spectrum to identify the critical peaks in the 640 keV region. RSEMCA also generated an error in the net count calculations by producing a negative peak count. This eliminates RSEMCA's ability to determine a mass percent of Pu-239 to Pu-240.

The results of the study suggest that RobWin performed better then RSEMCA. At present, RSEMCA is incapable of supporting DTRA's need because it cannot determine WGPu due to a mathematical error associated with the peak count calculations. The results also offer several areas for future research. The need for better spectral analysis software programs and detections systems will continue to grow as the world wrestles with nuclear dismantlement and an ever increasing amount of spent reactor fuel.

Appendix A (Key Gamma Rays)

The tables enclosed in this appendix list key gamma rays for the nuclide of interest in nuclear weapon detection. Those nuclides are: U-235, U-238, Pu-239, and Pu-240. The gamma rays listed are those that have a 1:100,000 chance of occurrence or better.

Table 12 (U-235 Key Gamma Rays)

Nuclide	Energy (keV)	Yield (%)	Rate (gammas/ sec*gram)
U-235 $T_{1/2}$ =7.038E+8 Years Alpha+ Gamma rays Specific Activity = 8.00E+4 Bq/gram	13.00	51.00	4.08E+4
	19.59	61.00	4.88E+4
	72.70	0.110	88
	89.9530	3.56	2848
	93.3500	5.81	4648
	94.0	0.400	320
	95.70	0.19	152
	105.0	2.69	2152
	109.160	1.54	1232
	140.76	0.220	176
	143.760	10.96	8768
	163.330	5.08	4064
	182.61	0.340	272
	185.715	57.2	4.576E+4
	194.940	0.630	504
	202.110	1.080	864
	205.311	5.01	4008
	221.380	0.120	96

Table 13 (U-238 Key Gamma Rays)

Nuclide	Energy (keV)	Yield (%)	Rate (gammas/ sec*gram)
U-238 $T_{1/2}$ = 4.468E+9 Years Alpha + Gamma rays Specific Activity = 1.24E+4 Bq/gram	13.00	8.0000	992.0
	49.55	0.0640	7.936
	89.9530	0.00070	0.0868
	93.3500	0.00114	0.14136
	105.00	0.00053	0.06572
	113.50	0.0102	1.2648

Table 14 (Pu-239 Key Gamma Rays)

Nuclide	Energy (keV)	Yield (%)	Rate (gammas/ sec*gram)
Pu-239 $T_{1/2}$ =24,110 yrs Alpha + Gamma rays Specific Activity = 2.30E+9 Bq/gram	12.97	0.01840	4.23E+05
	13.60	4.90000	1.13E+08
	30.04	0.00022	4.99E+03
	38.66	0.01050	2.42E+05
	42.06	0.00017	3.80E+03
	46.21	0.00074	1.70E+04
	46.69	0.00006	1.33E+03
	47.56	0.00006	1.29E+03
	51.62	0.02710	6.23E+05
	54.04	0.00020	4.53E+03
	56.83	0.00113	2.60E+04
	65.71	0.00005	1.06E+03
	67.67	0.00016	3.77E+03
	68.70	0.00030	6.90E+03
	68.74	0.00011	2.53E+03
	77.59	0.00041	9.43E+03
	78.43	0.00014	3.24E+03
	94.67	0.00380	8.74E+04
	96.13	0.00002	5.06E+02
	97.60	0.00008	1.84E+03
	98.44	0.00610	1.40E+05
	98.78	0.00122	2.81E+04
	103.06	0.00023	5.29E+03
	111.00	0.00290	6.67E+04
	115.38	0.00046	1.06E+04
	116.26	0.00060	1.37E+04
	119.72	0.00002	5.06E+02

	Energy (keV)	Yield (%)	Rate (gammas/ sec*gram)
	123.62	0.00002	4.60E+02
	124.51	0.00006	1.40E+03
	125.21	0.00007	1.63E+03
	129.30	0.00631	1.45E+05
	141.66	0.00003	7.36E+02
	143.35	0.00002	3.98E+02
	144.20	0.00028	6.51E+03
	146.09	0.00012	2.74E+03
	161.45	0.00012	2.83E+03
	171.39	0.00011	2.53E+03
	179.22	0.00007	1.52E+03
	188.23	0.00001	2.53E+02
	189.36	0.00008	1.91E+03
	195.68	0.00011	2.46E+03
	203.55	0.00057	1.31E+04
	225.42	0.00002	3.47E+02
	237.77	0.00001	3.31E+02
	243.38	0.00253	5.82E+04
	255.38	0.00008	1.84E+03
	263.95	0.00003	6.21E+02
	297.46	0.00005	1.15E+03
	311.78	0.00003	5.93E+02
	316.41	0.00001	3.04E+02
	320.86	0.00005	1.25E+03
	323.84	0.00005	1.24E+03
	332.85	0.00049	1.14E+04
	336.11	0.00011	2.58E+03
	341.51	0.00007	1.52E+03
	345.01	0.00003	5.75E+02
	345.01	0.00056	1.28E+04

	Yield (%)	Rate (gammas/ sec*gram)	Energy (keV)
	361.89	0.00001	2.81E+02
	367.07	0.00009	2.05E+03
	368.55	0.00009	2.02E+03
	375.05	0.00155	3.57E+04
	380.19	0.00031	7.02E+03
	382.75	0.00026	5.96E+03
	392.53	0.00021	4.72E+03
	393.14	0.00035	8.05E+03
	413.71	0.00147	3.37E+04
	422.60	0.00012	2.81E+03
	451.48	0.00019	4.35E+03
	645.94	0.00002	3.50E+02

Table 15 (Pu-240 Key Gamma Rays)

Nuclide	Energy (keV)	Yield (%)	Rate (gammas/ sec*gram)
Pu-240 $T_{1/2}$ = 6564 yrs Alpha + Gamma rays Specific Activity = 8.43E+9 Bq/gram	13.60	11.00000	9.27E+08
	45.24	0.04500	3.79E+06
	94.67	0.00003	2.23E+03
	98.44	0.00004	3.37E+03
	104.23	0.00708	5.97E+05
	111.00	0.00002	1.69E+03
	160.31	0.00040	3.37E+04
	212.46	0.00002	1.69E+03
	642.35	0.00001	1.10E+03

** Half lives, Gamma Energies and Yield % provided by Brookhaven National Labs.

Specific Activities provided by Handbook of Health Physics and Radiological Health, Pg 8-21.

Appendix B (Gamma Attenuation)

Under conditions of good geometry, the attenuation of a gamma radiation is:

$$I = I_0 e^{-ut}. \qquad 5$$

Where I is the gamma ray intensity at some distance from the source, I_0 is the gamma ray intensity at the source, u is the linear attenuation coefficient, and t is the thickness of the incident material.

Under conditions of poor geometry where a shield is very thick, scatter increases the gamma rays incident on the detector. The above equation underestimates the effectiveness of the thickness. The equation assumes that every photon that interacts with the shield will be removed from the beam and thus will not be available for counting by the detector. With poor geometry, a significant number of photons may be scattered by the shield into the detector, or photons that had been scattered out of the beam may be scattered back after a second collision as shown in Figure 39.

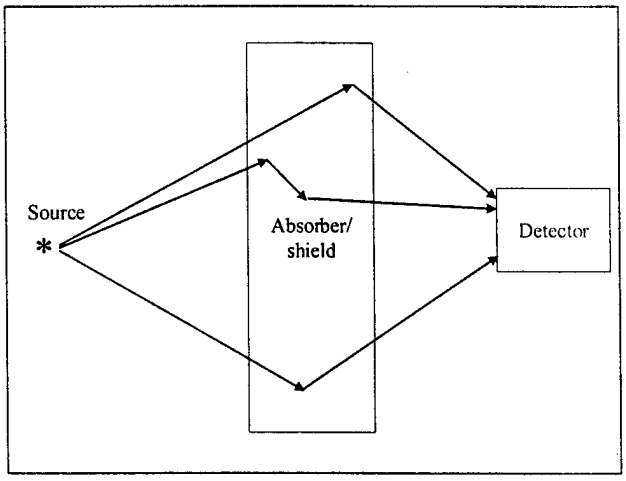

Figure 39 (Gamma-ray Absorption Under Conditions of Poor Geometry)

To account for the conditions of poor geometry, the above equation can be modified with a build up factor (B).

$$I = B\, I_0\, e^{-ut}. \qquad 6$$

The following tables utilize this equation to calculate the approximate gamma ray intensity expected incident upon the detector. Table 26 through Table 28 contain the buildup factors for water, air and iron. Notice that the buildup factors have a lower limit at 100 keV. This is because the gamma rays lower than 100 keV generally do not have the energy to scatter several times and still escape the material. A buildup factor of 1 will be used for cases where the gamma ray energies are significantly below 100 keV.

Figure 40 shows a generic storage container for Pu-239 as defined by DOE STG-3013-96. [18, A-11] Both the inner and outer containers are typically composed of 16 gauge (1.3 mm) stainless steel. This requires the escaping gamma rays to travel through an inner and outer casing of steel. If the material of the two casings is the same, then the total attenuation due to the stainless steel casing can be combined into one equation as shown below.

$$I = B\, I_0\, e^{-ut} + B\, I_0\, e^{-ut}. \qquad 7$$

$$I = B\, I_0\, (e^{-ut} + e^{-ut}) = B\, I_0\, e^{-u2t}. \qquad 8$$

Where t = thickness of steel container = 16 gauge = 1.3 mm

The material filling the storage container will effect the gamma ray attenuation. Because of uncertainty of material used, the attenuation will be calculated at both extremes. The upper extreme will assume air fills the void between the container walls. This will provide an upper activity limit since air does little to attenuate gamma rays.

The other extreme will assume paraffin fills the container. Paraffin is a common material used to shield WGPu because it is an excellent absorber of neutrons. These two activity calculations provide an upper and lower limit for the gamma ray activity at the outside of the second container.

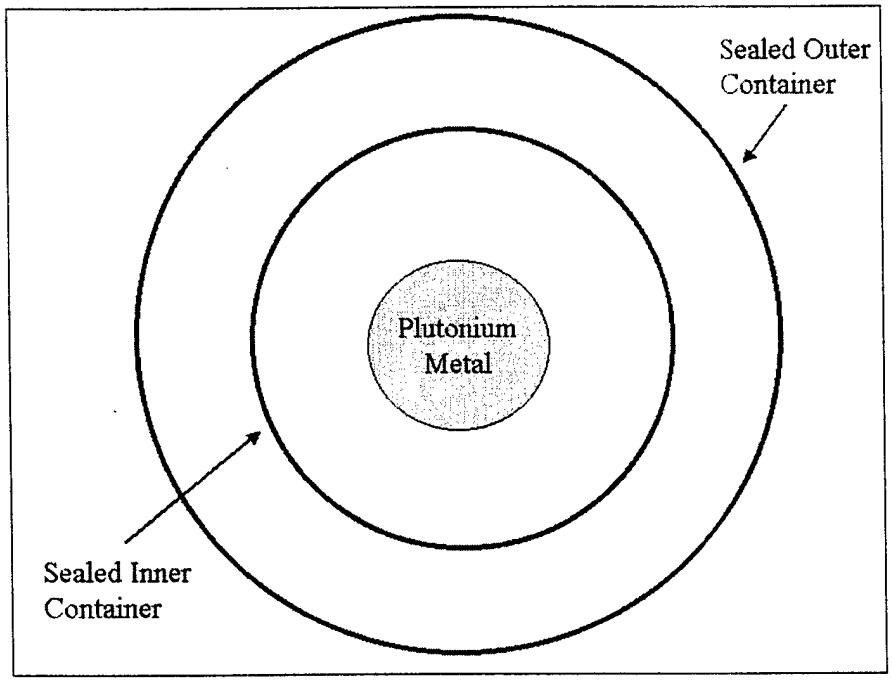

Figure 40 (Top View of Weapon Storage Container)

The following tables are for 0.5 kg isotope sources. Table 16 through Table 19 contain the gamma ray attenuation calculations for 45.72 cm (18 inches) of air and a two 1.3 mm iron walls. The approximate density of air and iron respectively is 0.00129 g/cm^3 and 7.86 g/cm^3. Table 20 through Table 23 contains gamma ray attenuation calculations through 45.72 cm of paraffin and two 1.3 mm iron walls. The linear attenuation

coefficients and build up factors for paraffin are the same as those for water. Paraffin has the same density of water, 1.0 g/cm^3 [2114, 6-5].

Table 16 (Gamma Ray Attenuation for U-235 through air and Iron Casing)

U-235 Key Gamma (KeV)	Frequency of occurrence (%)	Bq/gram	I_0 (Bq) for 0.5 kg	Build Up factor for air B	Mass Attenuation for air (cm2/g)	$I_P = B\ I_0\ e^{-\mu t}$ (Bq) air attenuation	Build Up factor for iron casing B	Mass Attenuation for iron (cm2/g)	$I = B\ I_P\ e^{-\mu t}$ (Bq) casing attenuation
13.00	51.00	4.08E+04	2.04E+07	2.35E+00	3.03E-03	4.79E+07	4.98E+00	9.00E+01	4.53E-23
19.59	61.00	4.88E+04	2.44E+07	2.35E+00	3.03E-03	5.73E+07	4.03E+00	2.60E+01	3.08E-01
72.70	0.11	8.80E+01	4.40E+04	2.35E+00	3.03E-03	1.03E+05	1.38E+00	8.00E-01	7.61E+04
89.95	3.56	2.85E+03	1.42E+06	2.35E+00	3.03E-03	3.35E+06	1.38E+00	4.50E-01	3.24E+06
93.35	5.81	4.65E+03	2.32E+06	2.35E+00	3.03E-03	5.46E+06	1.38E+00	4.00E-01	5.50E+06
94.00	0.40	3.20E+02	1.60E+05	2.35E+00	3.03E-03	3.76E+05	1.38E+00	4.00E-01	3.79E+05
95.70	0.19	1.52E+02	7.60E+04	2.35E+00	3.03E-03	1.79E+05	1.38E+00	4.00E-01	1.80E+05
105.00	2.69	2.15E+03	1.08E+06	2.34E+00	3.02E-03	2.52E+06	1.30E+00	3.50E-01	2.49E+06
109.16	1.54	1.23E+03	6.16E+05	2.33E+00	3.01E-03	1.44E+06	1.39E+00	3.50E-01	1.51E+06
140.76	0.22	1.76E+02	8.80E+04	2.28E+00	2.94E-03	2.01E+05	1.42E+00	2.50E-01	2.34E+05
143.76	10.96	8.77E+03	4.38E+06	2.27E+00	2.93E-03	9.95E+06	1.42E+00	2.50E-01	1.16E+07
163.33	5.08	4.06E+03	2.03E+06	2.23E+00	2.88E-03	4.53E+06	1.44E+00	1.90E-01	5.62E+06
182.61	0.34	2.72E+02	1.36E+05	2.20E+00	2.84E-03	2.99E+05	1.46E+00	1.70E-01	3.82E+05
185.72	57.20	4.58E+04	2.29E+07	2.19E+00	2.83E-03	5.01E+07	1.47E+00	1.70E-01	6.44E+07
194.94	0.63	5.04E+02	2.52E+05	2.17E+00	2.80E-03	5.47E+05	1.48E+00	1.60E-01	7.14E+05
202.11	1.08	8.64E+02	4.32E+05	1.16E+00	1.50E-03	5.01E+05	1.48E+00	1.60E-01	6.54E+05
205.31	5.01	4.01E+03	2.00E+06	2.15E+00	2.77E-03	4.31E+06	1.49E+00	1.50E-01	5.70E+06
221.38	0.12	9.60E+01	4.80E+04	2.12E+00	2.73E-03	1.02E+05	1.50E+00	1.50E-01	1.36E+05

Table 17 (Gamma Ray Attenuation for U-238 through air and Iron Casing)

U-238 Key Gamma (keV)	Frequency of occurrence (%)	Bq/gram	I_0 (Bq) for 0.5 kg	Build Up factor for air B	Mass Attenuation for air (cm2/g)	$I_P = B\ I_0\ e^{-ut}$ (Bq) air attenuation	Build Up factor for steel casing B	Mass Attenuation for iron (cm2/g)	$I = B\ I_P\ e^{-ut}$ (Bq) casing attenuation
13.00	8.00	9.92E+02	4.96E+05	2.35E+00	3.00E+00	9.77E+05	4.98E+00	9.00E+01	9.22E-25
49.55	0.06	7.94E+00	3.97E+03	2.35E+00	2.10E-01	9.21E+03	1.78E+00	2.00E+00	3.40E+03
89.95	0.00	8.68E-02	4.34E+01	2.35E+00	1.70E-01	1.01E+02	1.38E+00	4.50E-01	9.78E+01
93.35	0.00	1.41E-01	7.07E+01	2.35E+00	1.65E-01	1.64E+02	1.38E+00	4.00E-01	1.66E+02
105.00	0.00	6.57E-02	3.29E+01	2.34E+00	1.55E-01	7.62E+01	1.39E+00	3.50E-01	8.04E+01
113.50	0.01	1.26E+00	6.32E+02	2.32E+00	1.55E-01	1.45E+03	1.39E+00	3.50E-01	1.53E+03

Table 18 (Gamma Ray Attenuation for Pu-239 through air and Iron Casing)

Pu-239 Key Gamma (keV)	Frequency of occurrence (%)	Bq/gram	I_0 (Bq) for 0.5 kg	Build Up factor for air B	Mass Attenuation for air (cm2/g)	$I_P = B\ I_0\ e^{-\mu t}$ (Bq) air attenuation	Build Up factor for iron casing B	Mass Attenuation for iron (cm2/g)	$I = B\ I_P\ e^{-\mu t}$ (Bq) casing attenuation
12.97	0.01840	4.23E+05	2.12E+08	1.00E+00	3.00E+00	1.77E+08	1.00E+00	1.50E+02	1.32E-125
13.60	4.90000	1.13E+08	5.64E+10	1.00E+00	2.20E+00	4.95E+10	1.00E+00	1.50E+02	3.68E-123
30.04	0.00022	4.99E+03	2.50E+06	1.00E+00	3.50E-01	2.44E+06	1.00E+00	8.50E+00	6.99E-02
38.66	0.01050	2.42E+05	1.21E+08	1.00E+00	2.60E-01	1.19E+08	1.00E+00	3.60E+00	7.59E+04
51.62	0.02710	6.23E+05	3.12E+08	1.00E+00	2.10E-01	3.08E+08	1.00E+00	2.00E-01	2.05E+08
77.59	0.00041	9.43E+03	4.72E+06	1.00E+00	1.70E-01	4.67E+06	1.00E+00	7.00E-01	1.12E+06
94.67	0.00380	8.74E+04	4.37E+07	2.35E+00	1.65E-01	1.02E+08	1.38E+00	4.00E-01	6.20E+07
98.44	0.00610	1.40E+05	7.02E+07	2.35E+00	1.60E-01	1.63E+08	1.38E+00	3.70E-01	1.06E+08
98.78	0.00122	2.81E+04	1.40E+07	2.35E+00	1.60E-01	3.27E+07	1.38E+00	3.70E-01	2.12E+07
111.00	0.00290	6.67E+04	3.34E+07	2.33E+00	1.50E-01	7.70E+07	1.39E+00	3.50E-01	5.24E+07
129.30	0.00631	1.45E+05	7.26E+07	2.30E+00	1.50E-01	1.65E+08	1.41E+00	3.00E-01	1.26E+08
203.55	0.00057	1.31E+04	6.54E+06	2.16E+00	1.20E-01	1.40E+07	1.49E+00	1.50E-01	1.54E+07
225.42	0.00002	3.47E+02	1.74E+05	2.12E+00	1.15E-01	3.66E+05	1.51E+00	1.30E-01	4.23E+05
375.05	0.00155	3.57E+04	1.79E+07	1.83E+00	9.50E-02	3.25E+07	1.66E+00	9.50E-02	4.45E+07
413.71	0.00147	3.37E+04	1.69E+07	1.76E+00	9.50E-02	2.95E+07	1.70E+00	9.50E-02	4.13E+07
645.94	0.00002	3.50E+02	1.75E+05	1.56E+00	8.00E-02	2.71E+05	1.71E+00	7.00E-02	4.02E+05

** Table does not include all the key gamma rays for Pu-239. Gamma rays were chosen that were close to Pu-240 key gamma rays.

Table 19 (Gamma Ray Attenuation for Pu-240 through Air and Iron Casing)

Pu-240 Key Gammas (keV)	Frequency of occurrence (%)	Bq/gram	I_0 (Bq) for 0.5 kg	Build Up factor for air B	Mass Attenuation for air (cm2/g)	$I_P=B\ I_0\ e^{-\mu t}$ (Bq) air attenuation	Build Up factor for iron casing B	Mass Attenuation for iron (cm2/g)	$I=B\ I_P\ e^{-\mu t}$ (Bq) casing attenuation
13.60	11.00000	9.27E+08	4.64E+11	1.00E+00	4.00E+00	3.66E+11	1.00E+00	1.05E+02	2.36E-82
45.24	0.04500	3.79E+06	1.90E+09	1.00E+00	2.40E-01	1.87E+09	1.00E+00	2.50E+00	1.13E+07
94.67	0.00003	2.23E+03	1.12E+06	2.35E+00	1.80E-01	2.60E+06	1.38E+00	4.00E-01	1.58E+06
98.44	0.00004	3.37E+03	1.69E+06	2.35E+00	1.70E-01	3.92E+06	1.38E+00	3.80E-01	2.49E+06
104.23	0.00708	5.97E+05	2.98E+08	2.37E+00	1.70E-01	7.00E+08	1.38E+00	3.80E-01	4.44E+08
111.00	0.00002	1.69E+03	8.43E+05	2.32E+00	1.65E-01	1.94E+06	1.39E+00	3.50E-01	1.32E+06
160.31	0.00040	3.37E+04	1.69E+07	2.24E+00	1.40E-01	3.75E+07	1.44E+00	2.00E-01	3.58E+07
212.46	0.00002	1.69E+03	8.43E+05	2.14E+00	1.20E-01	1.79E+06	1.49E+00	1.50E-01	1.96E+06
642.35	0.00001	1.10E+03	5.48E+05	1.55E+00	8.50E-02	8.45E+05	1.72E+00	7.00E-02	1.26E+06

Table 22 (Gamma Ray Attenuation for Pu-239 through paraffin and Iron Casing)

Pu-239 Key Gamma (keV)	Frequency of occurrence (%)	Bq/gram	I_0 (Bq) for 0.5 kg	Build Up factor for paraffin B	Mass Attenuation for paraffin (cm2/g)	$I_P = B\ I_0\ e^{-\mu t}$ (Bq) paraffin attenuation	Build Up factor for iron casing B	Mass Attenuation for iron (cm2/g)	$I = B\ I_P\ e^{-\mu t}$ (Bq) casing attenuation
12.97	0.01840	4.23E+05	2.12E+08	1.00E+00	4.00E+00	7.98E-72	1.00E+00	1.50E+02	5.93E-205
13.60	4.90000	1.13E+08	5.64E+10	1.00E+00	4.00E+00	2.12E-69	1.00E+00	1.50E+02	1.58E-202
30.04	0.00022	4.99E+03	2.50E+06	1.00E+00	3.80E-01	7.11E-02	1.00E+00	8.50E+00	2.03E-09
38.66	0.01050	2.42E+05	1.21E+08	1.00E+00	3.00E-01	1.33E+02	1.00E+00	3.60E+00	8.51E-02
51.62	0.02710	6.23E+05	3.12E+08	1.00E+00	2.30E-01	8.45E+03	1.00E+00	2.00E-01	5.61E+03
77.59	0.00041	9.43E+03	4.72E+06	1.00E+00	1.95E-01	6.33E+02	1.00E+00	7.00E-01	1.51E+02
78.43	0.00014	3.24E+03	1.62E+06	1.00E+00	1.95E-01	2.18E+02	1.00E+00	7.00E-01	5.21E+01
94.67	0.00380	8.74E+04	4.37E+07	2.16E+02	1.90E-01	1.59E+06	1.38E+00	4.00E-01	9.71E+05
98.44	0.00610	1.40E+05	7.02E+07	2.16E+02	1.90E-01	2.56E+06	1.38E+00	3.70E-01	1.66E+06
98.78	0.00122	2.81E+04	1.40E+07	2.16E+02	1.90E-01	5.12E+05	1.38E+00	3.70E-01	3.31E+05
111.00	0.00290	6.67E+04	3.34E+07	2.11E+02	1.85E-01	1.49E+06	1.39E+00	3.50E-01	1.01E+06
129.30	0.00631	1.45E+05	7.26E+07	1.72E+02	1.80E-01	3.33E+06	1.41E+00	3.00E-01	2.54E+06
203.55	0.00057	1.31E+04	6.54E+06	1.08E+02	1.50E-01	7.43E+05	1.49E+00	1.50E-01	8.15E+05
225.42	0.00002	3.47E+02	1.74E+05	1.02E+02	1.45E-01	2.34E+04	1.51E+00	1.30E-01	2.71E+04
375.05	0.00155	3.57E+04	1.79E+07	3.24E+01	1.10E-01	3.79E+06	1.66E+00	9.50E-02	5.18E+06
413.71	0.00147	3.37E+04	1.69E+07	2.81E+01	1.00E-01	4.90E+06	1.70E+00	9.50E-02	6.86E+06
645.94	0.00002	3.50E+02	1.75E+05	1.13E+01	8.50E-02	4.04E+04	1.71E+00	7.00E-02	5.98E+04

** Table does not include all the key gamma rays for Pu-239. Gamma rays were chosen that were close to Pu-240 key gamma rays.

Appendix C (Source Activity)

The following equation converts the initial activity of a source to a current activity.

$$A = A_0 e^{-\lambda t} \qquad 9$$

and λ=ln 2/half life of the nuclide

Where A is the current activity of the source, A_0 is an initial activity of the source, λ is a decay constant equal to the inverse of the half-life and t is the time difference between the current activity from the date of initial activity. Table 24 contains the current activity for all the sources used. Not all the activity is incident upon the detector. To account for the activity incident on the detector we need to determine the solid angle (Ω) between the source and the detector as shown in Figure 41.

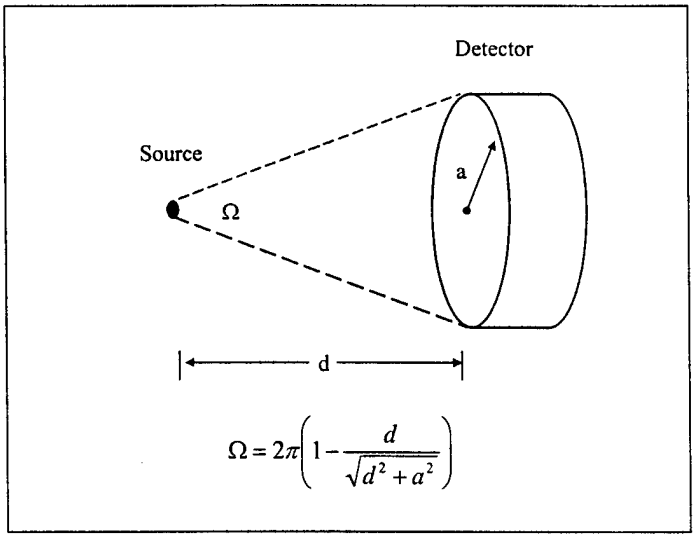

Figure 41 (Solid Angle for a Point Source)

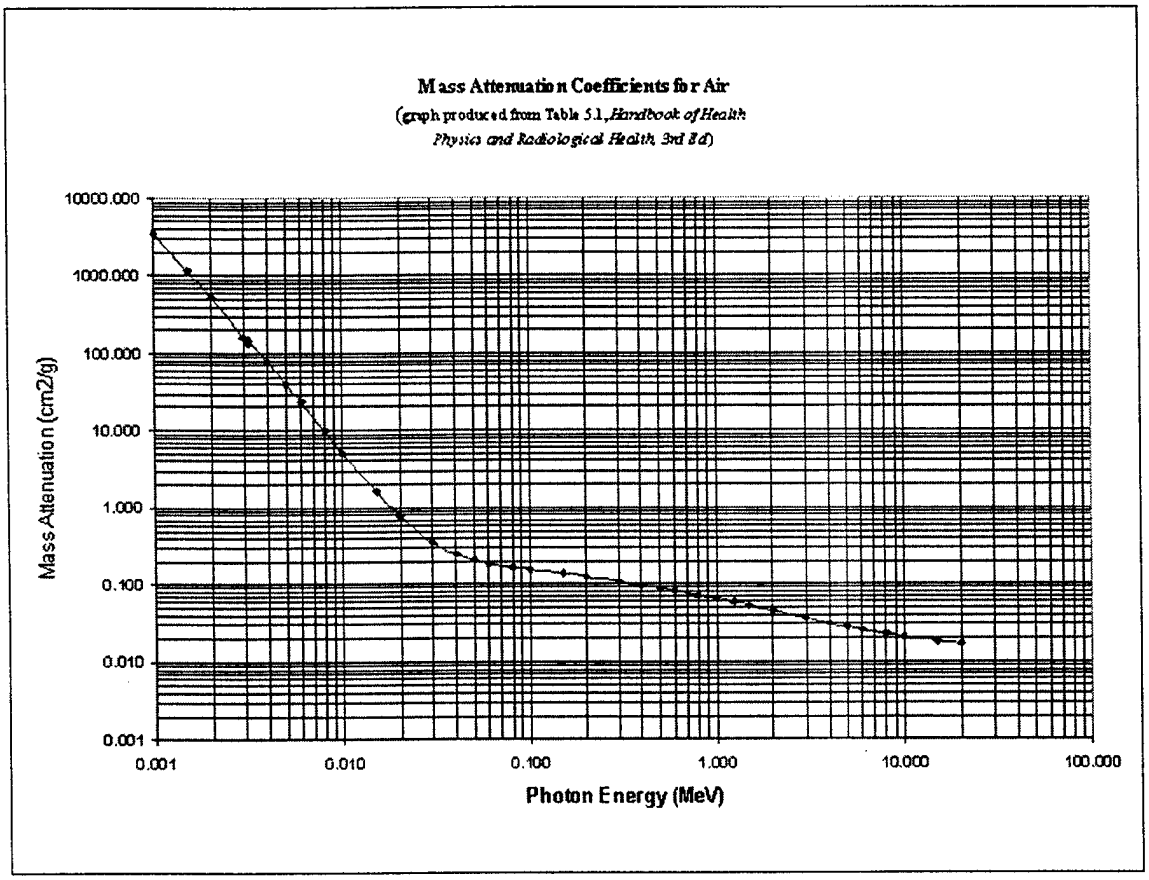

Figure 43 (Mass Attenuation Coefficient Curve for Air)

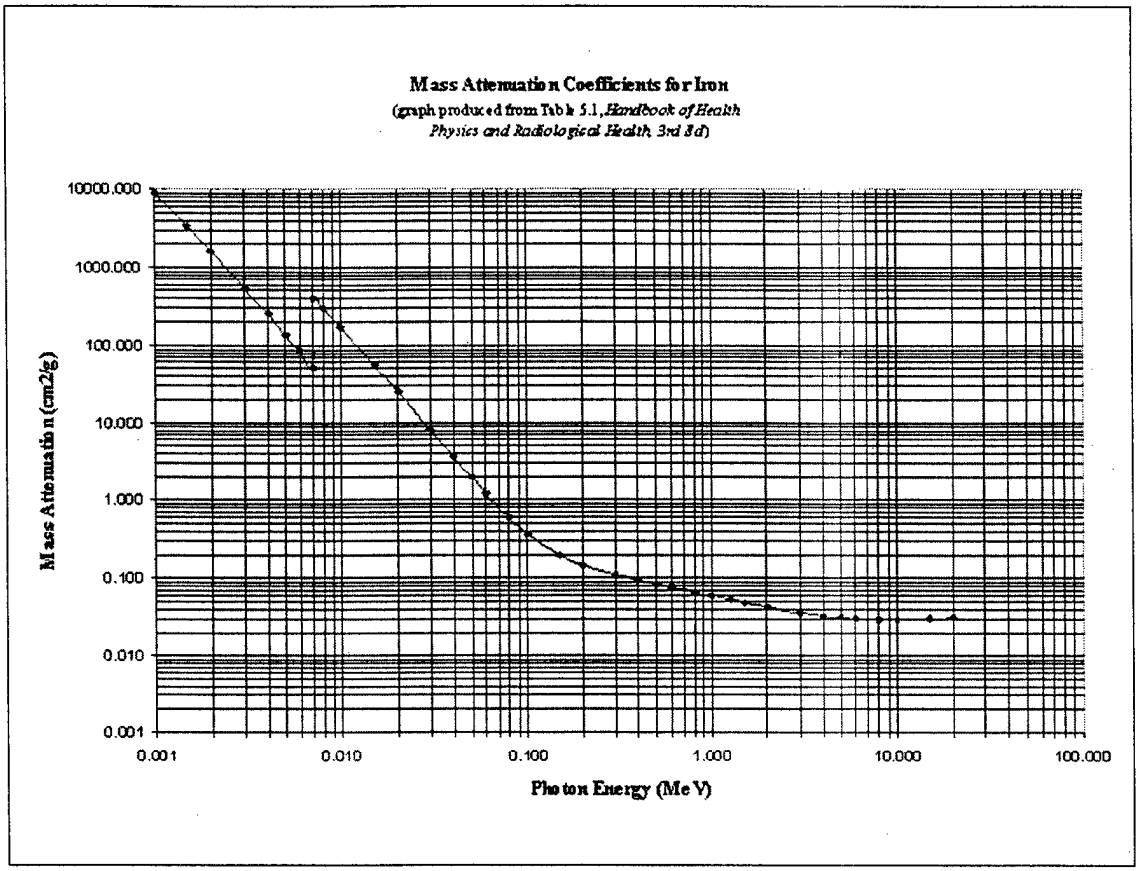

Figure 44 (Mass Attenuation Coefficient Curve for Iron)

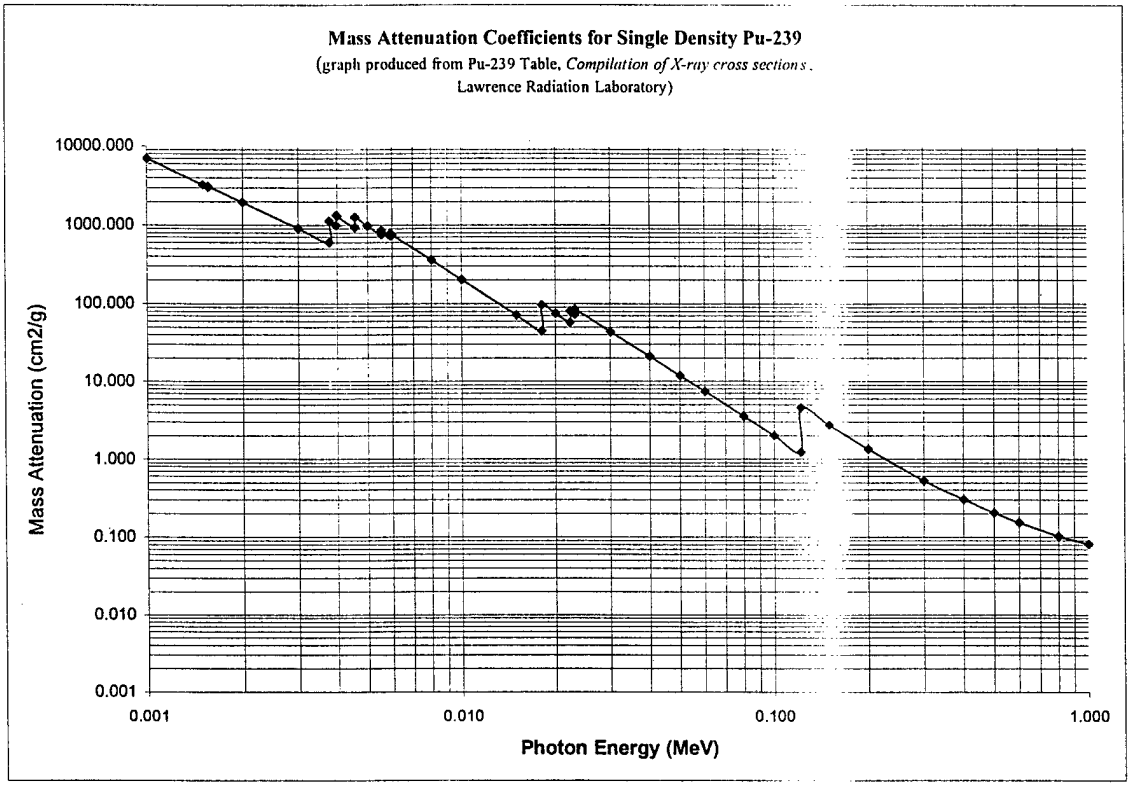

Figure 45 (Mass Attenuation Coefficient Curve for Pu-239)

Appendix E (BUILDUP FACTORS)

The following tables are reproduced using data provided by the *Handbook of Health Physics and Radiological Health, 3rd edition*. The lowest energy associated with buildup factors is 100 keV. This is because energies below 100 keV have little chance of multiple scatters back into the detection area. For energies below 100 keV a buildup factor of 1 will be assigned.

Table 26 (Buildup Factors for Water)

	Energy (MeV)									
	10 MeV	8 MeV	6 MeV	5 MeV	4 MeV	3 MeV	2 MeV	1 MeV	0.5 MeV	0.1 MeV
0.5 mfp	1.21	1.23	1.27	1.29	1.31	1.34	1.38	1.47	1.61	2.36
1.0 mfp	1.8	1.44	1.55	1.57	1.63	1.71	1.83	2.08	2.45	4.52
2.0 mfp	1.70	1.82	1.98	2.10	2.26	2.47	2.82	3.62	4.87	1.17E1
3.0 mfp	2.00	2.17	2.43	2.62	2.87	3.24	3.87	5.50	8.29	2.35E1
4.0 mfp	2.29	2.52	2.87	3.12	3.48	4.01	4.99	7.66	1.27E1	4.06E1
5.0 mfp	2.57	2.86	3.31	3.63	4.09	4.81	6.16	1.01E1	1.81E1	6.40E1
6.0 mfp	2.85	3.20	3.74	4.14	4.71	5.62	7.38	1.28E1	2.46E1	9.48E1
7.0 mfp	3.13	3.53	4.16	4.64	5.33	6.45	8.66	1.57E1	3.22E1	1.34E2
8.0 mfp	3.4	3.86	4.59	5.14	5.95	7.28	9.97	1.89E1	4.08E1	1.83E2
10.0 mfp	3.94	4.51	5.43	6.14	7.20	8.98	12.7	2.60E1	6.18E1	3.14E2
15.0 mfp	5.24	6.08	7.49	8.62	10.3	13.4	20.1	4.74E1	1.37E2	9.17E2
20.0 mfp	6.51	7.61	9.52	11.1	13.5	17.8	28.0	7.35E1	2.47E2	2.12E3
25.0 mfp	7.75	9.10	11.5	13.5	16.6	22.4	36.4	1.04E2	3.95E2	4.26E3
30.0 mfp	8.97	10.6	13.5	15.9	19.8	27.1	45.2	1.38E2	5.82E2	7.78E3
35.0 mfp	10.2	12.2	15.5	18.3	23.0	31.8	54.3	1.75E2	8.09E2	1.31E4
40.0 mfp	11.3	14.1	17.9	20.7	26.1	36.5	63.6	2.14E2	1.08E3	2.03E4

Table 27 (Buildup Factors for Air)

	Energy (MeV)									
	10 MeV	8 MeV	6 MeV	5 MeV	4 MeV	3 MeV	2 MeV	1 MeV	0.5 MeV	0.1 MeV
0.5 mfp	1.20	1.23	1.27	1.29	1.31	1.34	1.38	1.47	1.60	2.35
1.0 mfp	1.37	1.43	1.52	1.57	1.63	1.71	1.83	2.08	2.44	4.46
2.0 mfp	1.68	1.80	1.97	2.09	2.25	2.46	2.81	3.60	4.84	1.14E1
3.0 mfp	1.97	2.15	2.41	2.60	2.85	3.22	3.86	5.46	8.21	2.35E1
4.0 mfp	2.26	2.50	2.85	3.11	3.46	4.00	4.96	7.60	1.26E1	3.84E1
5.0 mfp	2.54	2.84	3.28	3.61	4.07	4.79	6.13	1.00E1	1.79E1	5.99E1
6.0 mfp	2.82	3.17	3.71	4.12	4.69	5.60	7.35	1.27E1	2.42E1	8.78E1
7.0 mfp	3.10	3.51	4.14	4.62	5.31	6.43	8.61	1.56E1	3.16E1	1.23E2
8.0 mfp	3.37	3.84	4.57	5.12	5.94	7.26	9.92	1.88E1	4.01E1	1.66E2
10.0 mfp	3.92	4.49	5.42	6.13	7.19	8.97	12.6	2.58E1	6.06E1	2.82E2
15.0 mfp	5.25	6.08	7.51	8.63	10.3	13.4	20.0	4.70E1	1.34E2	8.00E2
20.0 mfp	6.55	7.64	9.58	11.1	13.5	17.9	27.9	7.28E1	2.41E2	1.81E3
25.0 mfp	7.84	9.17	11.6	13.6	16.7	22.5	36.2	1.03E2	3.85E2	3.57E3
30.0 mfp	9.11	10.7	13.6	16.1	19.9	27.2	45.0	1.36E2	5.67E2	6.43E3
35.0 mfp	10.4	12.3	15.4	18.5	23.1	32.0	54.0	1.73E2	7.88E2	1.06E4
40.0 mfp	11.6	14.1	16.9	21.0	26.3	36.7	63.2	2.12E2	1.05E3	1.57E4

Table 28 (Buildup Factors for Iron)

	Energy (MeV)									
	10 MeV	8 MeV	6 MeV	5 MeV	4 MeV	3 MeV	2 MeV	1 MeV	0.5 MeV	0.1 MeV
0.5 mfp	1.15	1.18	1.22	1.26	1.31	1.35	1.40	1.53	1.79	1.38
1.0 mfp	1.27	1.33	1.42	1.49	1.59	1.70	1.84	2.14	2.66	1.60
2.0 mfp	1.48	1.60	1.79	1.93	2.12	2.39	2.76	3.50	4.57	1.94
3.0 mfp	1.69	1.88	2.17	2.39	2.68	3.10	3.74	5.04	6.75	2.13
4.0 mfp	1.93	2.17	2.57	2.86	3.27	3.86	4.80	6.79	9.23	2.31
5.0 mfp	2.19	2.50	2.99	3.37	3.89	4.66	5.93	8.74	1.21E1	2.48
6.0 mfp	2.47	2.85	3.45	3.91	4.55	5.51	7.12	1.09E1	1.53E1	2.63
7.0 mfp	2.78	3.22	3.93	4.47	5.23	6.39	8.37	1.32E1	1.88E1	2.77
8.0 mfp	3.12	3.62	4.44	5.07	5.95	7.30	9.67	1.57E1	2.27E1	2.90
10.0 mfp	3.87	4.50	5.54	6.33	7.46	9.23	1.24E1	2.11E1	3.14E1	3.13
15.0 mfp	6.29	7.18	8.72	9.92	1.17E1	1.45E1	2.00E1	3.71E1	5.88E1	3.61
20.0 mfp	9.59	1.06E1	1.25E1	1.41E1	1.64E1	2.04E1	2.85E1	5.62E1	9.39E1	4.00
25.0 mfp	1.40E1	1.48E1	1.69E1	1.87E1	2.16E1	2.67E1	3.77E1	7.79E1	1.36E1	4.34
30.0 mfp	1.96E1	1.98E1	2.17E1	2.37E1	2.70E1	3.33E1	4.74E1	1.02E1	1.86E1	4.63
35.0 mfp	2.67E1	2.56E1	2.68E1	2.89E1	3.25E1	4.04E1	5.77E1	1.28E1	2.42E1	4.85
40.0 mfp	3.54E1	3.24E1	3.21E1	3.40E1	3.79E1	4.78E1	6.84E1	1.56E1	3.05E1	4.98

Appendix F (Pu-239 Characterization)

The composition and isotope mix ratios are unknown for the Pu-239 source. Figure 46 shows the spectrum from the Pu-239 source collected by the NaI detector and the CZT detector. As with the multisource, the NaI was much more efficient and had very large count rates. However, the NaI lacked the resolution to identify the individual energy peaks. The CZT detector's resolution enables energy peak resolution, but because of its small active region becomes relatively useless beyond several hundred KeV.

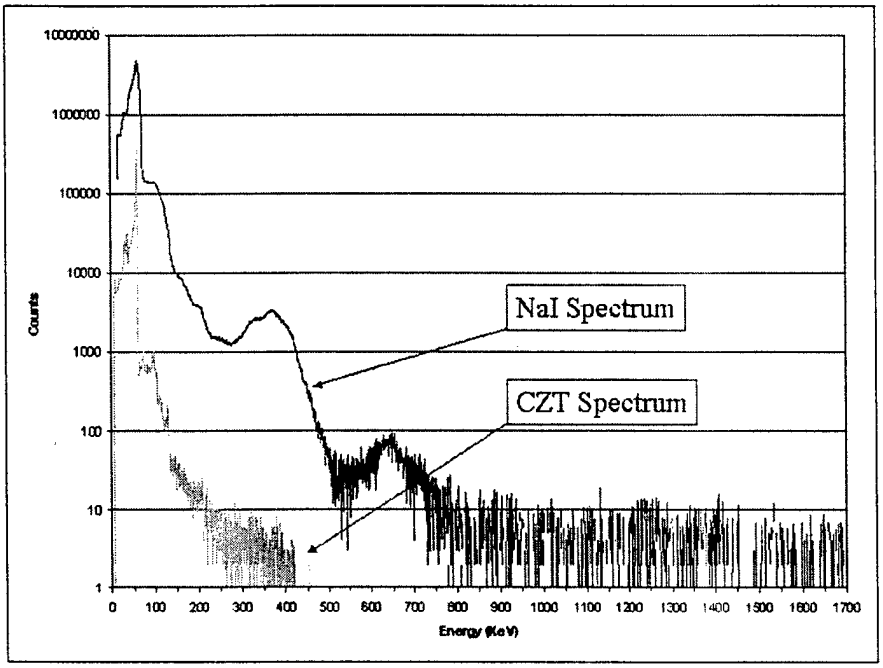

Figure 46 (Pu-239 Spectra Comparison)

Figure 47 provides a more detailed view of the lower energy levels. The CZT detector clearly identifies many peaks that are blended together by the NaI detector.

Several key peaks are identified below. RobWin and RSEMCA will use the CZT spectrum in an attempt to characterize the Pu-239 source.

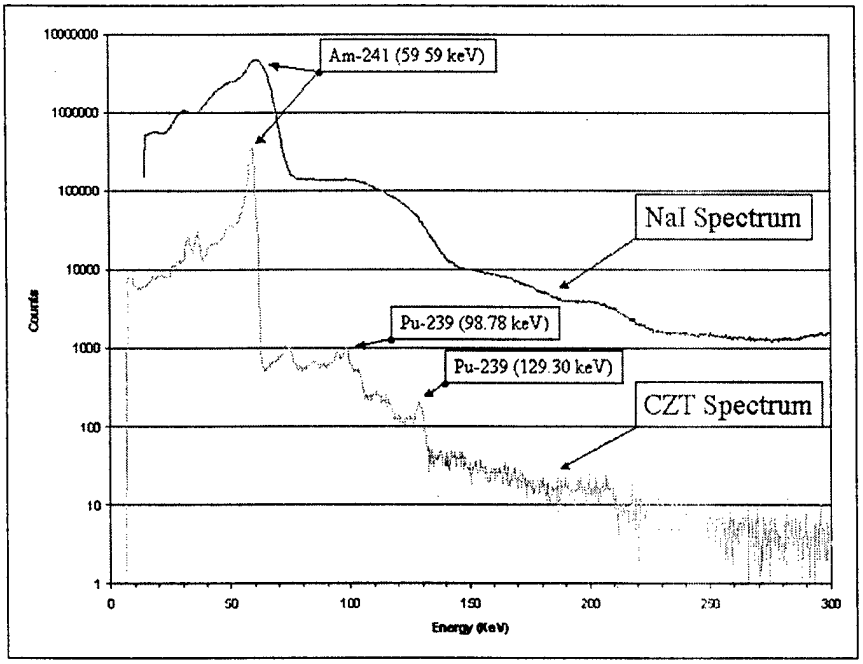

Figure 47 (Lower Energy Pu-239 Spectra Comparison)

Starting with the energy calibration from the CZT multisource, small modifications were made to adjust the calibration to the Pu-239 spectrum. Figure 48 shows the calibrated Spectrum for Pu-239. The energy calibrations used to fit the spectrum were:

$$Y(keV) = 1.064289E\text{-}6*x^2 + 0.3226212*x - 0.1620085$$

$$FWHM^2 = 46.34677 - 0.0394122*x$$

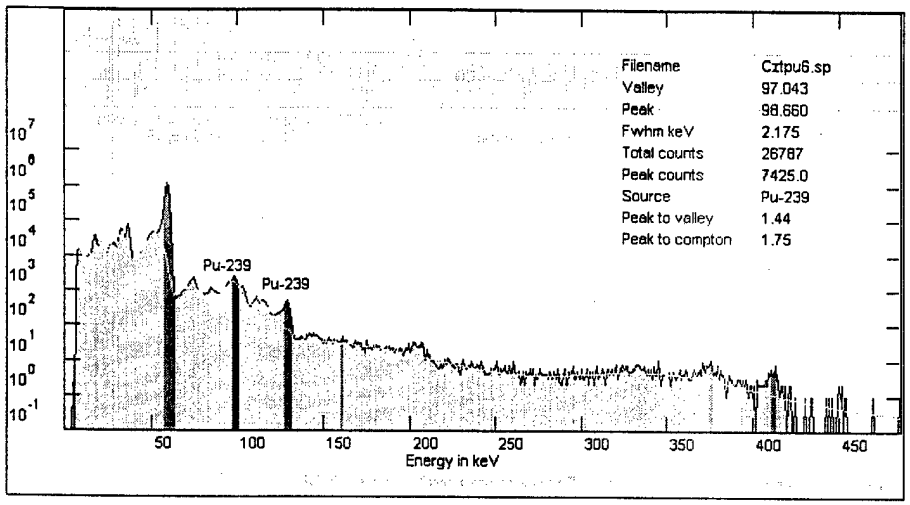

Figure 48 (Calibrated Pu-239 Spectrum)

The next three figures (Figure 49, Figure 50, and Figure 51) were attempts to locate a Pu-240 key gamma ray peak. There was a small indication of aPu-240 peak at 160.31 keV peak, but the peak counts are extremely small, 7.5 counts, and not enough to determine a mass ratio. Part of the problem in these lower energy ranges is that Pu-239 and Am-241 have gamma rays very close in energy, within1 keV, or the same as Pu-240 and the detectors cannot resolve them.

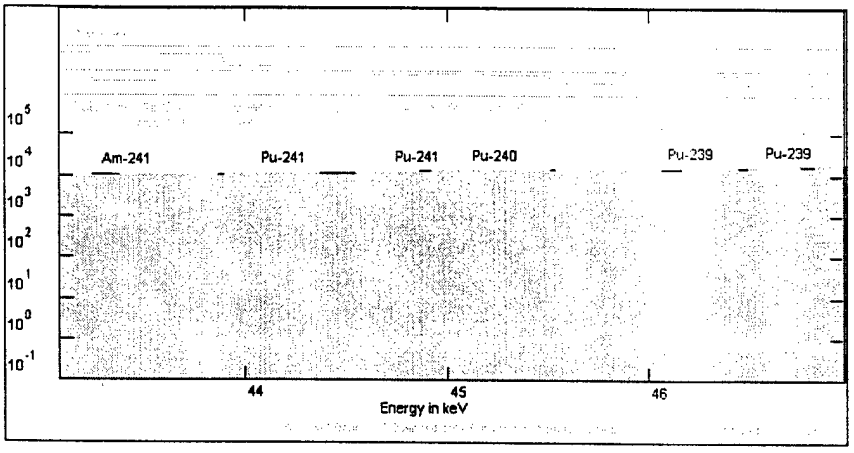

Figure 49 (Search for Pu-240 Peak at 45.24 keV)

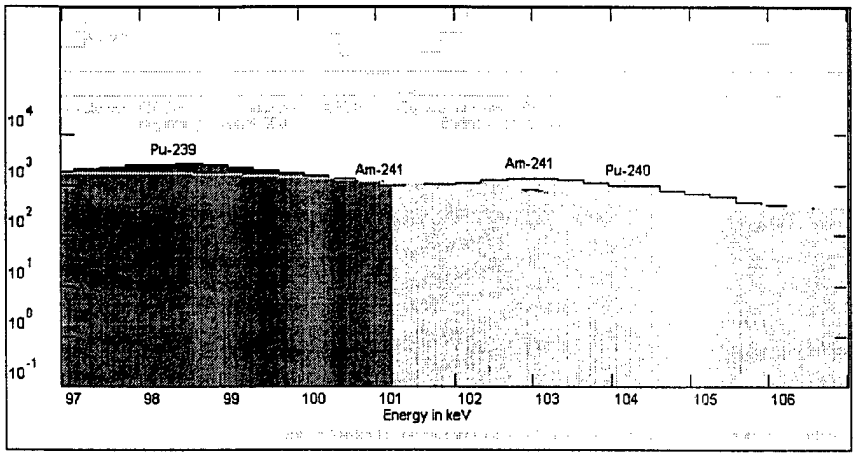

Figure 50 (Search for Pu-240 Peak at 104.23 keV)

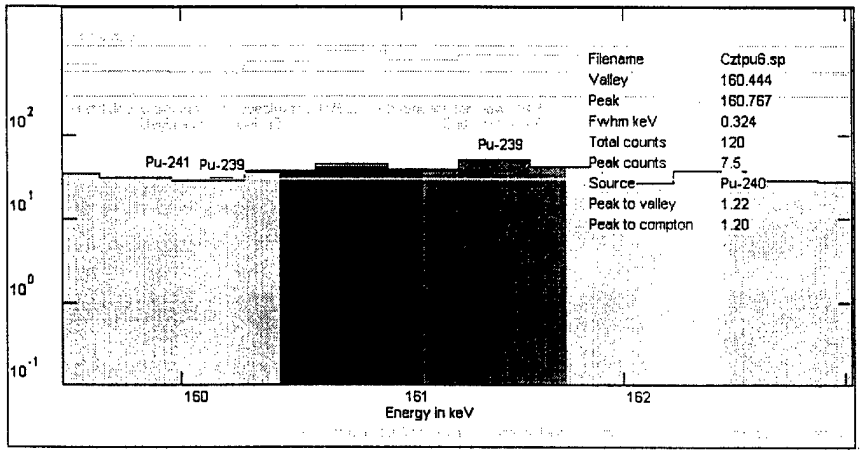

Figure 51 (Search for Pu-240 Peak at 160.31 KeV)

Am-241 gamma rays will most likely be present in a plutonium spectrum. If Pu-241 is present, it naturally decays through the emission of a beta to Am-241. The 59.59 keV peak shown in Figure 52 is most likely from Am-241.

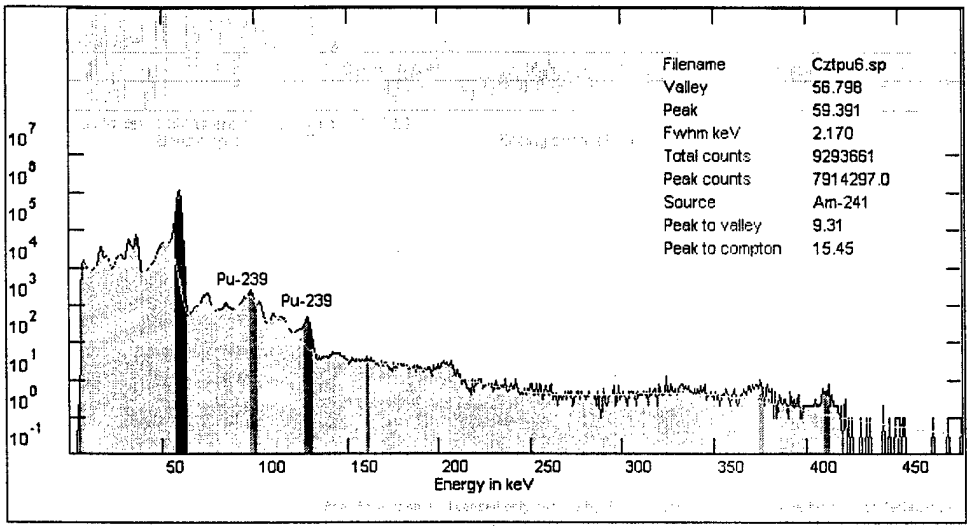

Figure 52 (Am-241 Peak at 59.54 keV)

Neither software program was capable of characterizing AFIT's Pu-239 source. This is more a fault of the detectors than it is the software. For determination of WGPu or RGPu, detectors need to operate in the 640 keV region to distinguish peaks between Pu-240 and Pu-239. The CZT detector cannot provide data in that region. The extremely large Am-241 peak at 59.54 keV would indicate a large concentration of Am-241. Not enough information exits to characterize the source and determine if it is WGPu.

Appendix G (Weapon Size Approximation)

Solid Sphere 500 g Pu-239

If the amount of Pu-239 available and the density (ρ) of Pu-239 are known, the volume can be derived.

$$\text{Volume} = \text{grams Pu-239}/\rho = 500\text{g}/19.85\ \text{g/cm}^3$$

$$\text{volume} = 25.1889\ \text{cm}^3$$

Knowing that volume = $(4/3)\ \pi\ r^3$, the dimension for the sphere can be calculated

$$r = (3*\text{Volume}/4\ \pi)^{1/3} = ((3*25.\ 1889)/4\ \pi)^{1/3}$$

So $r = 1.818$ cm as shown in Figure 53

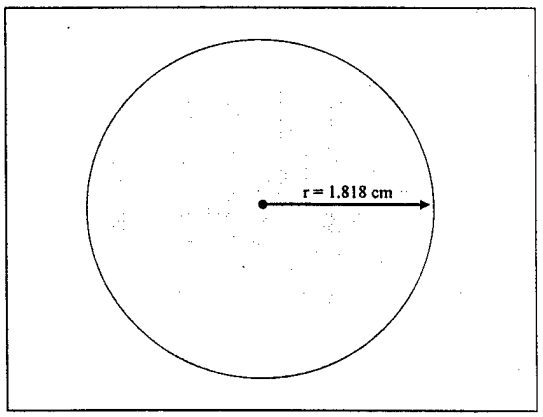

Figure 53 (Solid Pu-239 Sphere)

Hollow Sphere 500 g Pu-239 Calculations

Most modern weapons are made with a hollow core inside a Pu-239 sphere. This allows the gamma rays of the Pu-239 to escape the sphere and no attenuation loss due to travel though the Pu-239 mass.

The volume of 500 grams Pu-239 remains the same, however the size of the mass changes. The volume of Pu-239 is equal to the volume of the total sphere minus the volume of the hollow sphere. Using Figure 54 for a hollow sphere:

$$\text{Volume Pu-239} = \text{Total Volume} - \text{Hollow Sphere Volume}$$

$$\text{Volume Pu-239} = (4/3)\,\pi\,R^3 - (4/3)\,\pi\,r^3$$

Where $r = R-t$

The gamma rays of interest for Pu-239 are between 50 keV and 645 keV. To minimize scatter and allow the gamma rays to escape, the thickness of the Pu-239 shell must be less than 1 mean free path. The mean free paths for these gamma rays are found on Figure 55. A thickness of 0.01 cm is less than one mean free path for gamma rays greater than 80 keV. Using this thickness the size of the sphere can be determined.

$$\text{Volume Pu-239} = (4/3)\,\pi\,R^3 - (4/3)\,\pi\,(R-0.01)^3$$

$$25.1889\ \text{cm}^3 = (4/3)\,\pi\,R^3 - (4/3)\,\pi\,(R-0.01)^3$$

solving for R, the outer radius of the hollow sphere is 14.1629 cm.

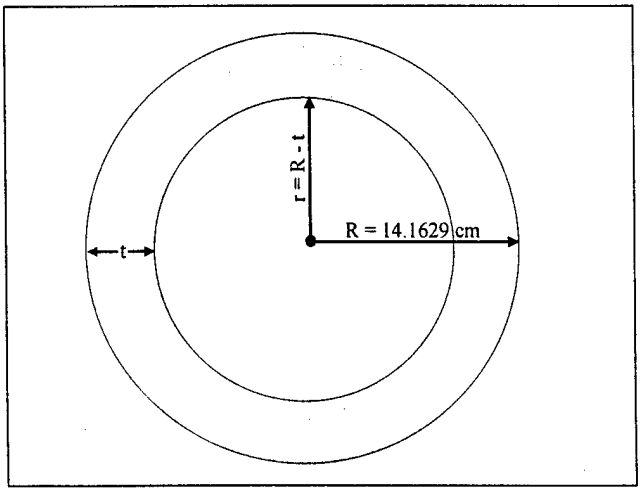

Figure 54 (Hollow Pu-239 Sphere)

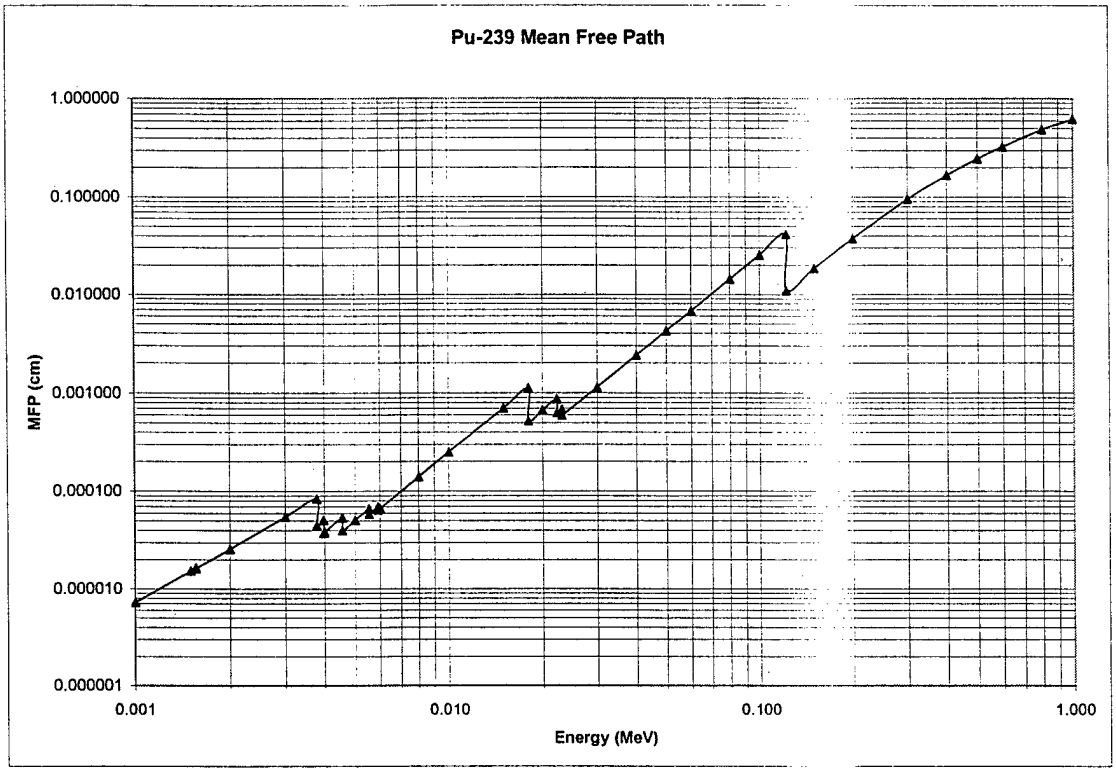

Figure 55 (Mean Free Path for Pu-239)

Appendix H (Weapon signature)

The number of gamma rays counted by the detector can be calculated using the initial gamma ray (Table 16 to Table 23), the detector's efficiency at for each gamma ray energy, a minimal weapon size, and some assumptions on collection distance. The following equation from Knoll is used to approximate the number of pulses recorded (S) [13, 118].

$$S = N\frac{4\pi}{\varepsilon_{ip}\Omega} \qquad 11$$

Where Ω represents the solid angle subtended by the detector at the source position, N is the number of radiation quanta incident on the detector, and ε_{ip} is the detector's intrinsic peak efficiency. For weapon detection, the source cannot be considered a point source and looks similar to Figure G-1.

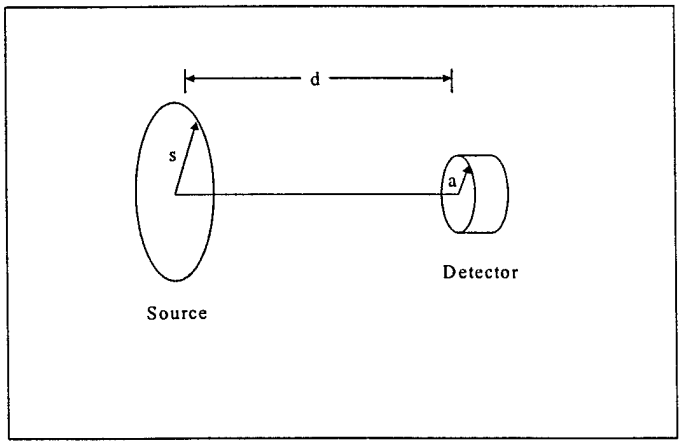

Figure 56 (Source Aligned with Detector)

In terms of Figure 56, the effective solid angle is solved using the integral

$$\Omega = \frac{4\pi a}{s}\int_0^\infty \frac{\exp(-dk)J_1(sk)J_1(ak)}{k}dk \qquad 12$$

where $J_1(x)$ are Bessel functions of x. An approximate solution is: [13, 119]

$$\Omega = 2\pi\left[1-\left(\frac{1}{(1+\beta)^{\frac{1}{2}}}\right)-\frac{3}{8}\left(\frac{\alpha\beta}{(1+\beta)^{\frac{5}{2}}}\right)+\alpha^2[F1]-\alpha^3[F2]\right]$$

with

$$F1=\frac{5}{16}\left(\frac{\beta}{(1+\beta)^{\frac{7}{2}}}\right)-\frac{35}{16}\left(\frac{\beta^2}{(1+\beta)^{\frac{9}{2}}}\right)$$

$$F2=\frac{35}{128}\left(\frac{\beta}{(1+\beta)^{\frac{9}{2}}}\right)-\frac{315}{256}\left(\frac{\beta^2}{(1+\beta)^{\frac{11}{2}}}\right)+\frac{1155}{1024}\left(\frac{\beta^3}{(1+\beta)^{\frac{13}{2}}}\right)$$

$$\alpha=\left(\frac{a}{d}\right)^2 \qquad \text{and} \qquad \beta=\left(\frac{s}{d}\right)^2$$

Appendix I (Detection Equipment Settings)

The following settings were used during this experiment:

b. CZT Detector Setup

1. eV Products CZT detector. Model – SPEAR with CAPture technology, 5mm x 5mm x 5mm crystal.

   Source Height – 0 cm, directly on face

2. Canberra Model 9645 High Voltage Power Supply.

   Settings: 504 volts
   Voltage Limit: 5002.93
   Overload Latch: Enable
   Inhibit Latch: Enable
   Inhibit Signal: 5V
   Output Polarity: Pos

3. Canberra Model 9615 Amplifier.

   Composite Gain: 75.00
   Course Gain: x50
   Fine Gain: 1.5000x
   S. Fine Gain: 1.00001x
   Pole Zero Value: 2816
   Shaping Time: 0.5 *u* sec
   Shaping Mode: Gaussian
   BLR Mode: Asym
   LTC Mode: Normal
   Input Mode: Normal
   Input Polarity: Pos
   Inhibit Polarity: Pos
   Pileup Rejection: On

4. Canberra Model 9633 Analog to Digital Converter (ADC).

   Range: 16384 channels
   Conversion Gain: 4096 channels
   Offset: 0
   ULD: 110.0%
   LLD: 1.0%
   Zero: 0.00
   Mode: PHA

Peak detect: Auto
Coincidence Mode: Coinc
Coincidence Timing: Late
Transfer Timing: Overlap

b. NaI Detector Setup

1. Harshaw NaI(TI) detector

   Source Height – 25 cm

2. Fluke Model 415A High Voltage Power Supply.

   Voltage: 1000 volts
   Voltage Limit: 3100 volts
   Output Polarity: Pos

3. EG&G Ortec Model 571 Spectroscopy Amplifier.

   Composite Gain: 22
   Course Gain: x20,
   Fine Gain: 1.1x
   Shape timing: 3.0 *u* sec
   Output Range: +10 volts
   BLR: Hi

4. Canberra Model 9633 Analog to Digital Converter (ADC).

   Range: 16384 channels
   Conv Gain: 4096 channels
   Offset: 0.0
   ULD: 110.00
   LLD: 2.0%
   Zero: 0.00
   Mode: PHA
   Peak detect: Auto
   Coincidence Mode: Coinc
   Coincidence Timing: Late
   Transfer Timing: Overlap

Appendix J (Genie Report Data File)

RSEMCA required specific data files not readily available with Genie. Report files were created for Genie to produce files compatible with RSEMCA.

Report File – Data.tpl

Genie 2000 uses this file to generate a report for use with RSEMCA software. The report contains a header and then a listing of counts per channel without the channel number. This file needs to be located in the "Ctlfiles" folder inside the "Genie2K" folder. The generated report is found in the "Repfiles" folder.

File Name: Data.tpl

```
$REM
$REM Sample Information Report Template
$REM
$SEC Header
$REM ----1---------2---------3---------4----------5---------6---------7
"*****************************************************************
**"
"*****     GAMMA SPECTRUM ANALYSIS      *****"
"*****************************************************************
**"
""
""
$DEFL STITLE SIDENT STYPE SGEOMTRY SQUANT SUNITS STIME CTITLE
$GETL 1 1 0
"Report Generated On          : |DDDDDDD |TTTTTTTTTT" #datetime #datetime
""
"Sample Title                 :
|AAAAAAAAAAAAAAAAAAAAAAAAAAAAAAAAAAAAAAA" #LIS1(1)
"Spectrum Description         : |AAAAAAAAAAAAAAAAAAAAAAAAAAAAAAA"
#LIS1(8)
"Sample Identification        : |AAAAAAAAAAAAAAA" #LIS1(2)
"Sample Type                  : |AAAAAAAAAAAAAAA" #LIS1(3)
"Sample Geometry              : |AAAAAAAAAAAAAAA" #LIS1(4)
""
"Peak Locate Threshold        : |F.FF" SENSITVTY
"Peak Locate Range (in channels) : |IIII - |IIII" PEAKSTART PEAKEND
```

```
"Peak Area Range (in channels)   : |IIII - |IIII" PASTART PAEND
$IF USEVARETOL
$SETE #FV1 VARTOLERANCE
"Identification Energy Tolerance : |FFF.FFF FWHM" #FV1
$ENDIF
$IFNOT USEVARETOL
$SETE #FV1 TOLERANCE
$SETD #FV1 ECALCNV
"Identification Energy Tolerance : |FFF.FFF |AA" #FV1 ECALUNITS
$ENDIF
""
"Sample Size                 : |EEEEEEEEEE |AAAAAAA" #LIS1(5) #LIS1(6)
""
"Sample Taken On               : |DDDDDDD |TTTTTTTTTT" #LIS1(7) #LIS1(7)
"Acquisition Started           : |DDDDDDD |TTTTTTTTTT" ASTIME ASTIME
""
"Live Time                   : |FFFFFFF.F seconds" ELIVE
"Real Time                   : |FFFFFFF.F seconds" EREAL
""
""
""
"          Energy Calibration Used Done On      : |DDDDDDD" ECALTIME
"          Efficiency Calibration Used Done On  : |DDDDDDD" DCALTIME
""
$REM
$REM Channel by Channel Data Report Template
$REM
$SEC Data
$REM
$REM INITIALIZE THE DATA CARRIERS
$REM
$SETE #IV1 1
$BT CHANNELS
$REM
"|IIIIIII "  SPECDATA(#IV1)
$REM
$SETA #IV1 1
$ET 1
$REM
```

Report File – Data2.tpl

Genie 2000 program uses this report file to generate a report containing only channel number and counts per channel. This file needs to be located in the "Ctlfiles" folder inside the "Genie2K" folder.

File Name: Data2.tpl

```
$REM
$REM Channel by Channel Data Report Template
$REM
$SEC Data
$REM
$REM INITIALIZE THE DATA CARRIERS
$REM
$SETE #IV1 1
$BT CHANNELS
$REM
"|IIII |IIIIIII " #IV1 SPECDATA(#IV1)
$REM
$SETA #IV1 1
$ET 1
$REM
```

Appendix K (Points of Contact)

Below is a list of points of contact for the equipment and software thoughtout this experiment:

a. Electronics

1) Canberra Industries, Inc., One State ST, Meriden, CT 06450. Phone: (203) 238-2351 Fax: (203) 235-1347

2) EG & G Ortec, 100 Midland Rd, Oak Ridge, TN 37830. Phone (615) 986-4212 or 1-800-251-9750

3) John Fluke MFG. CO.,INC., P.O. Box 7428, Seattle, Washington 98133.

b. Detectors

1) NaI Detector: Harshaw/Filtrol Partnership, 6801 Cochran Rd, Solon, OH 44139. Phone: (440) 248-7400

2) CZT Detector (Spear with CAPture Technology): eV PRODUCTS, *A Subsidiary of II-VI, Inc.,* 374 Saxonburg Blvd, Saxonburg, PA 16056. Phone: (724) 352-5288 Fax: (724) 352-4435 website:http://www.ii-vi.com/entry3-prod-ev.html

c. Software.

1) RobWin: Constellation Technology Corporation, 7887 Bryan Dairy Road, Largo, FL 33777. P.O.C.: George Lasche, email: Glasche@aol.com, URL: http://home.att.net/~George.Lasche/RobHome.html.

2) RSEMCA: Radiation Safety Engineering, Inc, P.O. Box 4729, Los Alamos, NM 87544. P.O.C.: Kenneth A. Van Riper, email: Kvr@rt66.com, URL: http://rt66.com/~kvr/kvr.html.

d. Sources.

1) Isotope Products Laboratories, 1800 N. Keystone ST, Burbank, CA 91504. Phone (818) 843-7000

2)Amersham International Limited, Amersham, UK

e. DTRA.

1) Lt Col Thomas Dunham, Arms Control Technology Division, email: Thomas.Dunham@DTRA.mil

2) Lt Col John Anton, Arms Control Program Manager, Arms Control Technology Division, email: John.Anton@DTRA.mil

12. Benedict, M., T. H. Pigford, and H. W. Levi. *Nuclear Chemical Engineering, 2nd Ed.* New York: McGraw-Hill, Inc., 1981.

13. Knoll, Glenn F. *Radiation Detection and Measurement, 3rd Ed.* New York: John Wiley & Sons, Inc., 2000.

14. McMaster, W.H., N. Kerr Del Grande, J.H. Mallet, and J.H. Hubbel. *Complication of X-ray Cross Sections, UCRL-50174, Sec.II, Rev. 1.* Livermore Radiation Laboratories, University of California, Livermore, May 1969.

15. Bridgman, Charles J. *The Physics of Nuclear Explosives and Their Effects.* Air Force Institute of Technology, Wright Patterson Air Force Base, December 1999.

16. Los Alamos National Labs. "Measurement Applications," Gamma-Ray Measurements – Isotopic Distribution, http://www.nis5.lanl.gov/measapps.htm.

17. Anton, LtCol John. email, Arms Control Program Manager, Arms Control Technology, Defense Threat Reduction Agency.

18. Department of Energy, *Standard DOE-STD-3013-96.* September 1996.

19. Lasche, G. P. email, RobWin Software Developer, Constellation Technologies.

20. Redus, Bob. "Charge Trapping in XR-100T-CZT Detectors," www.amptek.com.

21. Shleien, Bernard, Lester Slaback, and Brian Birky. *Handbook of Health Physics and Radiological Health, 3rd Ed.* Williams & Wilkins, Baltimore, 1998.

VITA

MAJ Tom Cartledge was born in White Plains, NY. He graduated from Valhalla High School in Valhalla, NY in June 1982. He entered undergraduate studies at the United States Military Academy in West Point, NY where he graduated with a Bachelor of Science degree in Engineering in May 1986 and received a Regular Commission as an Engineer officer in the United States Army.

His first assignment was with the 23d Engineer Battalion (Combat)(Mechanized) stationed in Hanau, Germany where he performed duties as platoon leader, company executive officer, and brigade engineer. Following Germany, he was assigned to FT Bragg, NC in July 1990 and held positions of Assistant Plans Officer and Company Commander for the 27th Engineer Battalion (Combat)(Airborne) and Company Commander for the 249th Engineer Battalion (Prime Power). While at FT Bragg, he deployed to Saudi Arabia for Operation Dessert Shield and Storm, Southern Florida for Hurricane Andrew relief efforts, Somalia for Operation Provide Hope, and Northern Iraq/Incirlik AFB for Operation Provide Comfort. In September 1995, he was reassigned to the Readiness Group at FT Devens, MA as an advisor to the Reserve Component units in New England. In September 1997, he was reassigned to FT Monroe, VA where he performed duties as the Japanese and Korean Program Manager and Executive Officer for the Deputy Chief of Staff for Doctrine. In August 1999 he entered the Graduate School of Engineering and Management, Air Force Institute of Technology. Upon graduation, he will be assigned to the Defense Threat Reduction Agency.

REPORT DOCUMENTATION PAGE

Form Approved
OMB No. 074-0188

PLEASE DO NOT RETURN YOUR FORM TO THE ABOVE ADDRESS.

1. REPORT DATE (DD-MM-YYYY)	2. REPORT TYPE	3. DATES COVERED (From – To)
02-03-2001	Master's Thesis	Aug 2000 – Mar 2001

4. TITLE AND SUBTITLE

COMPARISON OF SPECTRAL ANALYSIS SOFTWARE PROGRAMS (RobWin and RSEMCA)

5a. CONTRACT NUMBER

5b. GRANT NUMBER

5c. PROGRAM ELEMENT NUMBER

6. AUTHOR(S)

Cartledge, Thomas E., Major, U.S. Army

5d. PROJECT NUMBER

5e. TASK NUMBER

5f. WORK UNIT NUMBER

7. PERFORMING ORGANIZATION NAMES(S) AND ADDRESS(S)

Air Force Institute of Technology
School of Engineering and Management (AFIT/EN)
2950 P Street, Building 640
WPAFB OH 45433-7765

8. PERFORMING ORGANIZATION REPORT NUMBER

AFIT/GNE/ENP/01M-01

9. SPONSORING/MONITORING AGENCY NAME(S) AND ADDRESS(ES)

Defense Threat Reduction Agency
ATTN: TDCS/LtCol Anton
45045 Aviation Dr
Dulles, VA 20166-7517

10. SPONSOR/MONITOR'S ACRONYM(S)

11. SPONSOR/MONITOR'S REPORT NUMBER(S)

12. DISTRIBUTION/AVAILABILITY STATEMENT

APPROVED FOR PUBLIC RELEASE; DISTRIBUTION UNLIMITED.

13. SUPPLEMENTARY NOTES

14. ABSTRACT

The Defense Threat Reduction Agency (DTRA) has purchased two spectral analysis programs, RobWin and RSEMCA, to support arms control efforts. This thesis explored which program performed better for nuclear weapon identification and verification. The initial hypothesis was that both programs would perform similarly with only small differences in visual displays and operating functions. The thesis investigated three areas in order to evaluate the software's capabilities. The first area studied the benefits offered by different detectors, specifically the NaI and CZT detector. The second area analyzed the quantitative and qualitative capabilities of each program, and the third area reviewed the software's ability to detect weapon grade plutonium (WGPu). The results of the study show that RobWin performed better then RSEMCA. Only RobWin is capable of supporting DTRA's needs in treaty verification. RSEMCA is incapable of identifying WGPu due to a mathematical error associated with the peak count calculations. The detectors used in this thesis, the CZT and NaI, also failed to support DTRA's needs. Neither detector was capable of acquiring the necessary spectrum for identifying WGPu. Because of this thesis, recommendations were made for future work with CZT detectors, nuclear weapon detection, and software development.

15. SUBJECT TERMS

Spectral analysis, RobWin, RSEMCA, Defense Threat Reduction Agency, nuclear weapons, verification, identification, spectroscopy, gamma ray, CZT detector, and NaI detector

16. SECURITY CLASSIFICATION OF:			17. LIMITATION OF ABSTRACT	18. NUMBER OF PAGES	19a. NAME OF RESPONSIBLE PERSON
a. REPORT	b. ABSTRACT	c. THIS PAGE			LTC James C. Petrosky, ENP
U	U	U	UU	140	19b. TELEPHONE NUMBER (Include area code) (937) 255-3636, ext 4600

Standard Form 298 (Rev. 8-98)
Prescribed by ANSI Std. Z39-18

Form Approved
OMB No. 074-0188

FROM: AFIT/ENR (PATTY HARDIN)

TO: WHOM IT MAY CONCERN

SUBJECT: IF YOU HAVE CONCERNS/QUESTIONS/COMMENTS – PLEASE CONTACT ME.

Patty Hardin
Research Program Assistant
Office of Research and Consulting
Graduate School of Engineering and Management
Air Force Institute of Technology

Phone Number: (937) 255-3636 ext 4705
DSN 785-3636 ext 4705

EMAIL: patricia.hardin@afit.edu